Analysis of Cellular Mechanical Properties and Nuclear Lamin Proteins As Biomarkers for Whole-Cell Mechanophenotyping of Adipose-Derived Stem Cells

By

Rafael D. González Cruz, M.Eng.

B.S., Chemistry, University of Puerto Rico at Mayagüez, Mayagüez, PR 2009

M.Eng., Biomedical Engineering, Cornell University, Ithaca, NY 2010

Submitted in partial fulfillment of the requirements for the Degree of Doctor in Philosophy in Biomedical Engineering, a program in the Division of Biology and Medicine at Brown University

Department of Biomedical Engineering

PROVIDENCE, RHODE ISLAND, USA

MAY 2018

This dissertation by Rafael D. González Cruz is accepted in its present form by the program in Biomedical Engineering, in the Division of Biology and Medicine, as satisfying the dissertation requirements for the degree of Doctor in Philosophy.

_____	_____
Date	Eric M. Darling, Ph.D., Advisor

Recommended to the Graduate Council

_____	_____
Date	Diane Hoffman-Kim, Ph.D., Committee Chair
_____	_____
Date	Christian Franck, Ph.D., Reader
_____	_____
Date	Anita Shukla, Ph.D., Reader
_____	_____
Date	Kris N. Dahl, Ph.D., External Reader

Approved by the Graduate Council

_____	_____
Date	Andrew G. Campbell, Ph.D., Dean of the Graduate School

CURRICULUM VITAE

1. Name, position, department, contact

Rafael D. González Cruz, M.Eng.

PhD Candidate in Biomedical Engineering

Center for Biomedical Engineering

Brown University

rafael_gonzalez_cruz@brown.edu

(787)-546-9159

ORCiD: 0000-0001-6025-1686

2. Education

09/2003 – 05/2009	B.S. in Chemistry, University of Puerto Rico – Mayagüez
09/2009 – 05/2010	M.Eng. in Biomedical Engineering, Cornell University
09/2012 – Present	PhD in Biomedical Engineering, Brown University

3. Research Experience

a. Doctoral Student (PhD) in Biomedical Engineering at Brown University

PI: Eric M. Darling, PhD

i. Examination of cell surface marker proteins involved in mechanotransduction as novel biomarkers for cell sorting of stiff and soft live cells, with applications to stem cell and rare cell population enrichment

ii. Isolation and extraction of cell surface proteins from biotinylated cell lysates using biotin-based protein extraction kits

iii. Cell sorting of fixed osteoblasts and adipose-derived stem cells (ASCs) with distinct mechanical properties by analyzing differences in lamin A/C expression levels (induced by siRNA treatment)

iv. Found that lamin A and C are affected by disruption of the actin cytoskeleton in cells using cytoskeletal drugs and LMNA siRNA knockdown strategies using osteosarcoma cells

v. Found that nuclear lamin protein C is a strong predictor of cellular mechanical phenotype (stiffness) after quantifying its expression in mechanically distinct cells derived from different tissue sources

vi. Studied the mechanical properties of ASCs across several passages and their implications for stem cell differentiation towards specific lineages (*Adipocyte* Article)

b. Research Assistant at Brown University

PI: Eric M. Darling, PhD

i. Analyzed the correlation between mechanical properties of adipose-derived stem cells and their differentiation potential into bone, cartilage and fat tissue (*PNAS* Article)

ii. Learned atomic force microscope-(AFM) cellular indentation techniques

4. **Skills**

    a. **Instrumentation:** Atomic force microscopy (AFM)-based single-cell microindentation, flow cytometry, light microscopy

    b. **Molecular/Cellular Assays:** Protein extraction and quantification from live and fixed cells, Western blot, immunostaining, antibody validation, microcontact printing of proteins, siRNA gene silencing

    c. **Cell culture:** Cell line and primary cell cultures, adipose-derived stem cell (ASCs) isolation from lipoaspirate and culture, osteogenic and adipogenic differentiation of ASCs

5. **Publications**

    a. **González-Cruz RD**, Fonseca VC, Darling EM. (2012) Cellular mechanical properties reflect differentiation potential of adipose-derived mesenchymal stem cells. Proc Natl Acad Sci USA. 109 (24): E1523-9. PMCID: PMC3386052

    b. **González-Cruz RD**, Darling EM. (2013) Adipose-derived stem cell fate is predicted by cellular mechanical properties. Adipocyte. 2 (2): 87-91. PMCID: PMC3661107

    c. **González-Cruz RD**, Sadick, JS, Fonseca VC, Darling EM. (2018). Nuclear lamin C is linked to lineage-specific, whole-cell mechanical properties. Cell Molec. Bioeng. NIHMS935318

6. Conference Abstracts

a. **González-Cruz RD**, Fonseca VC, Darling EM. (2011) Stem cell mechanical biomarkers indicate differentiation potential. Podium presentation. 4th Northeast Regional IDeA Meeting. Newport, RI.

b. Fonseca VC, **González-Cruz RD**, Darling EM. (2011) Single-cell mechanical properties as an indicator of stem cell differentiation potential. Conference abstract. Biomedical Engineering Society Annual Meeting. Hartford, CT.

c. Darling EM, Desai HV, **González-Cruz RD**, Fonseca VC. (2012) Novel biomarkers for the identification of lineage-preference in mesenchymal stem cells. "Rising Star" podium presentation. BMES-SPRBM 2012 Conference. San Juan, Puerto Rico.

d. Darling EM, Labriola NR, **González-Cruz RD**, Fonseca VC. (2012) Cellular mechanical biomarkers for lineage-specific, stem cell enrichment. Podium presentation. Orthopaedic Research Society Annual Meeting. 58:0001. San Francisco, CA.

e. Darling EM, Labriola NR, **González-Cruz RD**, Kanthilal M, Sadick JS, Fonseca VC. (2015) The intersection of gene expression and mechanical phenotype. Conference abstract. Cellular and Molecular Bioengineering Conference. St. Thomas, USVI.

f. **González Cruz RD**, Fonseca VC, Kanthilal M, Sadick JS, Darling EM. (2015) LMNA gene and lamin A protein expression serve as novel biomarkers for characterizing mechanical phenotype. Conference abstract. Orthopaedic Research Society Annual Meeting, Las Vegas, NV.

g. **González Cruz RD**, Darling EM. (2015) Lamin A and B1 protein expression are indicative of whole-cell mechanical properties. Conference abstract. Society for Advancing Chicanos/Hispanics & Native Americans in Science National Conference. Washington, D.C.

h. **González Cruz RD**, Darling EM. (2016) Whole-cell mechanophenotype correlates to lamin protein and gene expression. Podium presentation. Cellular and Molecular Bioengineering Conference. New Orleans, LA.

7. Awards

a. SACNAS 2017/ASSIST Travel Award (2017)

b. Outstanding Research Presentation Award at the 2016 CMBE-ABioM (2016)

c. Travel Award CMBE Conference Travel Award (2016)

d. SACNAS 2015 Conference Travel Award (2015)

e. NIH Research Supplement Grant (to EMD Parent Grant, 2015-17)

f. Initiative to Maximize Student Development (IMSD) Fellowship (2013-15)

g. NIH Research Supplement (to EMD Parent Grant, 2011-12)

8. Service

a. To the university

i. Brown University IMSD Internal Advisory Board (2016-Present)

ii. Brown University PREP Post baccalaureate Program Mentor (2016-17)

iii. Society for the Advancement of Chicanos and Native Americans in Science (SACNAS) Brown University Chapter President (2015-2017)

iv. IMSD Scholar (2013-Present)

9. Teaching

a. Tissue Engineering Teaching Assistant BIOL 1140 (Fall 2013)

b. IMSD Essential Laboratory Calculations (Fall 2013)

ACKNOWLEDGEMENTS

I thank God, in His infinite grace and love, for providing me with the opportunity to gain the support of many wonderful people whose assistance and counsel were necessary for my successful academic journey from the small town of Aguada, Puerto Rico to Brown University and for the preparation of this written thesis.

First, I would like to thank my advisor, Eric Darling. I am particularly thankful for your guidance throughout my graduate training and encouragement to tackle difficult research questions while, at times, playing devil's advocate to make think deeply about my research and its implications for the field of stem cell biology and biomedical engineering. Thanks to your training, I feel confident in ability to pursue original research questions through the design of hypothesis-driven experiments and quantitative data analysis.

I also want to thank the members of my committee members, Profs. Diane Hoffman-Kim, Prof. Anita Shukla, Prof. Christian Franck, and Prof. Kris Noel Dahl. I am thankful to you for providing scientific guidance and constructive criticism towards the improvement of my research work in several occasions, including my qualifying examination, informal meetings, and now at my thesis defense. I am particularly thankful to Prof. Hoffman-Kim for providing both academic and life advice throughout different stages of my graduate career.

I am also thankful to the wonderful group of people that make the Darling Lab. Vera Fonseca, you were a critical part of my scientific growth and training while pursuing my career at Brown University. Your patience and kindness were incredibly helpful in learning techniques and measurements necessary for the completion of my experiments, which include cell culture, mechanical testing of cells, Western blot, etc. Your contributions to my scientific are forever recorded both in all my publications but also in the memories of your friendship.

I am also thankful for my lab mates, Nicholas Labriola, Bryan Sutermaster, Jessica Sadick, Manisha Shah, Roberto Gutiérrez, Adrienne Parsons, Hetal Marble, Olivia Beane, and Megan Dempsey. You all made lab a very social, friendly, and healthy environment for scientific research with your assistance in troubleshooting experiments, interpreting data, revising manuscripts, providing emotional support when experiments failed in the form of advice, jokes, memes, etc. My success in the lab would have not occurred without your assistance.

I am also thankful to the administrative staff of the 3rd floor of the Biomedical Center. I am particularly thankful to Ely Peimer, Jessica Bello, Kris McCutcheon, Melodie Vicenty, Crystal Miller, Gilberto Del Valle, and Leonard Erickson for your assistance with navigating logistics, research grant submissions, reagent ordering, and friendship. In that same vein, I am thankful for students and staff in this floor for providing support and friendship, with particular thanks to Liane Livi, for her incredible kindness, empathy, and friendship.

I am also thankful to the amazing staff from the Initiative to Maximize Student Development program. Deans Andrew Campbell and Elizabeth Harrington, thank you for allowing me to participate in the IMSD program and providing advice as well as opportunities to enhance my scientific training and professional development by attending IMSD modules, scientific conferences, etc. The training model for IMSD was instrumental in developing not only my scientific character but also strengthen my resolve in working to increase the representation of minority students like myself in institutions of higher learning such as Brown University. In a similar fashion, I am thankful to Prof. Medeva Ghee for providing opportunities to further my professional development and involvement with underrepresented student mentoring via the Leadership Alliance Program. Thank you, IMSD Program Coordinators Karen Ball and Jennifer Daly and OGPS Graduate Program Manager Tracey Cronin for being more than very helpful Program Coordinators/Managers but also friends that I could come and talk about life. Additionally, I am also thankful to Associate Dean for Diversity Initiatives, Marlina Duncan, and Director of the Brown Center for Students of Color (BCSC), Joshua Seguí, for their mentorship and counseling through my academic career through times of uncertainty as well as their friendship. Finally, I am thankful for my friends from the Society for the Advancement of Chicanos/Hispanics and Native Americans in Science (SACNAS)and the Puerto Rican Association at Brown University for providing a safe platform for professional development, emotional support, and opportunities to give back to the Brown and Providence community.

I am also thankful to my parents, David González Benique and Marisol del Carmen Cruz Santiago, for their unconditional love, support, instruction, guidance, and sacrifice throughout my life and up to this day. I am particularly thankful for my father's wisdom and my mother's love and prayers. I would also like to thank my uncle, Juan Inocencio Cruz Santiago, for being an early role model of academic perseverance and excellence and as well as for his financial support through college. I would also like to honor the memory of my late grandfather, Miguel Chaparro, for being a living example of overcoming adversity and becoming successful, despite growing up as an orphan. Their examples serve as a reminder of the sacrifices and hardships our people have endured to overcome the hurdles of social inequality and poverty and provide a better chance at socioeconomic mobility and stability to the next generation. This thesis is dedicated to them, in honor of such love.

I am also thankful to my beloved wife, Yarimar Ortiz Frontera, for her love, kindness, empathy, counsel, and support as I navigated the different stages of uncertainty and difficulty that comprised my journey from college to graduate school. I am quite certain I would have not overcome many personal situations that rose through that time span without her presence in my life.

Finally, I am also thankful for my science and math teachers, Chemistry and Biology college professors and scientific trainers, particularly my Chemistry teacher Irma Echevarría, Biochemistry professor, Prof. Doris Ramírez, and Masters advisor Prof. Cynthia A. Reinhart-King. Mrs. Echevarría took an interest in my academic goals, helped

me take AP classes and examinations, and took me to an open house of the University of Puerto Rico's Chemistry Department, from which I obtained my B.S. in Chemistry six years later. Professor Ramírez was responsible for helping me apply to the RiSE summer research internship program at Rutgers University that would introduce me to the field of biomedical engineering and later helped to apply for graduate school. Additionally, I am thankful to Prof. Sally Meiners (Rutgers University) and Prof. Reinhart-King (Cornell University) for their mentoring and providing the opportunity to work in the research fields of biomaterials and cellular biomechanics, respectively, while solidifying my resolve to pursue a research career in biomedical engineering. I would have not pursued a career in science had they not encouraged me the opportunities cultivate my scientific interests.

TABLE OF CONTENTS

LIST OF FIGURES

CHAPTER 2: Cellular mechanical properties reflect differentiation potential of adipose-derived mesenchymal stem cells

CHAPTER 4: Nuclear Lamin Protein C is Linked to Lineage-Specific, Whole-Cell Mechanical Properties

LIST OF TABLES

CHAPTER 2: Cellular mechanical properties reflect differentiation potential of adipose-derived mesenchymal stem cells

CHAPTER 3: Mechanophenotype changes of ASCs as a function of passage number: a small study

CHAPTER 1:

Motivation, Chapter Overview, and Background

1.1 MOTIVATION

The general motivation behind this body of work is to identify novel biomarkers that are intricately related to the cell's mechanical phenotype and use subsets of these markers for the isolation and enrichment of cells with specific mechanophenotypes from tissues with heterogeneous cellular populations. As a specific goal within the scope of this work, I examined the roles of: (a) whole-cell elastic and viscoelastic properties as novel indicators of lineage-specific differentiation potential of adipose-derived stem cells (ASCs, Chapter 2); (b) nuclear lamin proteins A, B1, and C as biomarkers of mechanical phenotype, as validated using mechanically distinct cell lines (Chapter 3); and (c) lamin A/C-based cell sorting of ASCs for the identification of novel surface biomarkers suited for high-throughput ASC sorting based on mechanophenotype (Chapter 4). While this work centers on a very specific biological system (ASCs and cell lines), the use of mechanical properties and mechano-related macromolecules can greatly motivate the study of mechanobiological phenomena in scenarios beyond the context of stem cell differentiation. Scenarios in which changes in mechanical phenotype and associated biomarkers can include cancer, bone and cartilage degeneration, and diseases resulting from defects in lamin protein encoding genes (laminopathies) such as muscular dystrophy and progeria, etc. It is my hope that the evidence presented in this thesis inspires future researchers to use mechanical properties and/or mechanobiomarkers reported in this work as detection, diagnostic, and/or enrichment tools in the biological scenarios mentioned above.

1.2 CHAPTER OVERVIEW

Chapter 2 examines the hypothesis that whole-cell mechanical properties, elastic and viscoelastic properties, are indicators of lineage-specific differentiation in clonal populations of adipose derived stem cells (ASCs). Specifically, it provides experimental evidence that ASC clonal populations are mechanically heterogeneous and that ASCs with high mechanical property parameters are more likely to differentiate towards osteogenic and chondrogenic linages, whereas the opposite trend in mechanophenotype favors adipogenesis. Chapter 3 explores the hypothesis that the expression of lamin proteins A/C, nuclear lamina proteins associated with cellular mechanotransduction, are strongly correlated to whole-cell mechanical properties and, by extension, could serve as biomarkers for determining a cell's inherent mechanophenotype. Specifically, it discusses experimental evidence that shows lamin C is the nuclear lamin protein with the strongest correlation to elastic and viscoelastic properties and that this relationship is dependent on an intact cytoskeleton in stiff cells. Chapter 4 proposes using lamin A/C as a biomarker to sort ASC populations that are hypothesized to be heterogeneous and, therefore, exhibit a different range of mechanical properties (based on results described in Chapter 1). Specifically, the sorted populations, high and low lamin A/C-sorted ASCs, can be subjected to proteomic analysis to identify cell surface markers that correspond to high lamin A/C, stiffer ASCs and low lamin A/C, more compliant ASCs. Chapter 5 discusses the future directions of the work presented in this thesis, placing particular emphasis in using the surface markers identified in Chapter 4 to sort live cells based on their mechanophenotype for stem cell enrichment and differentiation schemes.

1.3 BACKGROUND

1.3.1 Adipose-derived stem cells as therapeutic agents

Adipose-derived stem cells (ASCs) are non-hematopoietic, adult mesenchymal stem cells (MSCs) that represent a promising cell source for cell-based therapies and tissue engineering applications because these cells are multipotent, readily abundant in clinically relevant numbers, non-immunogenic, and easier to isolate than other MSCs.[1-3] Specifically, ASCs can be expanded in vitro to reach clinically relevant numbers and then differentiated into a variety of cells from ectodermal, mesodermal, and endodermal lineages when presented with lineage-specific induction cues.[1, 4-6] Because of their multipotency, ASCs have been used in a wide range of tissue engineering applications as well as in cell-based therapies.[7-9]

ASCs are readily derived from various sources of white adipose tissue adipose, which include subcutaneous, abdominal, inguinal, and auxiliary adipose tissues.[10] Each lipoaspirate sample can contain between 100 mL to over 3 L of fat tissue. From 300 mL of lipoaspirate, it is possible to obtain around 10 million adipose stromal/stem cells with 95% purity. From this SVF mixture, it is possible to isolate ASCs that can yield 5,000 colony-forming units (CFUs)/mL.[9] To put in perspective, the other major source of adult MSCs in body are bone-marrow derived MSCs that only yield between 100-1000 CFUs/mL of bone marrow with a more difficult (higher morbidity) isolation that mostly

targets femoral bone marrow tissue. These facts make ASCs the most accessible and abundant adult stem cell source in the human body.

1.3.2 Cellular heterogeneity in adipose tissue and the need for ASC enrichment

ASCs are derived from lipoaspirate tissue that is processed by enzymatic digestion and followed by centrifugal separation. This processed tissue is known as the stromal vascular fraction (SVF), which contains many other cell types besides ASCs.[11] These cells include fibroblasts, endothelial cells, pericytes, smooth cells, and a variety of blood cells, among others. Their presence in the SVF represents a problem for ASC-based therapeutics and tissue engineering applications because these schemes rely on the number of ASCs that can faithfully differentiate into the specific lineages that are being targeted for treatment. To address this issue, researchers have developed ASC isolation strategies to separate and enrich ASC populations from SVF samples. The most popular of these strategies involved screening the surface protein profiles of cells, or their immunophenotype, in the SVF and then sort them on markers that are specific for ASCs and not present in the other contaminating cell types.[12, 13] From an immunophenotypic perspective, ASCs must be negative for surface biomarkers that are predominantly expressed in the other cell populations present in the SVF while positive for markers that ensure their stemness, which could lead to endless combinations of markers being proposed for ASC identification. Therefore, the immunophenotypic definition of ASCs have been revised several times by the scientific community, with the latest scientific consensus for the minimal criteria for ASC immunophenotype being established jointly

by the International Federation of Adipose Therapeutics and Science and the International Society for Cell Therapy in 2013. These criteria state that ASCs freshly isolated from SVF should be positive for CD34 (early passage progenitor cell marker) and a bonafide viability marker but negative for CD45 (pan leukocyte marker), CD31 (endothelial marker), and CD235a (erythrocyte marker). For ASCs expanded in culture, the criteria specify that these cells should be positive for CD44, CD73, CD90 (mesenchymal markers) and CD105 (endoglin), but still negative for CD45 and CD31.[14]

The level of specificity required to obtain purer ASC populations from SVF demands the use of multiple surface marker panels to exclude unwanted cells like blood cells and endothelial cells and obtain a population of mesenchymal stem cells that includes ASCs. obtain the desired phenotypic specificity, which comes at the cost of cell yields. As a consequence, this approach limits the number of cells that can be obtained for clinical applications at the SVF stage. Once ASCs are isolated, they are expanded in monolayer cultures several times, under conditions that maintain their stemness, until their numbers are sufficient for clinical applications.[15] Through this process, not only ASCs proliferate but they also undergo changes in their surface marker profiles and lineage-specific differentiation potential, thus limiting the number of times ASCs can be passaged before their ability to differentiate into a particular cell type is compromised.[16-18]

1.3.3 Mechanical testing and mechanical properties of cells as biomarkers of cellular phenotype

As an alternative approach, a subset of researchers has looked into the mechanical properties of cells as biomarkers for mechanophenotype. These mechanical properties have been shown to be specific for certain cell types since cells from different lineages can display varying levels of resistance to deformation (elasticity) and flow (viscosity) in response to an applied force.[19-22] This dual mechanical behavior, known as viscoelasticity, is dependent on the composition and organization of subcellular structures, particularly the cytoskeleton. Assuming a cell behaves as an elastic material, its resistance to deformation is linearly proportional to the applied stress but inversely proportional to the resulting strain. This resistance to deformation is measured experimentally as the elastic modulus ($E_{elastic}$). Elastic materials with high elastic moduli are considered stiff because an increase in applied stress results in a negligible increase in their strain. Compliant elastic materials, though, have low elastic moduli because small increases in applied stress result in substantial deformation. Moreover, elastic materials subjected to a constant stress exhibit a constant strain and recover their original shape completely after the stress is removed. However, cells are viscoelastic materials and exhibit both elastic and viscous properties. Specifically, when a viscoelastic material is kept at a constant strain, the applied stress decreases over time, a phenomenon called stress relaxation. In stress relaxation, the viscoelastic properties of a material can be described by its instantaneous and relaxed moduli. The instantaneous modulus (E_0) is the resistance to deformation measured before the relaxation begins, whereas the relaxed

modulus (E_R) is the stiffness of the material at complete equilibrium. The material's apparent viscosity (μ_{app}) is determined by the resistance to flow upon the application of a stress. These mechanical properties, which can be extracted from experimental data using appropriate mathematical models, have emerged as biomarkers that are useful for discriminating among the elastic and viscoelastic properties of multiple cell types, including MSCs and differentiated cells.[20, 23, 24] Elastic and viscoelastic properties can be measured by various mechanical characterization methods, which include atomic force microscopy-based single cell indentations, micropipette aspiration, optical tweezers, microfluidics-based deformation cytometry, etc.[25] For the purposes of this thesis, all mechanical testing experiments were done with AFM-based single indentation measurements and only the discussion of such method will be included in this thesis.

Briefly, AFM-based microindentation allows the local measurement of cellular elastic properties by recording the deflection of a spherically-tipped cantilever while indenting a cell. Hooke's law, $F=k\Delta d$, is used to determine the applied force, where F is the force, k the spring constant or stiffness of the cantilever, and Δd is the deflection of the cantilever. From Hooke's law and indentation data, force-indentation curves are generated by plotting the force applied to the cell as a function of sphere indentation. From these curves, the cell's elastic properties (elastic or Young's modulus, $E_{elastic}$) and viscoelastic properties (E_0, E_R, and μ_{app}) can be determined by fitting the experimental data to a modified Hertz model that considers the indentation of a thin, flat surface with a spherical indenter.[20, 23]

$$F(\delta) = \frac{4R^{1/2}E_{elastic}}{3(1-\nu^2)}\delta^{3/2}C \quad \text{(Eq. 1)} \qquad F(t) = \frac{4R^{1/2}\delta^{3/2}E_R}{3(1-\nu)}\left(1+\frac{\tau_\sigma-\tau_\varepsilon}{\tau_\varepsilon}e^{-t/\tau_\varepsilon}\right)C \quad \text{(Eq. 2)}$$

$$E_0 = E_R\left(1+\frac{\tau_\sigma-\tau_\varepsilon}{\tau_\varepsilon}\right) \quad \text{(Eq. 3)} \qquad \mu = E_R\left(\tau_\sigma-\tau_\varepsilon\right) \quad \text{(Eq. 4)}$$

$$\mu = E_R(\tau_\sigma-\tau_\varepsilon)$$

Eq. 1 represents the elastic response of the probed cell when indented by the cantilever tip; Eq. 2 represents the stress relaxation, viscoelastic response of the cell after indentation. In these equations, F is the applied force, $E_{elastic}$ is the elastic Young's modulus, ν is Poisson's ratio (typically 0.5 for biological materials), R is the radius of the spherical tip, δ is the measured indentation, τ_σ is the stress relaxation time, τ_ε is the strain relaxation time, t is time, and C is a thin-layer correction factor designed to account for indentation depth, the radius of the spherical tip, and sample thickness. E_R is obtained by fitting the experimental data collected up to 30 seconds to Eq. 2. In order to find the remaining viscoelastic parameters, Eq. 3 and Eq. 4 can be used to define the instantaneous modulus and apparent viscosity (E_0 and μ_{app}, respectively). A 5 μm, spherically-tipped, cantilever is used to indent single cells over the nucleus at an indentation speed of 10 μm/s and indentation depth resulting in strains of less than 10%. Following indentation, a 30-second stress relaxation test is conducted to obtain time-dependent mechanical properties (viscoelastic properties E_0 and E_R). Cell heights will be recorded by obtaining the difference between the indentation contact point and that of the adjacent substrate.

While the mechanical testing methods briefly discussed above allow for characterization and discrimination of cells with distinct mechanical phenotypes, they

have two main limitations. First, their throughput does not match the high-throughput and yield offered by conventional cell sorting methods like fluorescence assisted cell sorting (FACS). Mechanical testing techniques like AFM-based cell indentation are usually end-point characterization techniques since most testing conditions, including the ones presented in thesis, occur in non-sterile environments. However, even if the setup could be adapted to create a sterile environment, the number of live cells that can be tested with AFM is exceedingly low (1 cells/s and 1 cell/30 s for elastic and viscoelastic property measurements, respectively; determined experimentally from AFM measurements in Chapters 3 and 4). The same numeric limitation applies to other testing methods such as micropipette aspiration and microbead rheological testing devices. Microfluidic devices could allow for higher mechanophenotypic sorting throughputs under sterile conditions, but the amount of volume these devices can handle as well as the cell yield (100 cells/s)[26] still pales in comparison to the higher outputs offered by conventional cell sorters (2500 cells/s); determined experimentally in Appendix A). This limitation is of great concern for studies requiring the sorting and characterization of millions of cells, which include clinical studies, cell-based therapies, and of particular interest to this study, proteomic analyses.

Second, the mechanical properties need to be tied to biological markers to understand the context in which the cells are exhibiting mechanophenotypic changes. Typically, mechanophenotypic changes are accompanied by changes in cell morphology and structural components like the actin cytoskeleton and cellular mechanotransduction machinery.[27-29] However, these changes alone are not enough to explain complex

biological phenomena and they need to be studied in parallel with biomolecules that are intricately involved in the biological scenarios of interest. For instance, in this thesis, I provide evidence for the role of mechanical properties as biomarkers is the context of stem cell differentiation as the correlation between elastic/viscoelastic properties and lineage-specific metabolites (see Chapter 3). Others have looked at mechanical properties of cells in the context of stem cell differentiation[24] and cancer,[29, 30] to name a few, but still had to conduct biological assays to connect the mechanical data to the biological problem under study.

In light of the aforementioned limitations, a combinatorial approach to be able to sort cells based on mechanophenotype in a high-throughput fashion and biological-guided context requires the examination of macromolecules that are involved in mechanophenotype and/or mechanotransduction as well as provide insight into the biological phenomena under study. Previous studies have looked at the role of several proteins that can trigger changes in either nuclear and/or cytoplasmic mechanical properties when their expression is altered by introducing changes in their local microenvironment. These proteins include integrins, linker of the nucleoskeleton and cytoskeleton (LINC) protein complex nesprins and SUN proteins, and nuclear lamin proteins.[31, 32] Integrins are of paramount importance because they can (a) trigger signaling cascades, such as Rho family GTPases and ß-catenin, that control ultimately control gene expression[33-36]; (b) sense the stiffness of the extracellular matrix and recruit focal adhesion complexes that then act upon the actin fibers to remodel the existing cytoskeleton.[37-39] Nesprins link cytoskeletal elements and transmit mechanical forces to

the nucleus by interacting with nuclear membrane SUN proteins.[32, 40] These SUN proteins interact directly with nuclear lamin proteins that relay those mechanical cues to induce chromatin rearrangements that result in gene expression changes.[41, 42] However, no studies have looked at the relationship of these markers with whole-cell mechanophenotype in a high-throughput fashion. That is, whether one or a subset of these proteins involved in mechanotransduction can be used as reliable biomarkers for cell stiffness the same way FACS surface markers are used to sort millions of cells.

1.3.4 Nuclear lamina proteins as potential biomarkers of cellular mechanical properties

Nuclear lamina proteins are involved in cellular mechanotransduction, maintaining nuclear integrity, and can alter gene expression because of their interactions with histones, transcription factors, and chromatin domains.[42-44] Specifically, they are at the receiving end of the mechanotransduction machinery, receiving direct mechanical force transduction from LINC complex proteins and/or paracrine signaling trigger by forces,[45, 46], which makes them very interesting mechanophenotypic biomarker candidates. Nuclear lamina proteins include lamins A and C, B1 and B2, which are encoded by genes *LMNA*, *LMNB1* and *LMNB2*, respectively.[47] The structural role of these proteins in the cell is of great importance as regulatory changes and/or mutations of the *LMNA* gene are not only responsible for gene expression changes in cells but also for several diseases known as laminopathies.[48] Specifically, deletions in *LMNA* genes can be responsible for diseases such as cardiomyopathies, muscular dystrophies, aging, etc.[49]

From a biomechanical perspective, cells harboring *LMNA* mutations exhibit distinct mechanical phenotypes from their wild-type counterparts; with cells having these mutations exhibited impaired mechanotransduction.[50] The mutations, of course, are specific to the genes being altered and their role in the *LMNA* gene transcription and mRNA translation processes. Progeria, for example, is a disease resulting in the mutation of *LMNA* gene that causes the lamin A precursor, prelamin A, to be improperly translated. As a result, cells with this mutation undergo accelerated aging as a phenotypic feature of this disease, but in their nucleus, prelamin A accumulates, making the nucleus stiffer but also more brittle and easier to rupture due faulty mechanotransduction and poor resistance to forces.[51, 52] Mutations were the *LMNA* gene is completely deleted results in cells being significantly more compliant, defective in mechanotransduction, and prone to exhibit nuclear damage when a force is applied.[50, 53] Interestingly, if portions of the *LMNA* that encode for either lamin A or C are functional and either protein is fully translated, the cell exhibits mechanophenotypes that are not dramatically different from wild-type cells.[54, 55] The absence of *LMNB1* expression failed to reciprocate these results. As result, the *LMNB1* gene is not involved in mechanotransduction and, potentially, it is neither involved in mechanophenotype, as suggested by data presented in Chapter 4. Altogether, these results show the importance of proper *LMNA* gene product transcription and translation responsible for the expression of lamin A and C proteins required for establishing a healthy cellular mechanophenotype.

Besides mutations, changes in *LMNA* gene regulation, due to chemical or physical cues, can also lead to mechanophenotype changes. In the context of stem cell

differentiation, both chemical and physical cues can influence the fate stem cells towards a particular lineage. Previous studies have demonstrated that matrix stiffness alone not only influences stem cell differentiation[56] but also *LMNA* gene expression.[57] Specifically, stiff matrices cause osteogenic *RUNX2* and myogenic *MYOD* genes, as well as the *LMNA* gene, to upregulate while the contrary is observed in soft substrates. However, adipogenic genes, such as *PPARG4*, were upregulated in soft substrates. Other studies show that adding molecules that stimulate the retinoic acid (RA) or activating the *Wnt* signaling pathway can also affect *LMNA* gene expression and, subsequently, stem cell differentiation.[36, 57] Interestingly, ECM stiffness can trigger both pathways. In the case of Wnt signaling, ECM stiffness promotes recruiting integrin ß1 recruitment of focal adhesion complex and ß-catenin becomes activated and transported into the nucleus to activate Wnt pathway related genes. Another interesting finding is that treatment of cells with *LMNA* mutations in a murine model of dilated cardiomyopathy exhibited improve cardiac function after Wnt pathway agonist treatment, which also suggests that small molecules and drugs that affect signaling pathways converging in the lamin nucleocytoskeleton could be interesting therapeutic agents for laminopathies or upregulation/downregulation of lamin gene expression. Altogether, this collection of studies demonstrates that lamin A/C could be a feasible biomarker for understanding the changes in whole-cell mechanophenotype in the context of cell lineage specification, stem cell differentiation, and disease progression.

1.4 CLOSING REMARKS

The studies presented within this thesis demonstrate the use of mechanical properties and mechano-related macromolecules such as lamin A/C as biomarkers of mechanical phenotype in the context of stem cell differentiation as correlated to lineage-specific metabolite production as well as lineage differentiation preference and passaging effects (Chapters 2 and 3), cell-specific mechanophenotyping (Chapter 4), and stem cell sorting based on lamin A/C expression (Appendixes A and B). The presented studies are meant to demonstrate, via hypothesis-driven, evidence-based research, that the combination of whole-cell mechanical properties with biological molecules involved in the different scenarios of interest is a robust approach to fully understand the role of mechanical properties in tissue engineering, regenerative medicine and disease.

1.5 REFERENCES

1. Zuk, P.A., M. Zhu, P. Ashjian, D.A. De Ugarte, J.I. Huang, H. Mizuno, Z.C. Alfonso, J.K. Fraser, P. Benhaim, and M.H. Hedrick, Human adipose tissue is a source of multipotent stem cells. Mol Biol Cell. 13(12): p. 4279-95.2002

2. Aust, L., B. Devlin, S.J. Foster, Y.D. Halvorsen, K. Hicok, T. du Laney, A. Sen, G.D. Willingmyre, and J.M. Gimble, Yield of human adipose-derived adult stem cells from liposuction aspirates. Cytotherapy. 6(1): p. 7-14.2004

3. Yanez, R., M.L. Lamana, J. Garcia-Castro, I. Colmenero, M. Ramirez, and J.A. Bueren, Adipose tissue-derived mesenchymal stem cells have in vivo immunosuppressive

properties applicable for the control of the graft-versus-host disease. Stem Cells. 24(11): p. 2582-91.2006

4. Zuk, P.A., M. Zhu, H. Mizuno, J. Huang, J.W. Futrell, A.J. Katz, P. Benhaim, H.P. Lorenz, and M.H. Hedrick, Multilineage cells from human adipose tissue: Implications for cell-based therapies. Tissue Eng. 7(2): p. 211-28.2001

5. Mizuno, H., P.A. Zuk, M. Zhu, H.P. Lorenz, P. Benhaim, and M.H. Hedrick, Myogenic differentiation by human processed lipoaspirate cells. Plast Reconstr Surg. 109(1): p. 199-209; discussion 210-1.2002

6. Guilak, F., K.E. Lott, H.A. Awad, Q. Cao, K.C. Hicok, B. Fermor, and J.M. Gimble, Clonal analysis of the differentiation potential of human adipose-derived adult stem cells. J Cell Physiol. 206(1): p. 229-37.2006

7. Choi, J.H., J.M. Gimble, K. Lee, K.G. Marra, J.P. Rubin, J.J. Yoo, G. Vunjak-Novakovic, and D.L. Kaplan, Adipose tissue engineering for soft tissue regeneration. Tissue Eng Part B Rev. 16(4): p. 413-26.2010

8. Beane, O.S. and E.M. Darling, Isolation, characterization, and differentiation of stem cells for cartilage regeneration. Ann Biomed Eng. 40(10): p. 2079-97.2012

9. Mizuno, H., M. Tobita, and A.C. Uysal, Concise review: Adipose-derived stem cells as a novel tool for future regenerative medicine. Stem Cells. 30(5): p. 804-10.2012

10. Dubois, S.G., E.Z. Floyd, S. Zvonic, G. Kilroy, X. Wu, S. Carling, Y.D. Halvorsen, E. Ravussin, and J.M. Gimble, Isolation of human adipose-derived stem cells from biopsies and liposuction specimens. Methods Mol Biol. 449: p. 69-79.2008

11. Yoshimura, K., T. Shigeura, D. Matsumoto, T. Sato, Y. Takaki, E. Aiba-Kojima, K. Sato, K. Inoue, T. Nagase, I. Koshima, and K. Gonda, Characterization of freshly

isolated and cultured cells derived from the fatty and fluid portions of liposuction aspirates. J Cell Physiol. 208(1): p. 64-76.2006

12. Gronthos, S., D.M. Franklin, H.A. Leddy, P.G. Robey, R.W. Storms, and J.M. Gimble, Surface protein characterization of human adipose tissue-derived stromal cells. J Cell Physiol. 189(1): p. 54-63.2001

13. Zimmerlin, L., V.S. Donnenberg, M.E. Pfeifer, E.M. Meyer, B. Peault, J.P. Rubin, and A.D. Donnenberg, Stromal vascular progenitors in adult human adipose tissue. Cytometry A. 77(1): p. 22-30.2010

14. Bourin, P., B.A. Bunnell, L. Casteilla, M. Dominici, A.J. Katz, K.L. March, H. Redl, J.P. Rubin, K. Yoshimura, and J.M. Gimble, Stromal cells from the adipose tissue-derived stromal vascular fraction and culture expanded adipose tissue-derived stromal/stem cells: A joint statement of the international federation for adipose therapeutics and science (ifats) and the international society for cellular therapy (isct). Cytotherapy. 15(6): p. 641-8.2013

15. Yu, G., X. Wu, M.A. Dietrich, P. Polk, L.K. Scott, A.A. Ptitsyn, and J.M. Gimble, Yield and characterization of subcutaneous human adipose-derived stem cells by flow cytometric and adipogenic mrna analyzes. Cytotherapy. 12(4): p. 538-46.2010

16. Mitchell, J.B., K. McIntosh, S. Zvonic, S. Garrett, Z.E. Floyd, A. Kloster, Y. Di Halvorsen, R.W. Storms, B. Goh, G. Kilroy, X. Wu, and J.M. Gimble, Immunophenotype of human adipose-derived cells: Temporal changes in stromal-associated and stem cell-associated markers. Stem Cells. 24(2): p. 376-85.2006

17. Wall, M.E., S.H. Bernacki, and E.G. Loboa, Effects of serial passaging on the adipogenic and osteogenic differentiation potential of adipose-derived human mesenchymal stem cells. Tissue Eng. 13(6): p. 1291-8.2007

18. Estes, B.T., A.W. Wu, R.W. Storms, and F. Guilak, Extended passaging, but not aldehyde dehydrogenase activity, increases the chondrogenic potential of human adipose-derived adult stem cells. J Cell Physiol. 209(3): p. 987-95.2006

19. Darling, E.M., S. Zauscher, and F. Guilak, Viscoelastic properties of zonal articular chondrocytes measured by atomic force microscopy. Osteoarthritis Cartilage. 14(6): p. 571-9.2006

20. Darling, E.M., S. Zauscher, J.A. Block, and F. Guilak, A thin-layer model for viscoelastic, stress-relaxation testing of cells using atomic force microscopy: Do cell properties reflect metastatic potential? Biophys J. 92(5): p. 1784-91.2007

21. Darling, E.M., M. Topel, S. Zauscher, T.P. Vail, and F. Guilak, Viscoelastic properties of human mesenchymally-derived stem cells and primary osteoblasts, chondrocytes, and adipocytes. J Biomech. 41(2): p. 454-64.2008

22. Darling, E.M., P.E. Pritchett, B.A. Evans, R. Superfine, S. Zauscher, and F. Guilak, Mechanical properties and gene expression of chondrocytes on micropatterned substrates following dedifferentiation in monolayer. Cell Mol Bioeng. 2(3): p. 395-404.2009

23. Dimitriadis, E.K., F. Horkay, J. Maresca, B. Kachar, and R.S. Chadwick, Determination of elastic moduli of thin layers of soft material using the atomic force microscope. Biophys J. 82(5): p. 2798-810.2002

24. Gonzalez-Cruz, R.D., V.C. Fonseca, and E.M. Darling, Cellular mechanical properties reflect the differentiation potential of adipose-derived mesenchymal stem cells. Proc Natl Acad Sci U S A. 109(24): p. E1523-9.2012

25. Suresh, S., Biomechanics and biophysics of cancer cells. Acta Biomater. 3(4): p. 413-38.2007

26. Otto, O., P. Rosendahl, A. Mietke, S. Golfier, C. Herold, D. Klaue, S. Girardo, S. Pagliara, A. Ekpenyong, A. Jacobi, M. Wobus, N. Topfner, U.F. Keyser, J. Mansfeld, E. Fischer-Friedrich, and J. Guck, Real-time deformability cytometry: On-the-fly cell mechanical phenotyping. Nat Methods. 12(3): p. 199-202, 4 p following 202.2015

27. Titushkin, I. and M. Cho, Modulation of cellular mechanics during osteogenic differentiation of human mesenchymal stem cells. Biophys J. 93(10): p. 3693-702.2007

28. Rodriguez, J.P., M. Gonzalez, S. Rios, and V. Cambiazo, Cytoskeletal organization of human mesenchymal stem cells (msc) changes during their osteogenic differentiation. J Cell Biochem. 93(4): p. 721-31.2004

29. Grady, M.E., R.J. Composto, and D.M. Eckmann, Cell elasticity with altered cytoskeletal architectures across multiple cell types. J Mech Behav Biomed Mater. 61: p. 197-207.2016

30. Cross, S.E., Y.S. Jin, J. Rao, and J.K. Gimzewski, Nanomechanical analysis of cells from cancer patients. Nat Nanotechnol. 2(12): p. 780-3.2007

31. Takai, E., K.D. Costa, A. Shaheen, C.T. Hung, and X.E. Guo, Osteoblast elastic modulus measured by atomic force microscopy is substrate dependent. Ann Biomed Eng. 33(7): p. 963-71.2005

32. Lombardi, M.L., D.E. Jaalouk, C.M. Shanahan, B. Burke, K.J. Roux, and J. Lammerding, The interaction between nesprins and sun proteins at the nuclear envelope is critical for force transmission between the nucleus and cytoskeleton. J Biol Chem. 286(30): p. 26743-53.2011

33. Arnsdorf, E.J., P. Tummala, R.Y. Kwon, and C.R. Jacobs, Mechanically induced osteogenic differentiation--the role of rhoa, rockii and cytoskeletal dynamics. J Cell Sci. 122(Pt 4): p. 546-53.2009

34. Arnsdorf, E.J., P. Tummala, and C.R. Jacobs, Non-canonical wnt signaling and n-cadherin related beta-catenin signaling play a role in mechanically induced osteogenic cell fate. PLoS One. 4(4): p. e5388.2009

35. Du, J., X. Chen, X. Liang, G. Zhang, J. Xu, L. He, Q. Zhan, X.Q. Feng, S. Chien, and C. Yang, Integrin activation and internalization on soft ecm as a mechanism of induction of stem cell differentiation by ecm elasticity. Proc Natl Acad Sci U S A. 108(23): p. 9466-71.2011

36. Du, J., Y. Zu, J. Li, S. Du, Y. Xu, L. Zhang, L. Jiang, Z. Wang, S. Chien, and C. Yang, Extracellular matrix stiffness dictates wnt expression through integrin pathway. Sci Rep. 6: p. 20395.2016

37. Wang, N., J.P. Butler, and D.E. Ingber, Mechanotransduction across the cell surface and through the cytoskeleton. Science. 260(5111): p. 1124-7.1993

38. Wang, N., Mechanical interactions among cytoskeletal filaments. Hypertension. 32(1): p. 162-5.1998

39. Matthews, B.D., D.R. Overby, R. Mannix, and D.E. Ingber, Cellular adaptation to mechanical stress: Role of integrins, rho, cytoskeletal tension and mechanosensitive ion channels. J Cell Sci. 119(Pt 3): p. 508-18.2006

40. Stewart-Hutchinson, P.J., C.M. Hale, D. Wirtz, and D. Hodzic, Structural requirements for the assembly of linc complexes and their function in cellular mechanical stiffness. Exp Cell Res. 314(8): p. 1892-905.2008

41. Haque, F., D. Mazzeo, J.T. Patel, D.T. Smallwood, J.A. Ellis, C.M. Shanahan, and S. Shackleton, Mammalian sun protein interaction networks at the inner nuclear membrane and their role in laminopathy disease processes. J Biol Chem. 285(5): p. 3487-98.2010

42. Solovei, I., A.S. Wang, K. Thanisch, C.S. Schmidt, S. Krebs, M. Zwerger, T.V. Cohen, D. Devys, R. Foisner, L. Peichl, H. Herrmann, H. Blum, D. Engelkamp, C.L. Stewart, H. Leonhardt, and B. Joffe, Lbr and lamin a/c sequentially tether peripheral heterochromatin and inversely regulate differentiation. Cell. 152(3): p. 584-98.2013

43. Shimi, T., K. Pfleghaar, S. Kojima, C.G. Pack, I. Solovei, A.E. Goldman, S.A. Adam, D.K. Shumaker, M. Kinjo, T. Cremer, and R.D. Goldman, The a- and b-type nuclear lamin networks: Microdomains involved in chromatin organization and transcription. Genes Dev. 22(24): p. 3409-21.2008

44. Gesson, K., P. Rescheneder, M.P. Skoruppa, A. von Haeseler, T. Dechat, and R. Foisner, A-type lamins bind both hetero- and euchromatin, the latter being regulated by lamina-associated polypeptide 2 alpha. Genome Res. 26(4): p. 462-73.2016

45. Dahl, K.N., A.J. Ribeiro, and J. Lammerding, Nuclear shape, mechanics, and mechanotransduction. Circ Res. 102(11): p. 1307-18.2008

46. Osmanagic-Myers, S., T. Dechat, and R. Foisner, Lamins at the crossroads of mechanosignaling. Genes Dev. 29(3): p. 225-37.2015

47. Lin, F. and H.J. Worman, Structural organization of the human gene encoding nuclear lamin a and nuclear lamin c. J Biol Chem. 268(22): p. 16321-6.1993

48. Ostlund, C., G. Bonne, K. Schwartz, and H.J. Worman, Properties of lamin a mutants found in emery-dreifuss muscular dystrophy, cardiomyopathy and dunnigan-type partial lipodystrophy. J Cell Sci. 114(Pt 24): p. 4435-45.2001

49. Worman, H.J., Nuclear lamins and laminopathies. J Pathol. 226(2): p. 316-25.2012

50. Lammerding, J., P.C. Schulze, T. Takahashi, S. Kozlov, T. Sullivan, R.D. Kamm, C.L. Stewart, and R.T. Lee, Lamin a/c deficiency causes defective nuclear mechanics and mechanotransduction. J Clin Invest. 113(3): p. 370-8.2004

51. Scaffidi, P. and T. Misteli, Lamin a-dependent misregulation of adult stem cells associated with accelerated ageing. Nat Cell Biol. 10(4): p. 452-9.2008

52. Verstraeten, V.L., J.Y. Ji, K.S. Cummings, R.T. Lee, and J. Lammerding, Increased mechanosensitivity and nuclear stiffness in hutchinson-gilford progeria cells: Effects of farnesyltransferase inhibitors. Aging Cell. 7(3): p. 383-93.2008

53. Lammerding, J. and R.T. Lee, The nuclear membrane and mechanotransduction: Impaired nuclear mechanics and mechanotransduction in lamin a/c deficient cells. Novartis Found Symp. 264: p. 264-73; discussion 273-8.2005

54. Lammerding, J., L.G. Fong, J.Y. Ji, K. Reue, C.L. Stewart, S.G. Young, and R.T. Lee, Lamins a and c but not lamin b1 regulate nuclear mechanics. J Biol Chem. 281(35): p. 25768-80.2006

55. Fong, L.G., J.K. Ng, J. Lammerding, T.A. Vickers, M. Meta, N. Cote, B. Gavino, X. Qiao, S.Y. Chang, S.R. Young, S.H. Yang, C.L. Stewart, R.T. Lee, C.F. Bennett, M.O. Bergo, and S.G. Young, Prelamin a and lamin a appear to be dispensable in the nuclear lamina. J Clin Invest. 116(3): p. 743-52.2006

56. Engler, A.J., S. Sen, H.L. Sweeney, and D.E. Discher, Matrix elasticity directs stem cell lineage specification. Cell. 126(4): p. 677-89.2006

57. Swift, J., I.L. Ivanovska, A. Buxboim, T. Harada, P.C. Dingal, J. Pinter, J.D. Pajerowski, K.R. Spinler, J.W. Shin, M. Tewari, F. Rehfeldt, D.W. Speicher, and D.E. Discher, Nuclear lamin-a scales with tissue stiffness and enhances matrix-directed differentiation. Science. 341(6149): p. 1240104.2013

CHAPTER 2

Cellular mechanical properties reflect differentiation potential of adipose-derived mesenchymal stem cells

Published in: Proc Natl Acad Sci U S A. 2012 Jun 12;109(24):E1523-9. doi: 10.1073/pnas.1120349109.

Rafael D. González-Cruz[a,b], Vera C. Fonseca[a,b], and Eric M. Darling[a,b,c,d,1]

[a]Department of Molecular Pharmacology, Physiology, and Biotechnology, [b]Center for Biomedical Engineering,[c] Department of Orthopaedics, and [d]School of Engineering, Brown University, Providence, RI, USA 02912.

2.1 ABSTRACT

The mechanical properties of adipose-derived stem cell (ASC) clones correlate with their ability to produce tissue-specific metabolites, a finding that has dramatic implications for cell-based regenerative therapies. Autologous ASCs are an attractive cell source due to their immunogenicity and multipotent characteristics. However, for practical applications ASCs must first be purified from other cell types, a critical step that has proven difficult using surface-marker approaches. Alternative enrichment strategies identifying broad categories of tissue-specific cells are necessary for translational applications. One possibility developed in our lab uses single-cell mechanical properties as predictive biomarkers of ASC clonal differentiation capability. Elastic and viscoelastic properties of undifferentiated ASCs were tested via atomic force microscopy and correlated with lineage-specific metabolite production. Cell sorting simulations based on these "mechanical biomarkers" indicated they were predictive of differentiation capability and could be used to enrich for tissue-specific cells, which if implemented could dramatically improve the quality of regenerated tissues.

2.2 INTRODUCTION

Adipose tissue contains a heterogeneous population of mesenchymal stem cells (MSCs) known as adipose-derived stem cells (ASCs). ASCs are capable of differentiating into a variety of lineage-specific cell types, including adipocytes, osteoblasts, and chondrocytes.[1-3] In comparison to MSCs derived from other tissues, ASCs are simple to isolate and available in large quantities.[4, 5] Because of the cells' mesodermal origin, ASCs have been used for many soft tissue and orthopaedic applications.[6-11] Unfortunately, ASC isolation is confounded by the lack of distinct and universally effective MSC biomarkers. Adipose tissue contains multiple cell types, including mature adipocytes, fibroblasts, smooth muscle cells, and endothelial cells[9], which can contaminate the stromal fraction collected during ASC isolation. While conventional methods such as flow cytometry can isolate stem cells using surface antigen expression[1, 2, 12], resulting cell yields are often less than 1%.[13, 14] Furthermore, the surface antigens present on ASCs can also be found on other cell types in adipose tissue, complicating the isolation of pure mesenchymal stem cell populations.[15-17] Collectively, these limitations suggest a need for alternative biomarkers that allow for ASC enrichment based on lineage potential.

Recently, single-cell mechanical properties were found to be akin to gene and protein expressions, capable of distinguishing differences in cellular subpopulations, disease state, and tissue sources.[18-22] Cells display varying levels of resistance to deformation (elasticity) and flow (viscosity) in response to an applied force. This behavior depends on the composition and organization of subcellular structures,

particularly the cytoskeleton. Previous studies describe the use of atomic force microscopy (AFM) to discriminate between elastic/viscous properties of MSCs and differentiated cells. From this work, a common set of parameters has been identified that act as mechanical biomarkers suitable for comparing among distinct cell types. These biomarkers describe the deformation response of a cell and include the elastic modulus ($E_{elastic}$), instantaneous modulus (E_0), relaxed modulus (E_R), apparent viscosity (μ), and cell size/height. These parameters are obtained by modeling the cell as a standard linear solid and acquiring data from indentation and stress relaxation tests.[21] In brief, $E_{elastic}$ represents the compliancy of the cell during a simple indentation test, E_0 and E_R are the initial and final moduli, respectively, during a stress relaxation test, and the apparent viscosity is a descriptor of how the cell deforms over time (see *Supplementary Information* Text for more detail). It is hypothesized that ASC mechanical biomarkers can be used to indicate not only cell type but also predict tissue-specific differentiation potential for stem cells. The goal of this study was to investigate the relationship between the mechanical properties of ASCs and their lineage differentiation capabilities. Specifically, 32 single-cell-derived clonal populations were established using ASCs harvested from human, subcutaneous fat. Cellular elastic and viscoelastic properties for each clonal population were determined via AFM by testing individual cells. Clones were then assessed for differentiation potential along adipogenic, osteogenic, and chondrogenic lineages. Correlations were determined between individual mechanical parameters and metabolite production, and simulations were used to determine potential tissue-specific enrichment for mechanical property-based sorting approaches.

2.3 MATERIALS AND METHODS

2.3.1 ASC Isolation and Clonal Population Expansion

Primary ASCs (Zen-Bio) were isolated from subcutaneous adipose tissue from healthy, nondiabetic, nonsmoking female donors aged 29–57 y ($N = 7$) and having an average body mass index (BMI) of 27.6 kg/m^2. ASC clonal populations were derived using the limiting dilution cloning method. Passage 2 (P2) ASCs were suspended in conditioned expansion medium[23], diluted to 1 cell/200 μL, and placed into thirty 96-well plates over three sessions. Conditioned expansion medium contained DMEM/F-12 (Lonza), 10% FBS (Zen-Bio), 5 ng/mL epidermal growth factor, 0.25 ng/mL transforming growth factor-beta 1 (TGF-β1), 1 ng/mL basic fibroblastic growth factor (R&D Systems), 100 U/mL penicillin, 100 μg/mL streptomycin, and 0.25 μg/mL amphotericin B, pen/strep/ampB (Invitrogen). Only wells with a single cell were kept to establish true clonal populations. At 90% confluence, clones were transferred to T-75 flasks (P3). At P4, cells were trypsinized, frozen, and kept in liquid nitrogen. Before mechanical and biochemical tests, clones were thawed and passaged once more (to P5).

2.3.2 Adipogenic and Osteogenic Differentiation

ASC clones ($n = 32$) were plated onto 96-well plates at a density of 8,000 cells/well and cultured with expansion medium until confluent. Medium was then replaced with 200 μL of adipogenic induction medium, osteogenic induction medium, or control medium ($n = 6$, 6, and 12, respectively).[23], Adipogenic medium contained DMEM/F-12, 3% FBS, 10 μg/mL insulin, 0.39 μg/mL dexamethasone, 55.6 μg/mL

isobutyl-1-methylxanthine (Sigma-Aldrich), 17.5 μg/mL indomethacin (Cayman Chemical), and pen/strep/ampB. Osteogenic medium contained DMEM/F-12, 10% FBS, 2.16 mg/mL β-glycerophosphate (10 mM), 50 μg/mL μascorbate-2-phosphate, 3.92 ng/mL dexamethasone, (Sigma-Aldrich), and pen/strep/ampB. Control medium contained DMEM/F-12, 10% FBS, and pen/strep/ampB. Cells were cultured for three weeks and then fixed in 3.7% paraformaldehyde [24]. Oil Red O (ORO, Sigma-Aldrich) staining was used to assess lipid accumulation in adipogenic and control samples. Alizarin Red S (ARS, Sigma-Aldrich) staining was used to assess calcified matrix deposition in osteogenic and control samples. After digital images were taken, ORO and ARS dyes were eluted from each sample, and optical densities were measured at 500 nm and 540 nm, respectively.[23], At this point, each well was stained with 4′,6-diamino-2-phenylindole (DAPI, Thermo Fisher Scientific), and optical densities were normalized on a per-cell basis.[25]

2.3.3 Chondrogenic Differentiation

ASC clones were placed in V-bottomed, 96-well plates at a density of 50,000 cells/well. Plates were centrifuged at 400 g to form cell pellets, and expansion medium was replaced with 200 μL of chondrogenic induction medium ($n = 6$) or control medium ($n = 6$).[23, 26] Chondrogenic medium contained high glucose Dulbecco's Modified Eagle Medium (DMEM), 10% FBS, 10 ng/mL TGF-β1, 50 μg/mL ascorbate-2-phosphate, 39.0 ng/mL dexamethasone, 1% ITS+ Premix (BD Biosciences), and pen/strep/ampB. Cell pellets were maintained in culture for three weeks. For analysis, half of the pellets [chondrogenic ($n = 3$) and control ($n = 3$)] were fixed in 3.7%

paraformaldehyde. The remaining pellets were digested with papain (Sigma-Aldrich). Fixed pellets were cryosectioned and immunostained using a Histostain-Plus Kit (Invitrogen) and a primary antibody specific to type II collagen (II-II6B3-s, Developmental Studies Hybridoma Bank). The papain-digested pellets were used to quantify sGAG content via the dimethylmethylene blue assay (Accurate Chem. and Sci. Corp.). The PicoGreen assay (Invitrogen) was used to quantify DNA amounts (480 nm excitation, 520 nm emission). For sGAG quantification, optical densities were measured at 595 nm. A standard curve was used to calculate total sGAG amounts in each pellet, which were then normalized on a per-DNA basis.

2.3.4 AFM Single-Cell Mechanical Testing

The mechanical properties of individual ASCs were measured using an atomic force microscope (MFP-3D-BIO, Asylum Research) using previously established techniques.[18, 20, 21] Additional explanation of the mechanical testing procedure can be found in the *Supplementary Information*. Briefly, spherically tipped cantilevers (5 μm diameter, $k \sim 0.03$ N/m, Novascan Technologies, Inc.) were used for indentation and stress relaxation experiments. Individual cells were mechanically tested using a single indentation/stress relaxation test over the perinuclear region of the cell. An approach velocity of 15 μm/s was used, followed by a 30 s relaxation period. Cells adhered on glass substrates were tested in spherical (n = 12–28 cells) and spread (n = 19–25 cells) morphologies. Spherical cell shapes were achieved by allowing ASCs to attach for approximately 30 min. Cells within a clonal population were then tested sequentially, with the entire session lasting less than 1.5 h. After 24 h, cells spread sufficiently to

exhibit flattened morphologies. Both cell shapes were confirmed visually prior to mechanical testing using phase contrast microscopy (Fig. S1). Cells attached to the glass substrate via adsorbed proteins from the culture medium, which was consistent across all clones. Specific ligand binding was not characterized in this study but could influence measured mechanical properties.[27, 28] During testing, indentation depths were maximized for spherical and spread morphologies (1.2 ± 0.3 μm and 0.43 ± 0.09 μm, respectively) but never exceeded 10% strain. The elastic modulus, $E_{elastic}$, was extracted from force (F) vs. indentation (δ) data using a modified Hertz model (Eq. 1)[20], where R is the relative radius of the tip, and v is the Poisson's ratio, assumed to be 0.5 for an incompressible material.[29] Parametric studies showed that varying v from 0.3 to 0.5 altered the measured properties by less than 20%. The parameters E_R, E_0, and μ (relaxed modulus, instantaneous modulus, and apparent viscosity) were determined using a thin-layer, stress relaxation model of a viscoelastic solid (Eq. 2-4)[20], where τ_σ and τ_ε are the relaxation times under constant load and deformation, respectively. C is a thin-layer correction factor relating indentation depth, tip radius, and sample thickness.[29]

$$F(\delta) = \frac{4R^{1/2}E_{elastic}}{3(1-\nu^2)}\delta^{3/2}C \quad \text{(Eq. 1)}$$

$$F(t) = \frac{4R^{1/2}\delta^{3/2}E_R}{3(1-\nu)}\left(1+\frac{\tau_\sigma-\tau_\varepsilon}{\tau_\varepsilon}e^{-t/\tau_\varepsilon}\right)C \quad \text{(Eq. 2)}$$

$$E_0 = E_R\left(1+\frac{\tau_\sigma-\tau_\varepsilon}{\tau_\varepsilon}\right) \quad \text{(Eq. 3)}$$

$$\mu = E_R\left(\tau_\sigma-\tau_\varepsilon\right) \quad \text{(Eq. 4)}$$

$$\mu = E_R(\tau_\sigma-\tau_\varepsilon)$$

Limitations to the testing approach included a likely overestimation of elastic moduli due to a relatively fast indentation velocity (i.e., fluid pressurization contributed to the measured modulus) and an underestimation of instantaneous moduli due to an

imperfect fit of the model to the initial drop during stress relaxation. However, testing procedures were identical for all cells, which allows for valid comparisons among clones in this study.

2.3.5 Cell Sorting Simulations

A basic sorting simulation was used to assess the potential enrichment of the investigated clonal populations using lineage-appropriate mechanical biomarkers. Analysis of the mechanical properties associated with the top quartile of clones for each of the adipogenic, osteogenic, and chondrogenic lineages identified single parameters that could potentially be used for sorting (Fig.4 *A*; adipogenesis, height; osteogenesis, E_R; chondrogenesis, μ). More sophisticated approaches that take into account all measured properties are possible through clustering or neural network techniques.[30] The sorting simulations involved a very basic assessment of which clonal populations would be kept if a threshold mechanical property level was set (Fig. 4 *C*–*E*). For example, keeping only clones with $E_R > 150$ Pa would result in 100% osteogenic differentiation potential in the resultant population. By moving the bar up to 200 Pa, all undiscarded clones would exhibit high osteogenic potential (Fig.4 *B*).

2.3.6 Statistical Analysis

Data collected from clonal populations ($n = 32$) were subjected to a Shapiro-Wilk normality test. Non-normally distributed mechanical properties were log-transformed before statistical analyses. Results for bar graphs and tables are presented as geometric mean ± SD. Differentiation potential data were normally distributed and are presented as arithmetic mean ± SD. *P*-values between differentiated and undifferentiated controls for

each clone were calculated using two-tailed, unpaired student's *t*-tests ($\alpha = 0.05$). To investigate correlations between mechanical properties and differentiation potential, Pearson correlation coefficients (r) were calculated from log-transformed data. Correlation coefficients are expressed as $r \pm 95\%$ confidence intervals. Statistical significance was achieved if $P < 0.05$. All statistical tests were performed using IBM SPSS 19 software (IBM).

2.4 RESULTS

2.4.1 Mechanical properties of ASCs are heterogeneous

Single-cell mechanical properties were measured using AFM for 32 ASC clonal populations. Cells were assessed in both spherical and spread morphologies by testing samples soon after seeding (approximately 30 min) or after one day. For both morphologies, cells were firmly attached to the underlying glass substrate during testing (Fig. S1). Clones exhibited substantial heterogeneity in their mean elastic and viscoelastic properties (Fig. 1; Fig. S2). When compared to spread ASCs, spherical cells were significantly more compliant, taller, and less viscous (Table 1). These expected results are associated with differences in cytoskeletal organization between spherical and spread morphologies. Regardless of cell shape, elastic and viscoelastic data fit well to Hertzian-based mathematical models ($R^2_{elastic} = 0.99$, $R^2_{viscoelastic} = 0.87$).

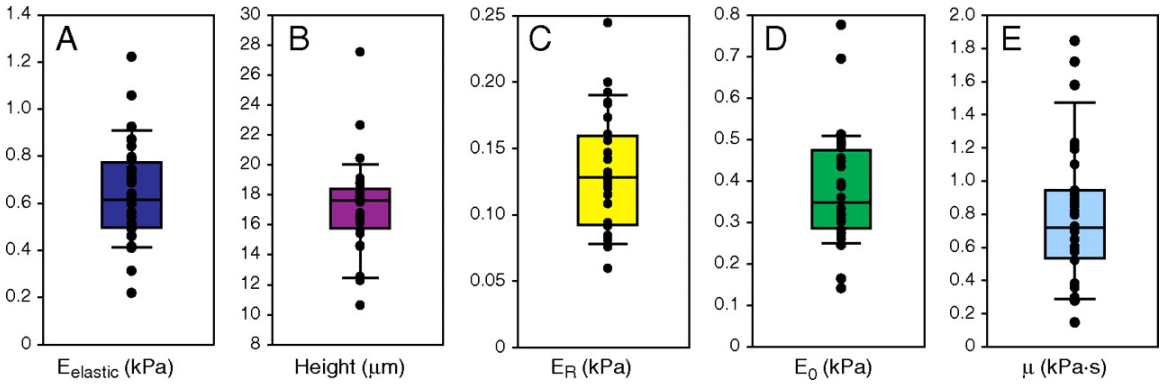

Figure 1: Mechanical heterogeneity of ASC subpopulations (**A-E**). Elastic and viscoelastic properties of thirty-two ASC clonal populations with spherical morphologies were measured by using AFM indentation and stress relaxation tests, respectively. Within each clonal population, at least 22 cells were tested. The following cellular mechanical properties were measured: elastic moduli (**A**), instantaneous moduli (**B**), relaxed moduli (**C**), apparent viscosities (**D**), and cell heights (**E**). Elastic and viscoelastic data fit well to Hertzian mathematical models ($R^2 = 0.99$ and $R^2 = 0.87$, respectively). Data presented as geometric mean ± SD.

Table 1: Summary of cellular mechanical properties for ASC clonal populations

Morphology	$E_{elastic}$ (kPa)	E_0 (kPa)	E_R (kPa)	μ_{app} (kPa•s)	Height (μm)
Spherical	0.6±0.2	0.4±0.1	0.1±0.04	0.7±0.4	16.9±3.1
Spread	1.6±0.5	1.1±0.3	0.6±0.2	2.6±1.6	4.6±0.5

Cellular mechanical properties are indicated by the following abbreviations: $E_{elastic}$ (elastic modulus), E_{equil} (equilibrium modulus), E_0 (instantaneous modulus), E_R (relaxed modulus), μ (apparent viscosity), and *Height* (cell height). Tabular data is presented as geometric means ± SD. Student's *t* tests between spherical and spread ASCs demonstrated significant differences between morphologies for all comparisons ($P < 0.001$).

2.4.2 Differentiation potential of ASC clonal populations

All ASC clonal populations were assessed for multipotentiality by differentiation along the adipogenic, osteogenic, and chondrogenic lineages (Fig. 2). Standard biochemical assays were used to quantify lineage-specific metabolite production on a per-cell or per-DNA basis. For each biochemical analysis, clones were arranged in ascendant order of lineage-specific metabolite production (Fig. 3). Positive differentiation was noted for samples that exhibited metabolite production above the 90th percentile of corresponding controls cultured in noninduction medium. Overall, 44% of clones were tripotent, 47% were bipotent, and 9% were unipotent. No clones showed a total lack of differentiation capability. For each lineage, significant differences in metabolite production existed between differentiated and undifferentiated ASCs. Oil Red O optical densities for clones in adipogenic conditions were significantly greater than those of undifferentiated controls ($P < 0.001$). Of all clones tested, 69% exhibited positive adipogenic differentiation. Alizarin Red S optical densities for clones in osteogenic

conditions were also significantly greater than those of undifferentiated controls ($P < 0.001$). Of all clones tested, 75% exhibited osteogenic differentiation potential.

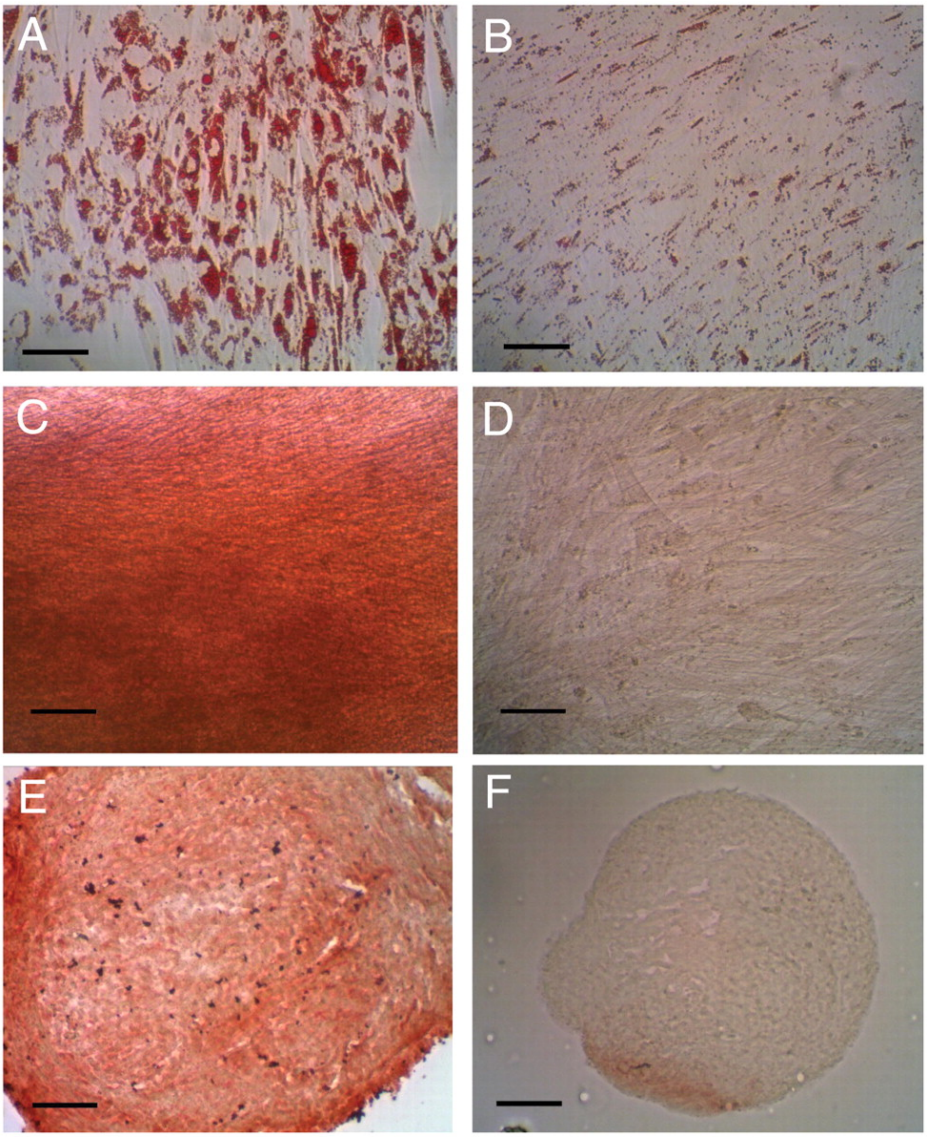

Figure 2: Confirmation of ASC differentiation towards mesodermal lineages via lineage-specific metabolite detection assays (**A-H**). Adipogenic differentiation was assessed by Oil Red O staining of intracellular lipid production in induced (**A**) and control (**B**) samples. Osteogenic differentiation was assessed by Alizarin Red S staining of calcium deposits in induced (**C**) and control (**D**) samples. Chondrogenic differentiation was assessed by type II collagen immunostaining in induced (**E**) and control (**F**) samples. Image magnification was 20X, and scale bars are 100 μm.

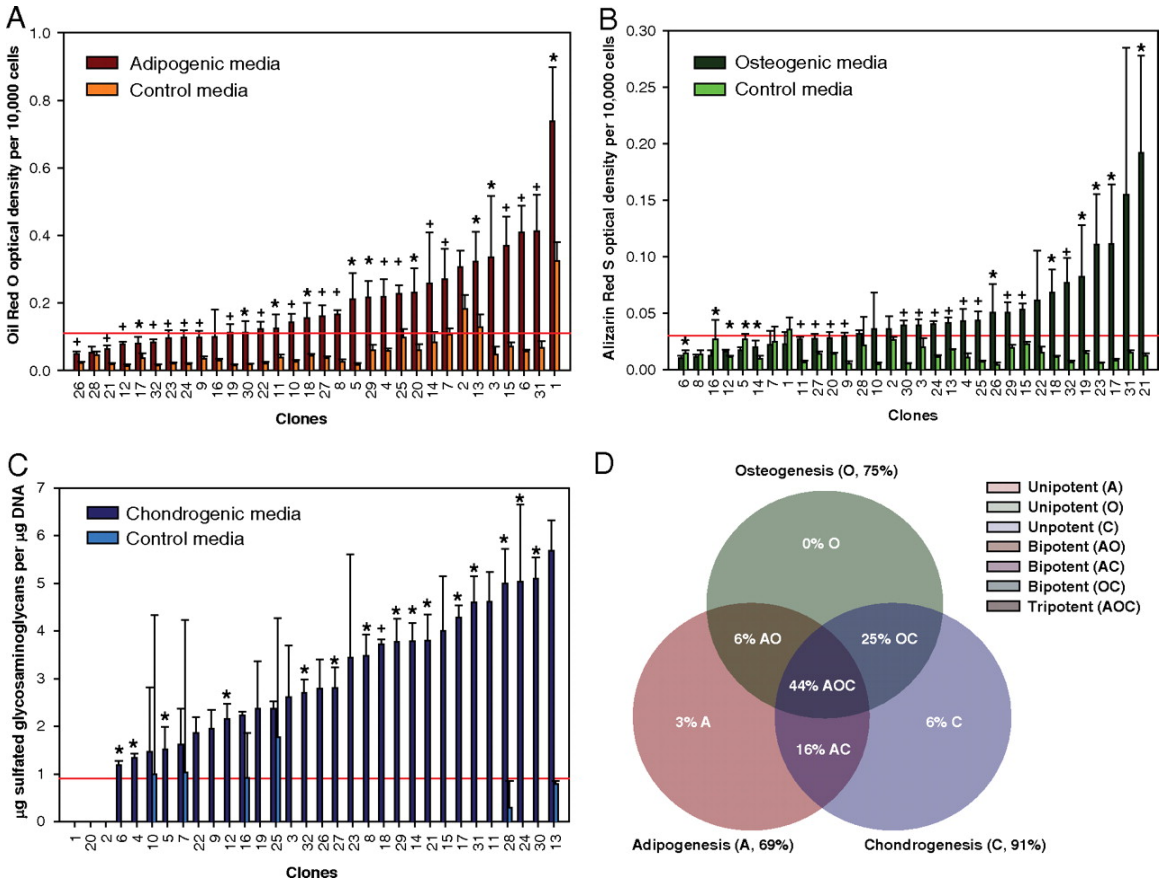

Figure 3: Adipogenic, osteogenic, and chondrogenic assessment of ASC clonal populations via lineage-specific metabolite quantification. Amounts of lineage-specific metabolites were determined by clone for adipogenesis (**A**), osteogenesis (**B**), and chondrogenesis (**C**). Each differentiation lineage showed extensive variability in metabolite production, emphasizing heterogeneity among the clonal populations. For each graph, the red line represents the 90th percentile associated with undifferentiated controls. This level acted a threshold value indicating positive or negative differentiation. Results were used to determine the multipotentiality of clones involved in this study (**D**). Data are presented as arithmetic means ± SD. Single asterisks denote statistical significance at a = 0.05 whereas plus signs denote statistical significance at a = 0.001 from corresponding controls.

The hypothesis that cellular mechanical biomarkers can be used as predictors of ASC differentiation potential was examined by determining correlations between ASC mechanical properties and lineage-specific metabolite production. Significant correlations existed for spherical cellular mechanical properties and the three lineages examined

(Table 2; Fig. S3), supporting the stated hypothesis and suggesting a novel means of classifying undifferentiated ASCs into tissue-specific groups.

Table 2: Correlations between ASC mechanical properties and their differentiation potential

Mechanical Property (MP)	Lineage	Pearson's r (±95% CI)	*p*-value	Normalized metabolite Production/MP x 10^3
$E_{elastic}$	Adipogenic	-0.51±0.27	0.003	-1.14
	Osteogenic	0.46±0.28	0.007	1.66
	Chondrogenic	0.59±0.24	0.004	0.71
E_0	Adipogenic	-0.50±0.27	0.003	-1.57
	Osteogenic	0.54±0.68	0.001	3.33
	Chondrogenic	0.60±0.23	0.0003	1.09
E_R	Adipogenic	-0.49±0.27	0.005	-5.54
	Osteogenic	0.48±0.28	0.005	10.44
	Chondrogenic	0.31±0.32	0.08	0.26
μ_{app}	Adipogenic	-0.27±0.33	0.14	-0.36
	Osteogenic	0.25±0.33	0.16	0.28
	Chondrogenic	0.56±0.25	0.0008	0.57
Height	Adipogenic	0.41±0.30	0.02	104.37
	Osteogenic	0.04±0.35	0.83	-8.05
	Chondrogenic	0.07±0.35	0.72	18.12

Cellular mechanical properties are indicated by the following abbreviations: $E_{elastic}$ (elastic modulus), E_0 (instantaneous modulus), E_R (relaxed modulus), μ (apparent viscosity) and Height (cell height). Error values for Pearson's correlation coefficient *r* represent ninety-five percent confidence intervals (95% C.I.). Correlations were calculated using log-transformed geometric means. To allow for comparisons among lineages, metabolite data were normalized to their respective, lineage-specific arithmetic mean and then fit with a linear regression. The slopes of these fits represent lineage-specific metabolite production per mechanical property (MP) measured as specified by the lineage. Adipogenic, osteogenic, and chondrogenic characteristic metabolites are intracellular lipids, extracellular matrix-bound calcium, and sulfated glycosaminoglycans, respectively. The mechanical property relationship to osteogenic potential showed steep, positive slopes (stiffer = more osteogenic) whereas adipogenic potential showed negative slopes (softer = adipogenic).

Analyses showed that adipogenesis was positively correlated with cell height and negatively correlated with E_{elastic}, E_R, and E_0. Osteogenesis was positively correlated with E_{elastic}, E_R, and E_0. Chondrogenesis was positively correlated with E_{elastic} and μ. The relative magnitude of the relationships was assessed by comparing slopes calculated from linear fits of normalized metabolite production per mechanical parameter. Generally, the osteogenic lineage was associated with steeper, positive slopes, followed by the chondrogenic lineage with shallower, positive slopes, and the adipogenic lineage with negative slopes. This relationship was reversed with respect to cell height. Surprisingly, no significant correlations were found using the mechanical properties of spread ASCs (Table S1). This finding might be expected based on previous reports that stem cells exhibit consistent mechanical properties when firmly attached compared to the suspended state.[31] Additionally, no discernible relationship existed between the mechanical properties of clones and uni/bi/tri-lineage potency states (Table S2; Fig. S4).

According to the current findings, these mechanical biomarkers could be used to sort ASCs into mechanically similar groups that correspond to specific lineages. Although lineage-specific metabolite production varied among clones, a subset could be considered high-potential populations. These groups of clones were defined as the top quartile of all populations examined, based on lineage-specific metabolite production, and are proposed as highly desirable, ASC subpopulations. The mechanical biomarkers for these clones showed distinct differences from the other populations (Fig. 4A). Highly osteogenic clones exhibited significantly higher E_{elastic}, E_R, and E_0 values ($P < 0.05$, $P < 0.001$, and $P < 0.01$, respectively). Highly chondrogenic clones showed

significantly higher μ values ($P < 0.05$). While not statistically significant, highly adipogenic clones were generally larger ($P = 0.09$) and more compliant ($P = 0.11$) than other clones.

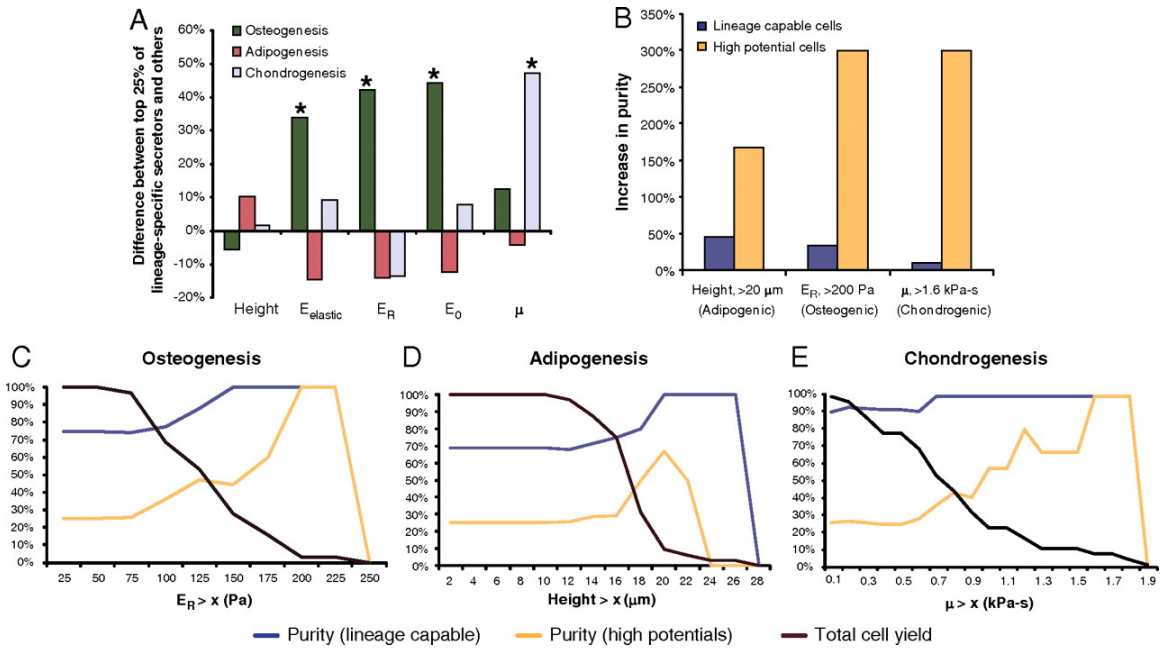

Figure 4: **Sorting simulations using pre-determined mechanical biomarker parameters for lineage-specific enrichment (A-E).** Mechanical and biochemical data were used to determine whether tissue-specific subpopulations might exist. Clones exhibiting high differentiation potential for certain lineages exhibited distinct mechanical properties (**A**). Simulations using these pre-determined mechanical biomarkers as sorting parameters showed that it would be possible to enrich for ASCs possessing lineage-specific differentiation potentials (**B**). However, higher cell purities were balanced by lower cell yields (**C-E**). Data in (**A**) and (**B**) are presented as geometric mean percentages. Single asterisks denote statistical significance at a = 0.05 between the upper 25% and lower 75% of clonal populations for each lineage.

2.4.3 Sorting simulations

Sorting simulations based on these mechanical parameters demonstrated the degree of lineage-specific enrichment possible using only cellular mechanical properties (Fig. 4B). Threshold values were determined for adipogenesis, osteogenesis, and chondrogenesis by assessing the effect of cell height, E_R, and μ, respectively, on population descriptors such

as lineage-capable purity, high potential purity, and overall cell yield (Fig. 4 *C–E*). Results showed that as progressively stricter sorting parameters were used, lineage-specific clone purity increased while cell yield decreased. High-potential populations typically were the larger (adipogenesis), stiffer (osteogenesis), or more viscous (chondrogenesis) clones, and therefore could be enriched simply by raising the corresponding threshold sorting parameters. For example, if only clones greater than 20 μm in cell height were collected, purity of adipogenic-positive clones was increased by 45%. Furthermore, the purity of highly adipogenic clones increased by 170%. Osteogenic clones could be enriched by selecting cells with $E_R > 0.2$ kPa, which resulted in a 33% increase in osteogenic-positive clones and a 300% increase in highly osteogenic clones. Chondrogenic clones could be selected using $\mu > 1.6$ kPa·s, resulting in a 10% increase in chondrogenic-positive cells and a 300% increase in highly chondrogenic clones. Total cell yield for these three cases would be 9%, 3%, and 6%, respectively, a substantial improvement over many antigen-based sorting schemes that result in < 1% yields.

2.5 DISCUSSION

The results of this study indicate that cellular mechanical properties are predictive of ASC differentiation and synthetic potential. Significant correlations existed between mechanical properties and lineage-specific metabolite production by ASC clones. These findings represent an advantageous means to characterize the differentiation potential of stem cells. Surface antigen-based enrichment techniques have had limited success identifying a stem cell biomarker useful for sorting ASCs.[32] High specificity is an advantage for many applications but is nonideal for targeting ASC subpopulations exhibiting variable phenotypes (e.g., multipotency, bipotency, or unipotency). Mechanical properties act as an indicator of the biochemical and structural characteristics of a cell and hold promise as a composite biomarker capable of identifying beneficial ASC subpopulations.

The observed heterogeneity in mechanical properties across clones and between morphologies can be attributed to variations in intracellular composition and organization. Previously, it was shown that differentiated cells and stem cells differ in their elastic and viscoelastic properties.[18] As stem cells differentiate toward specific lineages, their cytoskeleton rearranges until differentiation is achieved.[33-36] During this process, rearrangement is concurrent with a modulation of the cellular mechanical properties and any accumulation of intracellular metabolites. For osteogenesis, cells typically become stiffer, whereas for adipogenesis, cells become more compliant. Chondrogenesis induces intracellular changes that result in higher instantaneous and

relaxed moduli as well as higher apparent viscosities. These physical changes can occur to varying degrees before irreversible commitment to a single lineage. However, it is hypothesized that an ASC exhibits a mechanical phenotype associated with its preferred lineage, possibly because it has already begun the differentiation process.[34] This possibility is not an impediment to practical application, though, because the purpose of tissue-specific enrichment is to collect all cells capable of expressing the proper phenotype whether they are initially multipotent, unipotent, or fully differentiated.

ASC differentiation potentials showed that all clonal populations could differentiate along at least one lineage, while 91% of all clones could successfully differentiate along at least two lineages. Previous ASC clonal studies reported differentiation efficiencies well below the ones found here.[1, 23] However, differences in isolation and expansion approaches could account for this variation. The current study used the limiting dilution technique to establish single-cell clones, and only clones capable of doubling 20–25 times were evaluated. Furthermore, initial ASCs had already been passaged twice, whereas previous studies typically began with freshly isolated cells. This period of in vitro expansion could bias the cells slightly toward a more differentiation-prone state. Also, freshly isolated ASCs can be contaminated with other cell types present in adipose tissue. The presence of these contaminating cells can affect ASC differentiation potential.[37, 38] For example, if fibroblasts make up a significant portion of the harvest population, then overall osteogenic potential could be significantly reduced. Extended culture of undifferentiated ASCs can also affect ultimate differentiation potential. Specifically, monolayer expansion, under the conditions used in

the current study, was previously shown to increase the chondrogenic potential of ASCs prior to differentiation.[3, 39] Therefore, environmental conditioning could have been influential in the noticeably higher percentage of chondrogenic-positive clones found in this study.

As has been reported previously, adipose tissue contains ASC subpopulations with distinct differentiation potentials.[12, 15, 40-42] Surface antigen expression has been used to detect subpopulations capable of lineage-specific differentiation. However, this technique produces low cell yields and requires antibody conjugation, which may affect cellular function.[43] There are also concerns regarding ASC purity in these subpopulations because other cells, such as endothelial cells and fibroblasts, are found in the stromal fraction of adipose tissue and share surface antigens with ASCs.[15, 42] However, their mechanical properties are distinct from those measured for stem cells.[18, 44] Another level of complexity arises when discriminating between cells exhibiting the same surface markers but at different expression levels. The importance of this variation has yet to be investigated. In contrast to these surface antigen approaches, mechanical biomarkers function as a broad indicator of differentiation potential and require no modification of or invasion into individual cells.

Limitations do exist to using mechanical biomarkers for stem cell sorting approaches. Most of these arise from the challenge inherent in rapidly evaluating large cell numbers, which currently is a major advantage of flow cytometery. While AFM is an established technique for accurately measuring cellular elastic and viscoelastic properties,

testing the mechanical characteristics of a clinically relevant quantity of ASCs using this technique would be infeasible. Microfluidics-based approaches like cell deformation cytometry, size and physical characteristic sorting, and optical stretchers represent viable solutions to this limitation because of their high-throughput capabilities.[31, 45-47] It should be noted that the properties measured in the current study, which were for cells attached to a substrate, are unlikely to translate directly to cells in a fully suspended state. Previous, matched comparisons of AFM to micropipette aspiration results showed that measured modulus values were similar but apparent viscosities were much higher for fully suspended cells.[21] The current findings will need to be validated for implementation in a given sorting device, but many of the observed mechanical property differences should be apparent regardless of approach. Ultimately, the specific parameters used to identify targeted cell populations are irrelevant. The device needs only to distinguish among the deformation responses of individual cells and then group them accordingly.

2.6 CONCLUSION

The current study uses a small number of clones that are assumed to be representative of a larger, ASC population. If true, the relationship between mechanical properties and lineage-specific differentiation can be exploited to isolate cells capable of secreting large amounts of matrix molecules, which are critical for rapid tissue regeneration. The current findings are supported by previous reports of mechanical differences between undifferentiated stem cells and fully differentiated osteoblasts, adipocytes, and chondrocytes.[18, 33-35, 48] It remains to be seen whether this mechanical

biomarker-lineage relationship can be investigated on a larger scale, as well as whether it will improve functional tissue growth compared to using unsorted populations. Regardless, the results presented here present an intriguing role for the mechanical properties of undifferentiated stem cells. In summary, this study supports the hypothesis that ASC mechanical properties are indicative of differentiation potential. Furthermore, ASCs capable of producing high levels of lineage-specific metabolites were found to be mechanically distinct from other clones and could be a target for cellular enrichment. Simulations using the current data indicated that mechanical biomarker-based sorting would produce significant increases in cell purity. Future studies can build on these findings by targeting mechanically similar subpopulations that are well suited for tissue-specific regeneration.

2.7 ACKNOWLEDGEMENTS

We thank Dr. Farshid Guilak for providing resources to establish the clonal populations, as well as Poston Pritchett and Ghansham "Chris" Ramkhellawan for technical assistance and Jason Machan for advice on statistical analyses. This work was supported by National Institutes of Health (NIH) Grants from the National Institute of Arthritis and Musculoskeletal and Skin Diseases (NIAMS, AR054673) and National Institute of General Medical Sciences (NIGMS, GM104937). The contents of this publication are solely the responsibility of the authors and do not necessarily represent the official views of the NIAMS, NIGMS, or NIH.

2.8 AUTHOR CONTRIBUTIONS

EMD and VCF designed the experiments. EMD characterized the mechanical properties of all 32 clonal populations. VCF conducted all ASC differentiation experiments. RDGC and VCF imaged all differentiation experiments. RDGC and EMD analyzed all the data and wrote the manuscript. The authors declare no conflict of interest.

2.10 REFERENCES

1. Zuk, P.A., M. Zhu, H. Mizuno, J. Huang, J.W. Futrell, A.J. Katz, P. Benhaim, H.P. Lorenz, and M.H. Hedrick, Multilineage cells from human adipose tissue: Implications for cell-based therapies. Tissue Eng. 7[49]: p. 211-28.2001

2. Zuk, P.A., M. Zhu, P. Ashjian, D.A. De Ugarte, J.I. Huang, H. Mizuno, Z.C. Alfonso, J.K. Fraser, P. Benhaim, and M.H. Hedrick, Human adipose tissue is a source of multipotent stem cells. Mol Biol Cell. 13(12): p. 4279-95.2002

3. Estes, B.T., B.O. Diekman, and F. Guilak, Monolayer cell expansion conditions affect the chondrogenic potential of adipose-derived stem cells. Biotechnol Bioeng. 99(4): p. 986-95.2008

4. Katz, A.J., R. Llull, M.H. Hedrick, and J.W. Futrell, Emerging approaches to the tissue engineering of fat. Clin Plast Surg. 26(4): p. 587-603, viii.1999

5. Aust, L., B. Devlin, S.J. Foster, Y.D. Halvorsen, K. Hicok, T. du Laney, A. Sen, G.D. Willingmyre, and J.M. Gimble, Yield of human adipose-derived adult stem cells from liposuction aspirates. Cytotherapy. 6(1): p. 7-14.2004

6. Conejero, J.A., J.A. Lee, B.M. Parrett, M. Terry, K. Wear-Maggitti, R.T. Grant, and A.S. Breitbart, Repair of palatal bone defects using osteogenically differentiated fat-derived stem cells. Plast Reconstr Surg. 117(3): p. 857-63.2006

7. Cowan, C.M., Y.Y. Shi, O.O. Aalami, Y.F. Chou, C. Mari, R. Thomas, N. Quarto, C.H. Contag, B. Wu, and M.T. Longaker, Adipose-derived adult stromal cells heal critical-size mouse calvarial defects. Nat Biotechnol. 22(5): p. 560-7.2004

8. Jeon, O., J.W. Rhie, I.K. Kwon, J.H. Kim, B.S. Kim, and S.H. Lee, In vivo bone formation following transplantation of human adipose-derived stromal cells that are not differentiated osteogenically. Tissue Eng Part A. 14(8): p. 1285-94.2008

9. Yoshimura, K., T. Shigeura, D. Matsumoto, T. Sato, Y. Takaki, E. Aiba-Kojima, K. Sato, K. Inoue, T. Nagase, I. Koshima, and K. Gonda, Characterization of freshly isolated and cultured cells derived from the fatty and fluid portions of liposuction aspirates. J Cell Physiol. 208(1): p. 64-76.2006

10. Yoshimura, K., K. Sato, N. Aoi, M. Kurita, T. Hirohi, and K. Harii, Cell-assisted lipotransfer for cosmetic breast augmentation: Supportive use of adipose-derived stem/stromal cells. Aesthetic Plast Surg. 32(1): p. 48-55; discussion 56-7.2008

11. Yoshimura, K., Y. Asano, N. Aoi, M. Kurita, Y. Oshima, K. Sato, K. Inoue, H. Suga, H. Eto, H. Kato, and K. Harii, Progenitor-enriched adipose tissue transplantation as rescue for breast implant complications. Breast J. 16[49]: p. 169-75.2010

12. Rada, T., R.L. Reis, and M.E. Gomes, Distinct stem cells subpopulations isolated from human adipose tissue exhibit different chondrogenic and osteogenic differentiation potential. Stem Cell Rev. 7(1): p. 64-76.2011

13. Gronthos, S., D.M. Franklin, H.A. Leddy, P.G. Robey, R.W. Storms, and J.M. Gimble, Surface protein characterization of human adipose tissue-derived stromal cells. J Cell Physiol. 189(1): p. 54-63.2001

14. Jones, E.A., S.E. Kinsey, A. English, R.A. Jones, L. Straszynski, D.M. Meredith, A.F. Markham, A. Jack, P. Emery, and D. McGonagle, Isolation and characterization of bone marrow multipotential mesenchymal progenitor cells. Arthritis Rheum. 46(12): p. 3349-60.2002

15. Zannettino, A.C., S. Paton, A. Arthur, F. Khor, S. Itescu, J.M. Gimble, and S. Gronthos, Multipotential human adipose-derived stromal stem cells exhibit a perivascular phenotype in vitro and in vivo. J Cell Physiol. 214[49]: p. 413-21.2008

16. Alt, E., Y. Yan, S. Gehmert, Y.H. Song, A. Altman, D. Vykoukal, and X. Bai, Fibroblasts share mesenchymal phenotypes with stem cells, but lack their differentiation and colony-forming potential. Biol Cell. 103(4): p. 197-208.2011

17. Mitchell, J.B., K. McIntosh, S. Zvonic, S. Garrett, Z.E. Floyd, A. Kloster, Y. Di Halvorsen, R.W. Storms, B. Goh, G. Kilroy, X. Wu, and J.M. Gimble, Immunophenotype of human adipose-derived cells: Temporal changes in stromal-associated and stem cell-associated markers. Stem Cells. 24[49]: p. 376-85.2006

18. Darling, E.M., M. Topel, S. Zauscher, T.P. Vail, and F. Guilak, Viscoelastic properties of human mesenchymally-derived stem cells and primary osteoblasts, chondrocytes, and adipocytes. J Biomech. 41[49]: p. 454-64.2008

19. Darling, E.M., P.E. Pritchett, B.A. Evans, R. Superfine, S. Zauscher, and F. Guilak, Mechanical properties and gene expression of chondrocytes on micropatterned

substrates following dedifferentiation in monolayer. Cell Mol Bioeng. 2(3): p. 395-404.2009

20. Darling, E.M., S. Zauscher, J.A. Block, and F. Guilak, A thin-layer model for viscoelastic, stress-relaxation testing of cells using atomic force microscopy: Do cell properties reflect metastatic potential? Biophys J. 92(5): p. 1784-91.2007

21. Darling, E.M., S. Zauscher, and F. Guilak, Viscoelastic properties of zonal articular chondrocytes measured by atomic force microscopy. Osteoarthritis Cartilage. 14(6): p. 571-9.2006

22. Suresh, S., Biomechanics and biophysics of cancer cells. Acta Biomater. 3(4): p. 413-38.2007

23. Guilak, F., K.E. Lott, H.A. Awad, Q. Cao, K.C. Hicok, B. Fermor, and J.M. Gimble, Clonal analysis of the differentiation potential of human adipose-derived adult stem cells. J Cell Physiol. 206(1): p. 229-37.2006

24. Tapp, H., R. Deepe, J.A. Ingram, M. Kuremsky, E.N. Hanley, Jr., and H.E. Gruber, Adipose-derived mesenchymal stem cells from the sand rat: Transforming growth factor beta and 3d co-culture with human disc cells stimulate proteoglycan and collagen type i rich extracellular matrix. Arthritis Res Ther. 10(4): p. R89.2008

25. Carpenter, A.E., T.R. Jones, M.R. Lamprecht, C. Clarke, I.H. Kang, O. Friman, D.A. Guertin, J.H. Chang, R.A. Lindquist, J. Moffat, P. Golland, and D.M. Sabatini, Cellprofiler: Image analysis software for identifying and quantifying cell phenotypes. Genome Biol. 7(10): p. R100.2006

26. Estes, B.T., B.O. Diekman, J.M. Gimble, and F. Guilak, Isolation of adipose-derived stem cells and their induction to a chondrogenic phenotype. Nat Protoc. 5(7): p. 1294-311.2010

27. Gilchrist, C.L., E.M. Darling, J. Chen, and L.A. Setton, Extracellular matrix ligand and stiffness modulate immature nucleus pulposus cell-cell interactions. PLoS One. 6(11): p. e27170.2011

28. Takai, E., K.D. Costa, A. Shaheen, C.T. Hung, and X.E. Guo, Osteoblast elastic modulus measured by atomic force microscopy is substrate dependent. Ann Biomed Eng. 33(7): p. 963-71.2005

29. Dimitriadis, E.K., F. Horkay, J. Maresca, B. Kachar, and R.S. Chadwick, Determination of elastic moduli of thin layers of soft material using the atomic force microscope. Biophys J. 82(5): p. 2798-810.2002

30. Darling, E.M. and F. Guilak, A neural network model for cell classification based on single-cell biomechanical properties. Tissue Eng Part A. 14(9): p. 1507-15.2008

31. Maloney, J.M., D. Nikova, F. Lautenschlager, E. Clarke, R. Langer, J. Guck, and K.J. Van Vliet, Mesenchymal stem cell mechanics from the attached to the suspended state. Biophys J. 99(8): p. 2479-87.2010

32. Tuan, R.S., G. Boland, and R. Tuli, Adult mesenchymal stem cells and cell-based tissue engineering. Arthritis Res Ther. 5(1): p. 32-45.2003

33. Yourek, G., M.A. Hussain, and J.J. Mao, Cytoskeletal changes of mesenchymal stem cells during differentiation. ASAIO J. 53[49]: p. 219-28.2007

34. Yu, H., C.Y. Tay, W.S. Leong, S.C. Tan, K. Liao, and L.P. Tan, Mechanical behavior of human mesenchymal stem cells during adipogenic and osteogenic differentiation. Biochem Biophys Res Commun. 393(1): p. 150-5.2010

35. Titushkin, I. and M. Cho, Modulation of cellular mechanics during osteogenic differentiation of human mesenchymal stem cells. Biophys J. 93(10): p. 3693-702.2007

36. Ofek, G., V.P. Willard, E.J. Koay, J.C. Hu, P. Lin, and K.A. Athanasiou, Mechanical characterization of differentiated human embryonic stem cells. J Biomech Eng. 131(6): p. 061011.2009

37. Lennon, D.P., S.E. Haynesworth, D.M. Arm, M.A. Baber, and A.I. Caplan, Dilution of human mesenchymal stem cells with dermal fibroblasts and the effects on in vitro and in vivo osteochondrogenesis. Dev Dyn. 219(1): p. 50-62.2000

38. Peptan, I.A., L. Hong, and J.J. Mao, Comparison of osteogenic potentials of visceral and subcutaneous adipose-derived cells of rabbits. Plast Reconstr Surg. 117(5): p. 1462-70.2006

39. Estes, B.T., A.W. Wu, R.W. Storms, and F. Guilak, Extended passaging, but not aldehyde dehydrogenase activity, increases the chondrogenic potential of human adipose-derived adult stem cells. J Cell Physiol. 209(3): p. 987-95.2006

40. Sengenes, C., K. Lolmede, A. Zakaroff-Girard, R. Busse, and A. Bouloumie, Preadipocytes in the human subcutaneous adipose tissue display distinct features from the adult mesenchymal and hematopoietic stem cells. J Cell Physiol. 205(1): p. 114-22.2005

41. Zimmerlin, L., V.S. Donnenberg, M.E. Pfeifer, E.M. Meyer, B. Peault, J.P. Rubin, and A.D. Donnenberg, Stromal vascular progenitors in adult human adipose tissue. Cytometry A. 77(1): p. 22-30.2010

42. Rada, T., T.C. Santos, A.P. Marques, V.M. Correlo, A.M. Frias, A.G. Castro, N.M. Neves, M.E. Gomes, and R.L. Reis, Osteogenic differentiation of two distinct subpopulations of human adipose-derived stem cells: An in vitro and in vivo study. J Tissue Eng Regen Med.2011

43. Trickett, A. and Y.L. Kwan, T cell stimulation and expansion using anti-cd3/cd28 beads. J Immunol Methods. 275(1-2): p. 251-5.2003

44. Kuznetsova, T.G., M.N. Starodubtseva, N.I. Yegorenkov, S.A. Chizhik, and R.I. Zhdanov, Atomic force microscopy probing of cell elasticity. Micron. 38(8): p. 824-33.2007

45. Rosenbluth, M.J., W.A. Lam, and D.A. Fletcher, Analyzing cell mechanics in hematologic diseases with microfluidic biophysical flow cytometry. Lab Chip. 8(7): p. 1062-70.2008

46. Sraj, I., C.D. Eggleton, R. Jimenez, E. Hoover, J. Squier, J. Chichester, and D.W. Marr, Cell deformation cytometry using diode-bar optical stretchers. J Biomed Opt. 15(4): p. 047010.2010

47. Gossett, D.R., W.M. Weaver, A.J. Mach, S.C. Hur, H.T. Tse, W. Lee, H. Amini, and D. Di Carlo, Label-free cell separation and sorting in microfluidic systems. Anal Bioanal Chem. 397(8): p. 3249-67.2010

48. Tan, S.C., W.X. Pan, G. Ma, N. Cai, K.W. Leong, and K. Liao, Viscoelastic behaviour of human mesenchymal stem cells. BMC Cell Biol. 9: p. 40.2008

2.10 SUPPLEMENTARY INFORMATION (SI)

SI Text: Basic Theory for the Mechanical Tests Associated with the Study

Cells display varying levels of resistance to deformation (elasticity) and flow (viscosity) in response to an applied force. This dual mechanical behavior, known as viscoelasticity, is dependent on the composition and organization of subcellular structures, particularly the cytoskeleton. Assuming a cell behaves as an elastic material, its resistance to deformation is linearly proportional to the applied stress but inversely proportional to the resulting strain. This resistance to deformation is measured experimentally as the elastic modulus ($E_{elastic}$). Elastic materials with high elastic moduli are considered stiff because an increase in applied stress results in a negligible increase in their strain. Compliant elastic materials, though, have low elastic moduli because small increases in applied stress result in substantial deformation. Moreover, elastic materials subjected to a constant stress exhibit a constant strain and recover their original shape completely after the stress is removed. However, cells are viscoelastic materials and exhibit both elastic and viscous properties. Specifically, when a viscoelastic material is kept at a constant strain, the applied stress decreases over time, a phenomenon called stress relaxation. In stress relaxation, the viscoelastic properties of a material can be described by its instantaneous and relaxed moduli. The instantaneous modulus (E_0) is the resistance to deformation measured before the relaxation begins, whereas the relaxed modulus (E_R) is the stiffness of the material at complete equilibrium. The material's apparent viscosity (μ_{app}) is determined by the resistance to flow upon the application of a

stress. These mechanical properties, which can be extracted from experimental data using appropriate mathematical models, have emerged as biomarkers that are useful for discriminating among the elastic and viscoelastic properties of multiple cell types, including MSCs and differentiated cells**.**

SI Figures

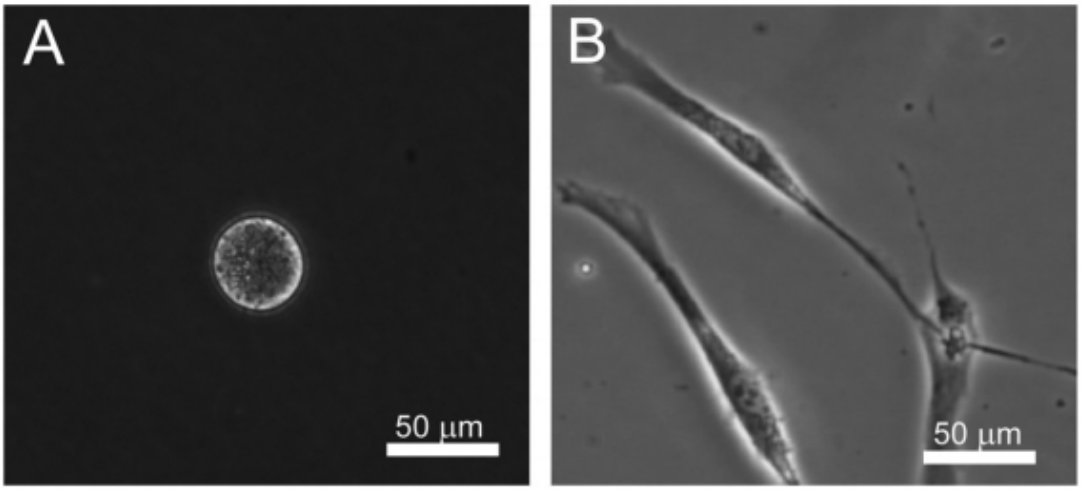

Figure S1. Morphology of spherical and spread adipose-derived stem cells (ASCs) using phase contrast imaging. P5 ASCs plated for 0.5–1.5 h on a glass substrate exhibit a rounded cell shape (A). After 24 h, ASCs spread extensively and exhibited a flattened morphology (B). Single indentation and relaxation tests were conducted over the center of the cell or the nucleus, respectively. (Scale bars, 50 μm).

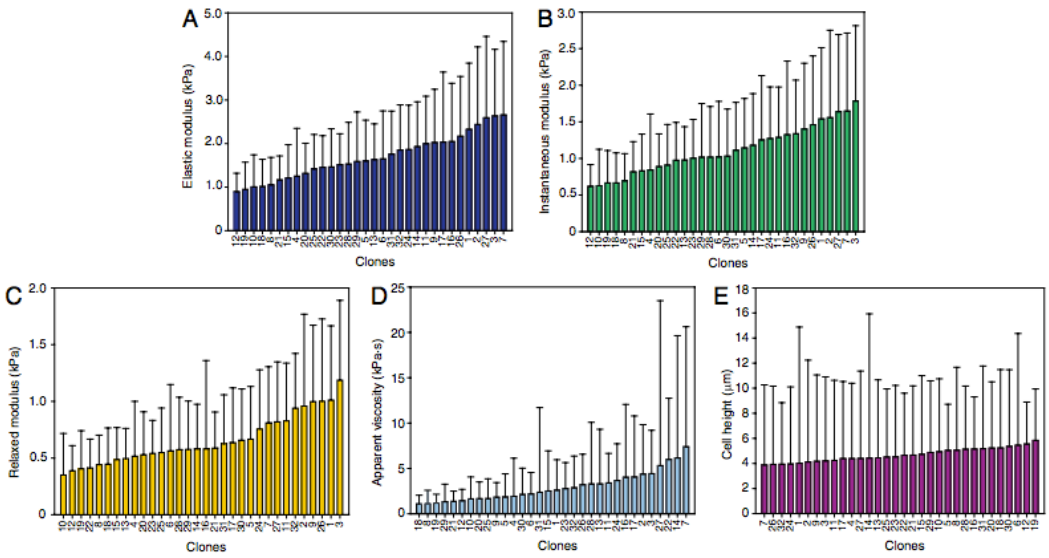

Figure S2. Mechanical properties of ASC subpopulations for the spread morphology also exhibited heterogeneity. Elastic and viscoelastic properties of 32 ASC clonal populations with spread morphologies were measured by using atomic force microscopy (AFM) indentation and stress relaxation tests, respectively. Within each clonal population, an average of 23 cells was tested via AFM. Measured mechanical properties included elastic modulus (A), instantaneous modulus (B), relaxed modulus (C), apparent viscosity (D), and cell height (E). As for the spherical morphology, elastic and viscoelastic data were fit well with Hertzian mathematical models (R^2 = 0.99 and R^2 = 0.88, respectively). Data is presented as geometric mean ± standard deviation.

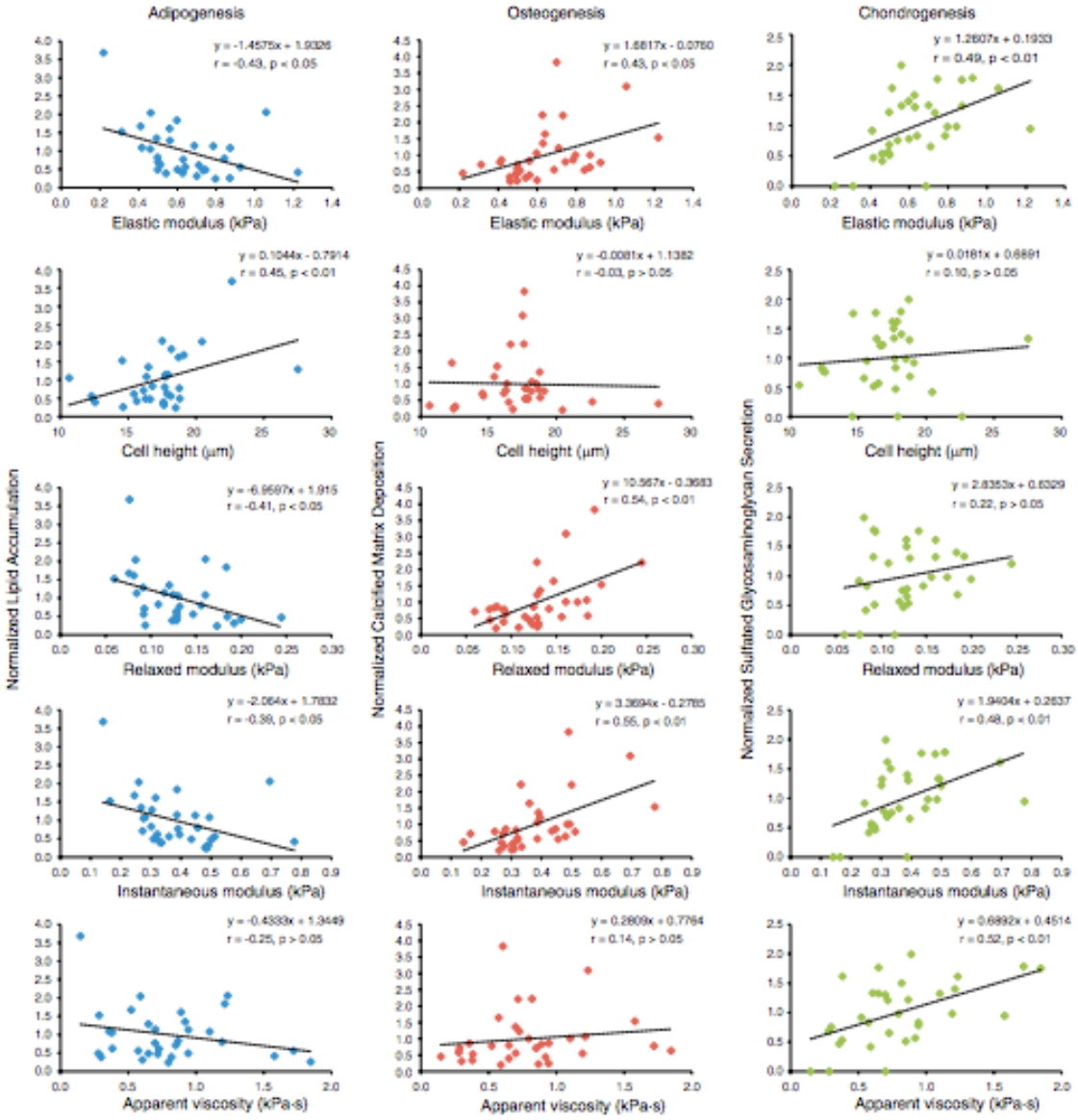

Figure S3. Cellular mechanical properties correlated with the differentiation potential of ASCs across adipogenic, osteogenic, and chondrogenic lineages. The mechanical properties of 32 ASC clonal populations were characterized via AFM. These data were then correlated with their differentiation potential toward adipogenic (blue dots, left column), osteogenic (red dots, central column), and chondrogenic (green dots, right column) lineages. In all clonal populations, differentiation along the three lineages was assessed via biochemical assays that quantified lipid accumulation, extracellular matrix calcium deposition, and sulfated glycosaminoglycan secretion, respectively. For presentation purposes, biochemical data were normalized to the geometric mean of all clones for each lineage. Pearson's correlation coefficient, r, indicated the correlation between each mechanical property and the normalized metabolite production for all clonal populations. Statistical significance was present if $P < 0.05$.

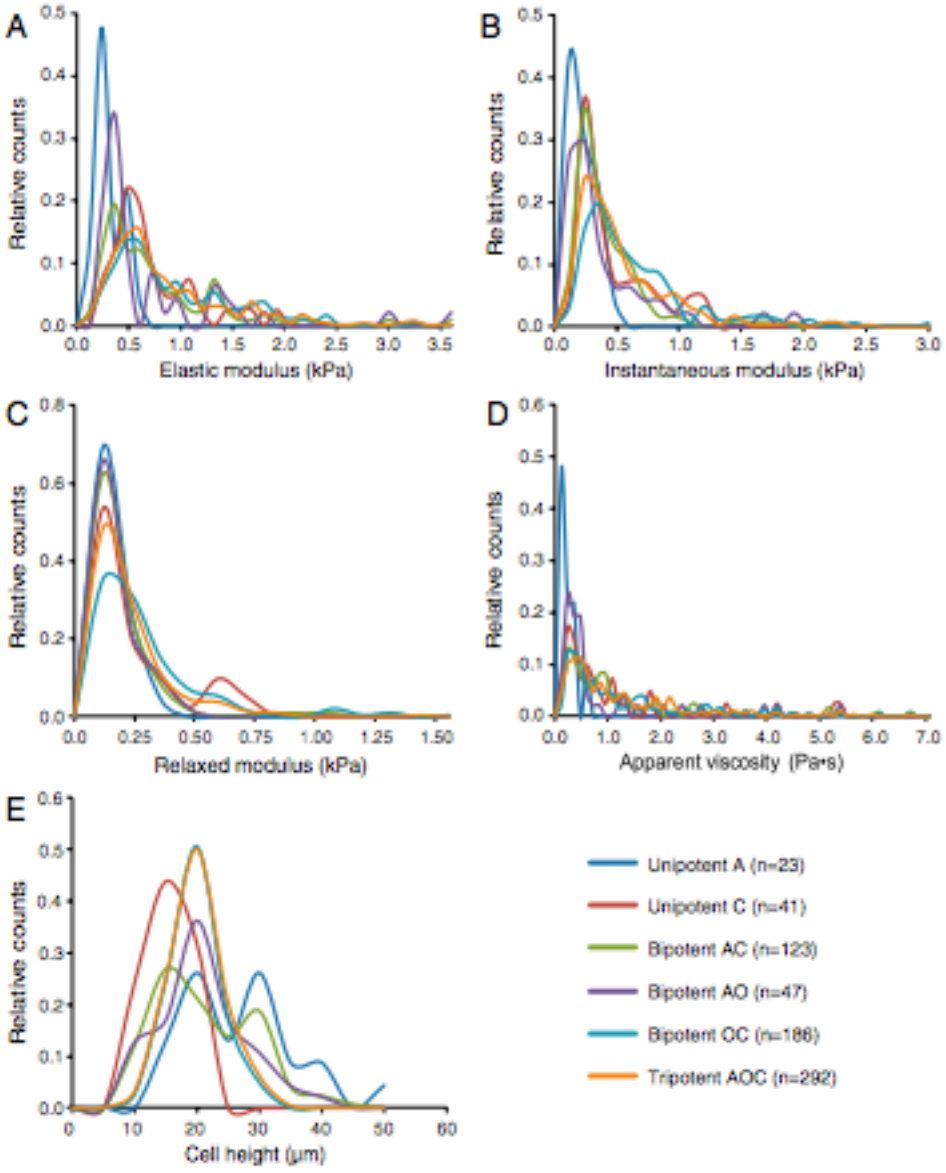

Figure S4. Mechanical property distributions for ASC clonal populations (spherical morphology) showed that no clear relationship existed with respect to potency. Broadly overlapping distributions were seen for $E_{elastic}$ (A), E_0 (B), E_R (C), μ_{app} (D), and cell height (E). Distributions were normalized to total cell numbers within each potency group. Note that sample sizes for the different potencies are highly variable, lessening the universal reliability of these distributions. For example, the Unipotent A distribution (dark blue line) includes 23 cells from a single, qualifying clone. The Unipotent C distribution (red line) includes 41 cells from two qualifying clones. Contrast those with the Tripotent AOC distribution (orange line), which includes 292 cells from 14 qualifying clones. See Table S2 for numerical data.

Table S2: Summary of mechanical properties for spherical and spread ASCs from clonal populations

Morphology	$E_{elastic}$ (kPa)	E_0 (kPa)	E_R (kPa)	μ_{app} (kPa-s)	Height (μm)
Spherical	0.6±0.2	0.4±0.1	0.1±0.04	0.7±0.4	16.9±3.1
Spread	1.6±0.5	1.1±0.3	0.6±0.2	2.6±1.6	4.6±0.5

Cellular mechanical properties are indicated by the following abbreviations: $E_{elastic}$ (elastic modulus), E_{equil} (equilibrium modulus), E_0 (instantaneous modulus), E_R (relaxed modulus), μ_{app} (apparent viscosity), and *Height* (cell height). Tabular data is presented as geometric means ± standard deviation. Student's *t* tests between spherical and spread ASCs demonstrated significant differences between morphologies for all comparisons ($p < 0.001$).

Table S2: Ranges of mechanical properties for spherical clones based on their differentiation potential

			$E_{elastic}$ (kPa)		E_0 (kPa)		E_R (kPa)	
Clone Potency	**Clones**	**Cells**	Average	Range	Average	Range	Average	Range
Unipotent (A)	1	23	0.2±0.1	0.1-0.6	0.2±0.1	0.1-0.4	0.1±0.1	0.0-0.2
Unipotent (Ch)	2	41	0.6±0.4	0.2-1.9	0.4±0.3	0.1-1.2	0.2±0.2	0.0-0.7
Bipotent (AC)	6	137	0.6±0.5	0.1-2.7	0.4±0.3	0.1-1.7	0.1±0.1	0.0-1.0
Bipotent (AO)	2	47	0.6±0.7	0.1-3.6	0.3±0.4	0.1-1.8	0.1±0.1	0.0-0.4
Bipotent (OC)	8	186	0.9±0.6	0.1-4.1	0.6±0.5	0.1-3.2	0.2±0.2	0.0-1.4
Tripotent (AOC)	13	278	0.8±0.8	0.1-8.1	0.5±0.5	0.1-3.7	0.2±0.2	0.0-1.3

			μ_{app} (kPa·s)		Cell height (μm)	
Clone Potency	**Clones**	**Cells**	Average	Range	Average	Range
Unipotent (A)	1	23	0.2±0.1	0.1-0.6	24.4±9.6	10.2-49.2
Unipotent (Ch)	2	41	1.1±1.6	0.1±7.6	12.9±3.3	7.3±19.7
Bipotent (AC)	6	137	1.1±1.3	0.0-6.7	18.7±7.6	5.9-40.6
Bipotent (AO)	2	47	0.8±1.1	0.1-5.3	18.3±6.8	5.4-37.6
Bipotent (OC)	8	186	1.3±1.5	0.1-9.7	17.2±3.9	8.4-28.4
Tripotent (AOC)	13	278	1.3±1.6	0.0-12.0	17.5±4.4	6.7-32.0

CHAPTER 3

Mechanophenotype changes of ASCs as a function of passage number: a small study

Published in: Adipocyte, 2013 Apr 1;2:87-91. doi: 10.4161/adip.23015.

Rafael D. González-Cruz[a,b], and Eric M. Darling[a,b,c,d]

[a]Department of Molecular Pharmacology, Physiology, and Biotechnology, [b]Center for Biomedical Engineering, [c]Department of Orthopaedics, and [d]School of Engineering, Brown University, Providence, RI, USA 02912.

3.1 ABSTRACT

Adipose-derived stem cells (ASCs) show great promise for tissue engineering applications and cell-based therapies because of their multipotency, relative abundance and immunosuppressive properties. However, ASCs must be isolated from heterogeneous cell populations present in adipose tissue. In this brief report, we provide a concise summary of the history and use of cellular mechanical properties as novel, label-free biomarkers to predict the differentiation potential of ASCs toward adipogenic, osteogenic and chondrogenic lineages. Additionally, we have found that passage number influences the mechanical properties of ASCs along with a discussion of potential environmental factors that could affect these properties. Altogether, this report provides evidence for the reliability of cellular mechanical properties as biomarkers for ASC differentiation potential and outlines how they can be used to sort ASCs with lineage-specific preferences for particular applications.

3.2 INTRODUCTION

Despite the abundance of MSCs in adipose tissue when compared with other tissues of mesodermal origin, current isolation techniques such as FACS still yield very low cell numbers. As a result, purified ASC populations must be expanded in vitro until they reach a population size that is feasible for clinical applications. However, previous studies suggest that the time cells spend in culture could affect their phenotype and, subsequently, their differentiation potential.[1, 2] In one study that used FACS to sort ASCs, cell surface marker expression changed as a function of passage number.[1] Immediately after being isolated, ASCs exhibited high expression levels of CD34, a stem cell-associated marker. However, CD34 expression decreased drastically after only one passage. Similarly, expression levels of hematopoietic marker CD45, initially low in freshly isolated cells, further decreased and became negligible soon after ASCs were expanded.[3] On the other hand, the expression of surface markers such as CD49d, CD73 and CD90, which are expressed at moderate levels in freshly isolated cells, increased dramatically as ASCs were expanded in vitro.[1, 4]Altogether, these studies suggest that current ASC expansion conditions effectively enrich for multipotent stem cells of mesenchymal origin.

Additionally, other studies reported that the expression of other surface markers like CD44 and CD73, which are highly expressed in chondrocytes and osteoblasts, increased dramatically in expanded ASCs. These results suggest that ASC surface marker expression resembled that of chondrocytes and osteoblasts as their passage number

increased. Separate studies, focusing on changes in ASC differentiation potential as a function of passage number, also reported striking differences between the adipogenic, chondrogenic and osteogenic potential of ASCs at different passages.[2, 5, 6] Specifically, results indicated that ASC adipogenic potential was enhanced at early passages (P2-P5) but decreased at later passages. Conversely, ASC chondrogenic and osteogenic potential increased at later passages. Altogether, these results strongly indicate that the time ASCs spend in culture during their expansion strongly influences their fate.

The previous work shown in Chapter 2 investigated the mechanical properties and differentiation potential of ASCs at a specific passage number (P5). In this Chapter, the mechanical properties of undifferentiated ASCs were examined as a function of passage time, which in this thesis, refers to resuspending nearly confluent monolayer cultures and dividing them into subsets to continue their in vitro expansion. Subsequent experiments investigated how ASC mechanical properties change over time in culture.

3.3 METHODS

3.3.1 Mechanical testing of serially passaged ASCs

The mechanical properties of P3, P4 and P5 ASCs were measured using AFM, as described previously.[7] We tested a minimum of 18 cells per passage. Statistical significance between the mechanical properties from P3, P4 and P5 ASCs was determined by one-factor ANOVA with Fisher's LSD post-hoc test ($p < 0.05$).

3.4 RESULTS

3.4.1 Mechanophenotype of ASCs changes with passage number

We examined ASC elastic and viscoelastic properties at P3–P5 to determine the extent of any changes, as well as their potential impact on cell sorting approaches. Results indicated that the mechanical properties of spherical ASCs differ significantly by passage number (Table 1). Specifically, P3 ASCs were more compliant and less viscous than P4 and P5 ASCs. Increased passage resulted in a less compliant phenotype.

Table 1: Mechanical properties of serially passaged ASCs

Passage	$E_{elastic}$ (Pa)	E_R (Pa)	μ_{app} (Pa•s)	Cell height (μm)
P3	345 ± 150	61 ± 33	321 ± 278	12.8 ± 4.8
P4	884 ± 497	86 ± 69	734 ± 636	15.6 ± 3.7
P5	800 ± 511	292 ± 254	1690 ± 1899	8.9 ± 3.7

The mechanical properties of P3, P4 and P5 ASCs were measured using AFM, as described previously.[7] We tested a minimum of 18 cells per passage. Statistical significance between the mechanical properties from P3, P4 and P5 ASCs was determined by one-factor ANOVA with Fisher's LSD post-hoc test ($p < 0.05$). Differences in $E_{elastic}$ and E_0 were significant between P3 and P4, but not P5, ASCs. However, differences in E_{equil}, E_R and cell height were not significant between P3 and P4 ASCs but were significant between those passage groups and P5 ASCs. μ_{app} increased with passage number, and the observed differences across all passages were significant. Data are shown as arithmetic mean ± standard deviation.

3.5 DISCUSSION

These findings suggest that the amount of time ASCs are exposed to environmental signals in their culture environment could be strongly affecting their mechanical properties and their differentiation potential as well. During their expansion,

ASCs are adhered to a rigid plastic substrate and surrounded by a specialized media cocktail composed of nutrients and soluble growth factors. These two environmental stimuli, substrate rigidity and bioactive molecules, are known to play a role in the differentiation potential of MSCs, including ASCs. Previous studies in which MSCs were cultured on substrates that mimicked tissue-specific elasticity showed that substrate compliance could direct stem cell differentiation.[8] Regarding the effects of passage number on ASC differentiation potential, previous studies show that ASCs expanded in monolayer cultures, but in the presence of chondrogenic-inducing soluble factors like bone morphogenic protein 6, enhanced ASC chondrogenic potential.[9] Interestingly, culturing and passaging mature chondrocytes in these two-dimensional conditions leads to their dedifferentiation, which occurs concomitantly with an increase in the cells' viscoelastic moduli.[10] However, the phenotype of these dedifferentiated chondrocytes can be partially rescued if they are re-seeded on a micropatterned, two-dimensional substrate that imparts the cells with a round morphology.[11]

3.6 CONCLUSION

In the end, passage number is an important factor in predicating stem cell fate because it is associated with how long ASCs are exposed to chemical and mechanical signals, which not only elicit biological changes, but also mechanical property changes.

3.7 ACKNOWLEDGEMENTS

The authors thank Hetal V. Desai for providing insightful advice. This work was supported in part by National Institutes of Health grants AR054673 and GM104937.

3.8 REFERENCES

1. Mitchell, J.B., K. McIntosh, S. Zvonic, S. Garrett, Z.E. Floyd, A. Kloster, Y. Di Halvorsen, R.W. Storms, B. Goh, G. Kilroy, X. Wu, and J.M. Gimble, Immunophenotype of human adipose-derived cells: Temporal changes in stromal-associated and stem cell-associated markers. Stem Cells. 24(2): p. 376-85.2006

2. Wall, M.E., S.H. Bernacki, and E.G. Loboa, Effects of serial passaging on the adipogenic and osteogenic differentiation potential of adipose-derived human mesenchymal stem cells. Tissue Eng. 13(6): p. 1291-8.2007

3. Zimmerlin, L., V.S. Donnenberg, M.E. Pfeifer, E.M. Meyer, B. Peault, J.P. Rubin, and A.D. Donnenberg, Stromal vascular progenitors in adult human adipose tissue. Cytometry A. 77(1): p. 22-30.2010

4. Yoshimura, K., T. Shigeura, D. Matsumoto, T. Sato, Y. Takaki, E. Aiba-Kojima, K. Sato, K. Inoue, T. Nagase, I. Koshima, and K. Gonda, Characterization of freshly isolated and cultured cells derived from the fatty and fluid portions of liposuction aspirates. J Cell Physiol. 208(1): p. 64-76.2006

5. Estes, B.T., A.W. Wu, R.W. Storms, and F. Guilak, Extended passaging, but not aldehyde dehydrogenase activity, increases the chondrogenic potential of human adipose-derived adult stem cells. J Cell Physiol. 209(3): p. 987-95.2006

6. Estes, B.T., B.O. Diekman, and F. Guilak, Monolayer cell expansion conditions affect the chondrogenic potential of adipose-derived stem cells. Biotechnol Bioeng. 99(4): p. 986-95.2008

7. Darling, E.M., M. Topel, S. Zauscher, T.P. Vail, and F. Guilak, Viscoelastic properties of human mesenchymally-derived stem cells and primary osteoblasts, chondrocytes, and adipocytes. J Biomech. 41(2): p. 454-64.2008

8. Engler, A.J., S. Sen, H.L. Sweeney, and D.E. Discher, Matrix elasticity directs stem cell lineage specification. Cell. 126(4): p. 677-89.2006

9. Estes, B.T., A.W. Wu, and F. Guilak, Potent induction of chondrocytic differentiation of human adipose-derived adult stem cells by bone morphogenetic protein 6. Arthritis Rheum. 54(4): p. 1222-32.2006

10. Darling, E.M., P.E. Pritchett, B.A. Evans, R. Superfine, S. Zauscher, and F. Guilak, Mechanical properties and gene expression of chondrocytes on micropatterned substrates following dedifferentiation in monolayer. Cell Mol Bioeng. 2(3): p. 395-404.2009

11. Gossett, D.R., H.T. Tse, S.A. Lee, Y. Ying, A.G. Lindgren, O.O. Yang, J. Rao, A.T. Clark, and D. Di Carlo, Hydrodynamic stretching of single cells for large population mechanical phenotyping. Proc Natl Acad Sci U S A. 109(20): p. 7630-5.2012

CHAPTER 4

Nuclear Lamin Protein C is Linked to Lineage-Specific, Whole-Cell Mechanical Properties

Published in: Cell. Mol. Bioeng. 2018. doi: 10.1007/s12195-018-0518-y (Accepted, in Press)

Rafael D. González-Cruz[a,b], Jessica S. Sadick[a], Vera C. Fonseca[a,], and Eric M. Darling[a,b,c,d]

[a]Department of Molecular Pharmacology, Physiology, and Biotechnology, [b]Center for Biomedical Engineering,[c] Department of Orthopaedics, and [d]School of Engineering, Brown University, Providence, RI, USA 02912.

4.1 ABSTRACT

Lamin proteins confer nuclear integrity and relay external mechanical cues that drive changes in gene expression. However, the influence these lamins have on whole-cell mechanical properties is unknown. We hypothesized that protein expression of lamins A, B1, and C would depend on the integrity of the actin cytoskeleton and correlate with cellular elasticity and viscoelasticity. To test these hypotheses, we examined the protein expression of lamins A, B1, and C across five different cell lines with varied mechanical properties. Additionally, we treated representative "soft/stiff" cell types with cytochalasin D and *LMNA* siRNA to determine the effect of a more compliant whole-cell phenotype on lamin A, B1 and C protein expression. A positive, linear correlation existed between lamin C protein expression and average cell moduli/apparent viscosity. Though moderate correlations existed between lamin A/B1 protein expression and whole-cell mechanical properties, they were statistically insignificant. Inhibition of actin polymerization, via cytochalasin D treatment, resulted in reduced cell elasticity, viscoelasticity, and lamin A and C protein expression in "stiff" MG-63 cells. In "soft" HEK-293T cells, this treatment reduced cell elasticity and viscoelasticity but did not affect lamin B1 or C protein expression. Additionally, *LMNA* siRNA treatment of MG-63 cells decreased whole-cell elasticity and viscoelasticity. These findings suggest that lamin C protein expression is strongly associated with whole-cell mechanical properties and could potentially serve as a biomarker for mechanophenotype.

4.2 INTRODUCTION

Whole-cell mechanical properties have emerged as important phenotypic traits that can identify specific cell types, differentiation states, and disease progression.[1, 2] Cellular mechanophenotypes are defined by an amalgam of both elastic and viscous components that give cells a characteristic, inherent mechanical property, as reviewed elsewhere.[3] These components are responsible for relaying physical cues from their surrounding microenvironment, across the cytoskeletal network, and into the nucleus via nucleocytoskeletal protein complexes known as linker of the nucleus to cytoskeleton (LINC).[4] Previous studies have shown that altering the mechanical properties of tissue-specific cell types results not only in structural and morphological changes but also in genetic modifications that may lead to different phenotypic traits.[5-7] At the heart of the mechanotransduction cascade, nuclear envelope lamin proteins are responsible for receiving these mechanical cues from the LINC complex and contributing to chromatin rearrangements that influence gene expression.[8, 9] Lamins are intermediate filament proteins that exist in most mammalian cells and include lamins A and C, splice variants of the *LMNA* gene,[10] lamins B1 and B2, encoded by genes *LMNB1* and *LMNB2*, respectively.[11, 12] Specifically, lamins A and C have been shown to affect nuclear and cellular deformability, mechanotransduction, cell polarization, and migration.[13-18] Gene and protein expression for lamin A/C is affected by changes in the physical and chemical microenvironment.[19] Most importantly, lamin A and C protein expression vary across tissues known to exhibit different mechanical properties.[20] Consequently, changes in lamin A/C expression may indicate changes in cellular phenotype that affect biological

processes of clinical relevance, such as stem cell differentiation, development of laminopathies, and cancer progression.[21-23] The role of lamins B1 and B2 in mechanotransduction are less apparent. Previous studies indicate that these lamins are not significant contributors to nuclear mechanical properties or cellular mechanotransduction. However, these results have been observed mostly in fibroblastic cell types where lamin A/C seems to predominantly influence cellular mechanophenotype. In other studies, lamin B1 has been found to be important in maintaining nuclear structural integrity and anchoring the nucleus to the LINC protein complex.[28,29] This work suggests a potential connection between lamin B1 and the mechanophenotype of compliant cells, such as neuronal and hematopoietic cell types, which express low levels of lamin A compared to lamins B1 and B2.[20]

Given the differential expression of lamin proteins in cells from different tissue sources, stages of differentiation, and inherent mechanophenotype, we hypothesized that lamin A, B1, and C protein levels would correlate with cellular elasticity and viscoelasticity and act as a biomarker of wholecell mechanical properties. To test this hypothesis, we examined lamin protein expression for five different cell types exhibiting differences in their elastic and viscoelastic properties. The human cell lines used in this study were normal human fibroblasts (NHF), osteosarcoma cells (MG-63), ovarian granulose cells (KGN), embryonic kidney cells (HEK-293T), and neuroblastoma cells (SH-SY5Y). Atomic force microscopy (AFM)-based single-cell indentation tests were conducted to determine cellular elastic and viscoelastic properties. Protein expression was evaluated using western blots. Correlation analyses between cellular mechanical

properties and lamin protein levels illustrated the potential roles of lamin A, B1, and C as biomarkers for mechanophenotype. Furthermore, the interdependency of the actin cytoskeleton, lamin A/C gene expression, and whole-cell mechanophenotype was explored using cytochalasin D (CytoD) and siRNA treatments.

4.3 METHODS

4.3.1 Cell culture conditions

Passage 7 NHF, MG-63, KGN, HEK293T, and SH-SY5Y cells were cultured until 80-90% confluence before being used for experiments. NHF and KGN cells were cultured in High glucose, Dulbecco Modified Eagle's Medium (hg DMEM, Hyclone, GE Healthcare, UT) containing 10% fetal bovine serum (FBS, Zen-Bio, NC), and 1% penicillin and streptomycin (P/S, Hyclone). MG-63 and HEK293T cells were cultured in Minimum Essential Medium Eagle (MEM 1X, Cellgro, VA) containing 10% FBS, and 1% P/S. SH-SY5Y cells were cultured in hg DMEM, 10% FBS, 1% P/S, and 1% glutamine. For whole-cell mechanical tests, 2.5 x 104 cells were seeded on square, glass coverslips (18 mm x 18 mm) placed in 50 mm culture dishes, given cell typespecific media, and allowed to attach and spread at 37°C for two days prior to testing.

4.3.2 AFM-based mechanical characterization

AFM-based, single cell indentation tests were used to measure whole-cell mechanical properties (MFP-3D-Bio, Asylum Research, CA). Spherically tipped cantilevers (diameter = 5 μm, Novascan Technologies, IA) had a nominal stiffness of k =

0.03 N/m. Cells were indented over the perinuclear region at a constant indentation velocity of 10 μm/s using a force trigger of 1 nN, yielding cell strains < 10%. Stress relaxation experiments maintained an approximately constant indentation for 30 seconds prior to retracting. Indentation and force data were used to determine cellular elasticity ($E_{elastic}$) and viscoelasticity (relaxed modulus, E_R; and apparent viscosity, μ_{app}) using a modified Hertz contact model and thin-layer stress relaxation. model (Fig. S1).[30-32]

For CytoD (Enzo Life Sciences, NY) experiments, representative "stiff" (MG-63) and "soft" (HEK-293T) cells were treated with growth medium (no treatment, NT), growth medium with 0.05% dimethyl sulfoxide (DMSO, Acros Chemicals, China) in distilled water, or growth medium with 0.05% DMSO and 2 μM CytoD one hour before testing. For *LMNA* gene knockdown experiments, "stiff" MG-63 cells were treated with either 50 nM LMNA siRNA (siLMNA, s8221, 4390824, sense: 5′-CCAAAAAGCGCAAACUGGATT-3′, antisense: 5′-UCCAGUUUGCGCUUUUUGGTG-3′, *LMNA* Silencer Select Validated siRNA, Ambion, Thermo Fisher Scientific) or 50 nM Scramble siRNA (siScramble, 4390843, Silencer Select Negative Control #1 siRNA, Ambion, Thermo Fisher Scientific) for 72 hours before mechanical testing. Sample sizes for mechanical characterization of all cell types are as follows: NHF (n = 49), MG-63 (n = 55, n = 43-55 for CytoD, n = 25-46 for siRNA), KGN (n = 67), HEK-293T (n =67, n = 32-67 for CytoD), and SH-SY5Y (n = 56). Mechanical measurements, for all conditions and cell types, were repeated across three separate sessions to account for any systematic errors.

4.3.3 Lamin protein expression assays

Western blot assays were conducted in triplicate to investigate lamin A, B1, and C protein expression in NHF, MG-63, KGN, HEK-293T and SH-SY5Y cells as well as in MG-63 and HEK-293T cells treated with CytoD. For blots used to investigate differential protein expression across mechanically distinct cells, nearly confluent cell cultures were lysed on ice for 30 minutes using either a sodium dodecyl sulfate (SDS)/urea buffer or a radioimmunoprecipitation (RIPA) lysis buffer. The SDS/urea buffer consisted of 2M urea (Sigma Aldrich, MO), 34 mM sodium dodecyl sulfate (SDS, ThermoFisher Scientific), and 50 mM Tris-HCl (ThermoFisher Scientific) at pH = 8.0 in triplicate. The RIPA buffer (sc-24948, Santa Cruz Biotechnologies, CA) consisted of 1X lysis buffer (1X tris buffer saline, 1% Nonidet P-40, 0.5% sodium deoxycholate, 0.1% SDS, 0.004% sodium azide, pH = 7.4), 2mM phenylmethylsulfonyl fluoride in DMSO, 10 μL of a proprietary protein inhibitor cocktail in DMSO, and 1 mM sodium orthovanadate. For blots used to investigate CytoD effects on lamin protein expression, nearly confluent MG-63 and HEK-293T cultures were treated with CytoD for 1 hour and lysed using RIPA lysis buffer as instructed by manufacturer specifications. Total protein concentrations from protein lysates, extracted either using SDS/urea or RIPA lysis buffer, were determined using a bicinchoninic acid (BCA) Assay (Pierce™, ThermoFisher Scientific) prior to gel loading. These two lysis buffers were examined to account for the possibility of different protein solubilities, with RIPA being standard in the field and SDS/urea being potentially more suitable for extracting hydrophobic proteins like lamins and β-tubulin. 33 For all lysates, 10 μg of protein were loaded and separated on SDS-PAGE Any KD gels (Bio-Rad, CA) and transferred onto Immobilon™-FL polyvinylidene fluoride membranes

(Millipore, MA). Membranes detected via fluorescence were blocked in nonmammalian Odyssey® Blocking Buffer (LiCOR, NE) for 1 hour at room temperature to limit interference with the IRDye™ secondary antibodies. Following blocking, the membranes were incubated with rabbit anti-human lamin A/C (1:500 dilution, 2032S, Cell Signaling Technology, MA), polyclonal goat anti-human lamin B1 (1:250 dilution, sc-6217, Santa Cruz Biotechnologies), and mouse anti-human β-tubulin (1:1000 dilution, E7-s, Developmental Studies Hybridoma Bank, IA) primary antibodies overnight at 4°C. Membranes were washed three times at 15-minute intervals in 1X Tris Buffer Saline Tween (TBST, ThermoFisher Scientific) and then incubated separately with infrared fluorophore-labeled donkey anti-rabbit IRDye® 680RD (1:5000 dilution, 925-68073, LiCOR), donkey anti-goat IRDye® 800CW (1:5000 dilution, 926-32214, LiCOR), and goat anti-mouse IRDye® 800CW (1:5000 dilution, 925-32210, LiCOR) secondary antibodies for 1 hour each. Membranes were washed three more times at 15-minute intervals in 1X TBST between secondary antibody incubations. Membranes treated with all IRDye® secondary antibodies were visualized using the Odyssey CLx near-infrared scanner (LiCOR). For all western blots, densitometry analyses were done using ImageJ version 1.51d. Protein expression data were normalized to β-tubulin expression.

4.3.4 *LMNA* and *LMNB1* gene expression assays

Lamin gene expression was assessed by qPCR. mRNA was extracted from three sample replicates for each cell type using QuickRNA Miniprep Kits (Zymo Research, CA), as instructed by manufacturer guidelines. Reverse transcription of RNA was accomplished using a SuperScript III First Strand cDNA Synthesis Kit (0.5-1

mg/reaction, Life Technologies, MA). TaqMan Gene Expression Assay human primers (Life Technologies) for genes of interest *LMNA* (Hs00153462_m1) and *LMNB1* (Hs01059210_m1) and reference gene GAPDH (Hs03929097_g1) were used for all qPCR runs. Fluorescence levels were measured using an ABI 7900HT Fast Real-Time PCR Detection Instrument (Life Technologies) and analyzed using the inverse ΔCt method. Relative expression of *LMNA* and *LMNB1* was calculated by normalizing expression to GAPDH. All qPCR runs were done in technical triplicate.

4.3.5 Immunofluorescence staining

Fixed, untreated and CytoD-treated MG-63 and HEK-293T cells were labeled for lamin A/C protein expression using 4 μg/mL of mouse IgG1 anti-lamin A/C monoclonal primary antibody (E-1, sc-376248, SCBT) and 1 μg/mL of Alexa Fluor 488- conjugated goat anti-mouse IgG1 secondary antibody (A-21121, Thermo Fischer Scientific), respectively, using standard immunostaining procedures. Actin cytoskeleton was labeled with 0.1 μg/mL Alexa Fluor 647-conjugated phalloidin toxin (Invitrogen). Lamin A/C and actin cytoskeleton staining was determined visually at 20X magnification using a Nikon Eclipse Ti-U epifluorescence camera (Nikon Instruments, Melville, NY). Images were captured using a QiCAM 12-bit digital camera (QImaging, Surrey, BC, Canada).

4.3.6 Statistical analysis

Data normality was assessed using a Shapiro-Wilks test. Mechanical property and protein expression data used for correlation analyses (from five cell types) were non-normal. Therefore, statistically significant comparisons among groups were determined

using two-sided Kruskal-Wallis tests with Dunn's post hoc test. Mechanical property data for CytoD experiments followed a log-normal distribution, and following transformation, were analyzed using two-sided, one-way ANOVA with Tukey post hoc tests. Protein expression data for CytoD experiments were normally distributed and analyzed similarly. Correlation analyses between mechanical property data and protein expression were determined by calculating Pearson's r coefficient for each set of properties. All experiments were done in triplicate. Statistical analyses were performed using SigmaPlot software.

4.4 RESULTS

4.4.1 Whole-Cell Mechanical Properties of Lineage-Specific Cell Types

Single-cell indentation tests were conducted via AFM to characterize the elastic ($E_{elastic}$) and viscoelastic (E_R, μ_{app}) properties of five lineage-specific cell types (Fig. 1A and Table S1).

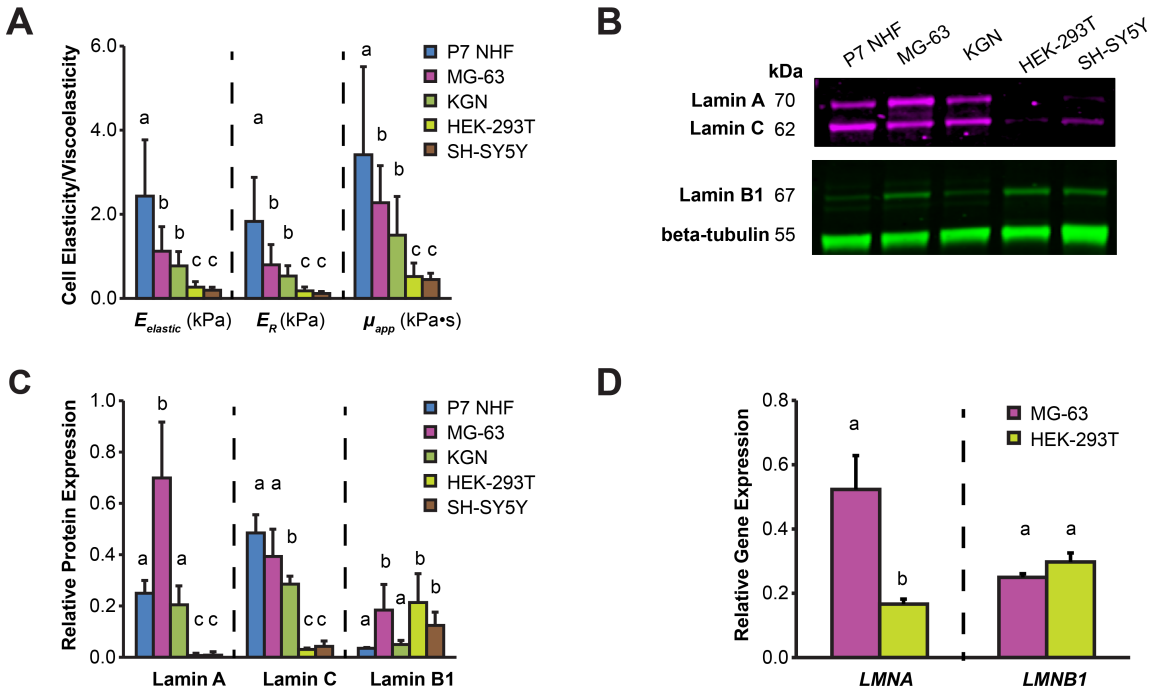

Figure 3: Mechanical properties and lamina protein levels for five, mechanically distinct cell types. (A) Cellular elastic and viscoelastic properties for NHF, MG-63, KGN, HEK-293T, and SH-SY5Y cells. Cellular elasticity was determined from elastic modulus ($E_{elastic}$); cellular viscoelasticity was determined by relaxed modulus (E_R) and apparent viscosity (μ_{app}). (B-C) Lamin A, C, and B1 representative protein expressions. Densitometry values normalized to β-tubulin expression. (D) *LMNA* and *LMNB1* gene expressions associated with "stiff" MG-63 and "soft" HEK-293T cells. Mechanical property and gene expression data represented as arithmetic means ± standard deviation. Statistical significance ($p < 0.05$) was determined using Kruskal-Wallis non-parametric tests with Tukey post hoc tests. Groups with different lowercase letters exhibit statistically significant differences.

Specifically, the tested cells NHF, MG-63, KGN, HEK-293T, and SH-SY5Y were chosen based on their resemblance to primary cells derived from connective tissue, bone,

epithelium, kidney, and brain, respectively, since these tissues are mechanically distinct from one another. The cells tested showed a consistent trend in their $E_{elastic}$, E_R, and μ_{app} values: NHF > MG-63 > KGN > HEK-293T ~ SH-SY5Y. Stiffer cell types had higher $E_{elastic}$, E_R, and μ_{app} values. Comparisons of mechanical properties between individual cell types were statistically significant ($p < 0.05$), with the exceptions of comparisons between MG-63 vs. KGN cells and HEK-293T vs. SH-SY5Y cells ($p > 0.05$). These results show that lineage-specific cells exhibit distinct elastic and viscoelastic properties.

4.4.2 Lamin protein and gene expression analysis

BCA assays were used to determine total protein concentration from lysates extracted from the five cell types, using either SDS/urea or RIPA lysis buffer (Fig. S2). Results showed that SDS/urea extracted more total protein than RIPA, suggesting improved solubilization and potentially better representation of the proteins present. Thus, data presented in the main text focused on SDS/urea extracted samples, with data from RIPA-extracted samples being presented in Supplemental Materials Section. Trends among cell types were largely conserved between the two extraction methods, suggesting that while less protein was solubilized with RIPA, the relative composition of proteins was similar to SDS/urea samples. Western blot was used to assess representative lamin protein expression for five cell types (Figs. 1B-1C, Fig. S2). A consistent relationship was observed for lamin A protein expression: MG-63 > NHF ~ KGN > HEK-293T ~ SH-SY5Y. A similar relationship was observed for lamin C protein expression: MG-63 ~ NHF > KGN > HEK-293T ~ SH-SY5Y. No particular relationship was observed for lamin B1 protein expression: NHF ~ KGN < MG-63 ~ HEK-293T ~ SH-SY5Y. qPCR

was used to examine *LMNA* and *LMNB1* gene expression for representative stiff, MG-63 and soft, HEK-293T cells (Fig 1D). Results showed that *LMNA* expression was 3-times greater in MG-63 than HEK-293T cells ($p < 0.05$). *LMNB1* was not significantly different between cell types.

4.4.3 Mechanical property-lamin protein correlations

Correlation analyses were conducted to determine the relationship between elastic/viscoelastic properties and lamin protein expression (Fig. 2). Lamin C protein expression was positively correlated with $E_{elastic}$, E_R, and μ_{app}, as evidenced by their respective Pearson's *r* coefficients: $r_{Eelastic} = 0.90$ ($p < 0.05$), $r_{ER} = 0.94$ ($p < 0.05$), and $r_{\mu app} = 0.97$ ($p < 0.05$). Lamin A protein expression was moderately correlated with $E_{elastic}$, E_R, and μ_{app} in a positive fashion but not to the level of statistical significance: $r_{Eelastic} = 0.42$ ($p = 0.44$); $r_{ER} = 0.44$ ($p = 0.41$) and $r_{\mu app} = 0.60$ ($p = 0.23$). Lamin B1 expression was negatively correlated with Eelastic, ER, and μapp, but again, not to the level of statistical significance: $r_{Eelastic} = -0.59$ ($p = 0.24$); $r_{ER} = -0.59$ ($p = 0.23$) and $r_{\mu app} = -0.53$ ($p = 0.30$). Correlation analyses were also run for data obtained using RIPA buffer lysates, detected using either fluorescence or chemiluminescence methods (Figs. S3 and S4). RIPA samples detected via fluorescence (N = 1) exhibited similar

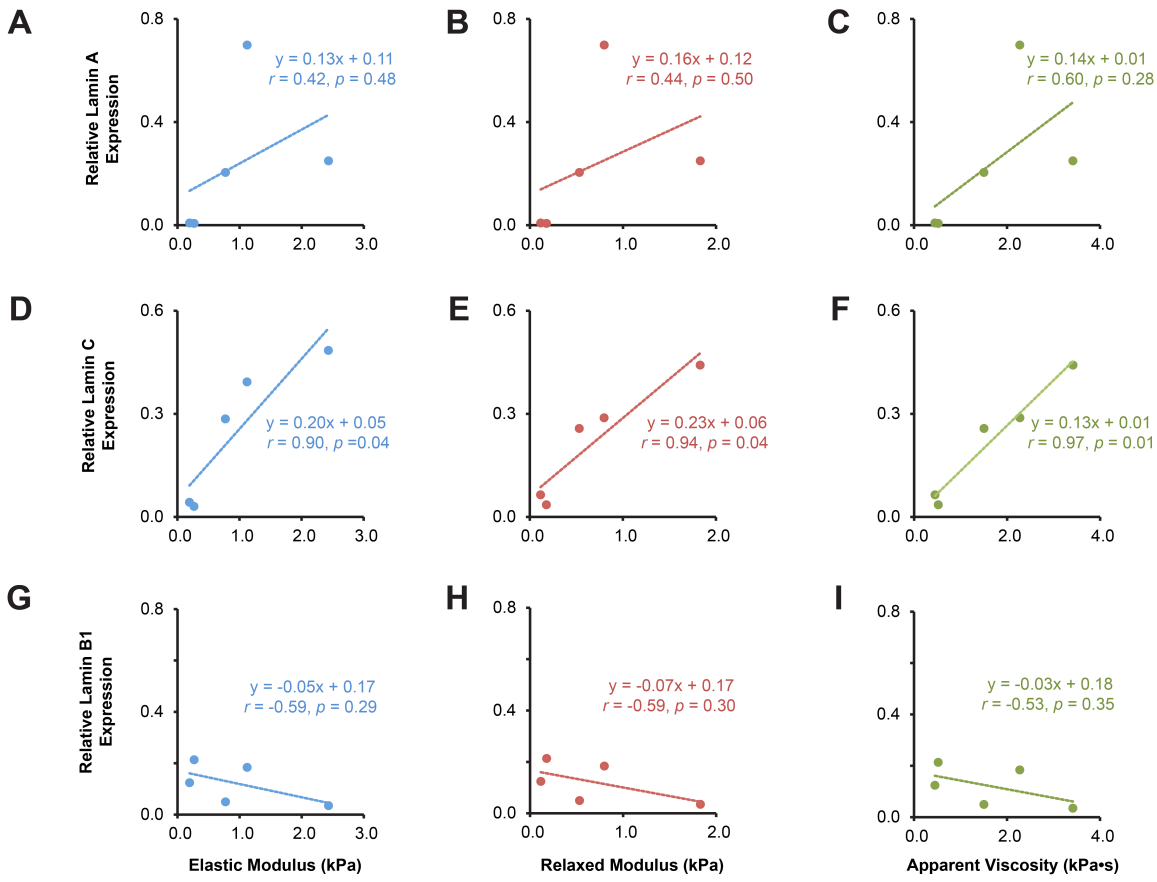

Figure 4: Relative lamin A, C, and B1 expressions correlate with cellular elasticity and viscoelasticity across the five cell types tested. Correlations were examined between mechanical properties and lamin A (A-C), lamin C (D-E), or lamin B1 (G-H) expressions from protein samples extracted using SDS/urea lysis buffer. Pearson's r correlation coefficients are reported for the linear and inverse exponential fits associated with the data. Each data point corresponds to the median values of elastic modulus, relaxed modulus, or apparent viscosity measured for each cell type, plotted against the associated, average lamina protein expression.

positive/negative trends for mechanical properties vs. lamins A/B1/C to SDS/urea samples detected the same way, although the shape of the fits varied slightly (Fig. S3). However, RIPA samples detected via chemiluminescence (N = 3) exhibited different trends from RIPA samples detected via fluorescence, with lamin A exhibiting the strongest relationship with mechanical properties rather than lamin C (Fig. S4). Additional analyses showed that lamin A and C protein correlations were moderately strong but not statistically significant ($r_{A\text{-}C}$ = 0.72, p = 0.11), whereas correlations

between lamin A and B1 and lamin C and B1 were weak and not statistically significant (Fig. S5, $r_{A\text{-}B1} = 0.09$, p = 0.88; $r_{C\text{-}B1} = 0.54$, $p = 0.30$, respectively).

4.4.4 Actin Cytoskeleton Disruption and *LMNA* Silencing

Representative "stiff" MG-63 and "soft" HEK-293T cells were treated with CytoD to determine whether elastic/viscoelastic properties and lamin A, B1, and C protein expression were affected by disrupting the actin cytoskeleton. As expected, the elastic and viscoelastic properties of CytoD-treated MG-63 cells were substantially lower than untreated cells, with a concurrent increase in cell height (Fig. 3A, $p < 0.05$).

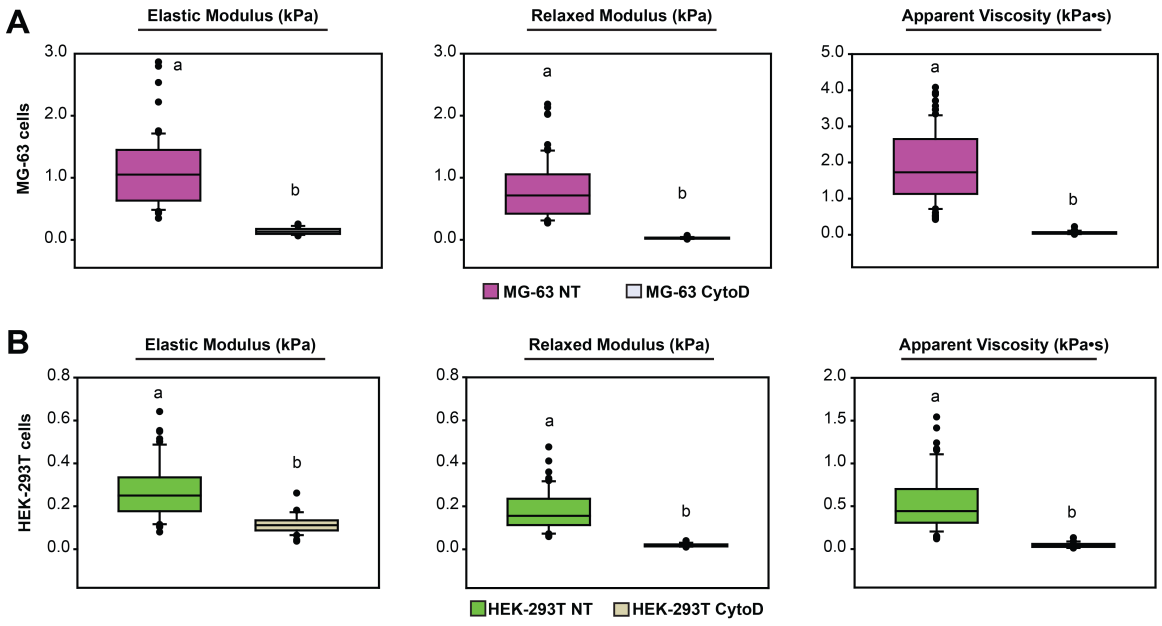

Figure 3: Disruption of actin cytoskeleton affects the mechanophenotype of stiff and soft cells. (A) Elastic moduli, relaxed moduli, and apparent viscosities for "stiff" MG-63 cells exposed to either no treatment (NT) or 2 µM cytochalasin D (CytoD). (B) Elastic moduli, relaxed moduli, apparent viscosities, and cell heights for NT or CytoD, "soft" HEK-293T cells. Statistical significance ($p < 0.05$) was determined using one-way ANOVA with Tukey post hoc tests. Groups with different lowercase letters exhibit statistically significant differences.

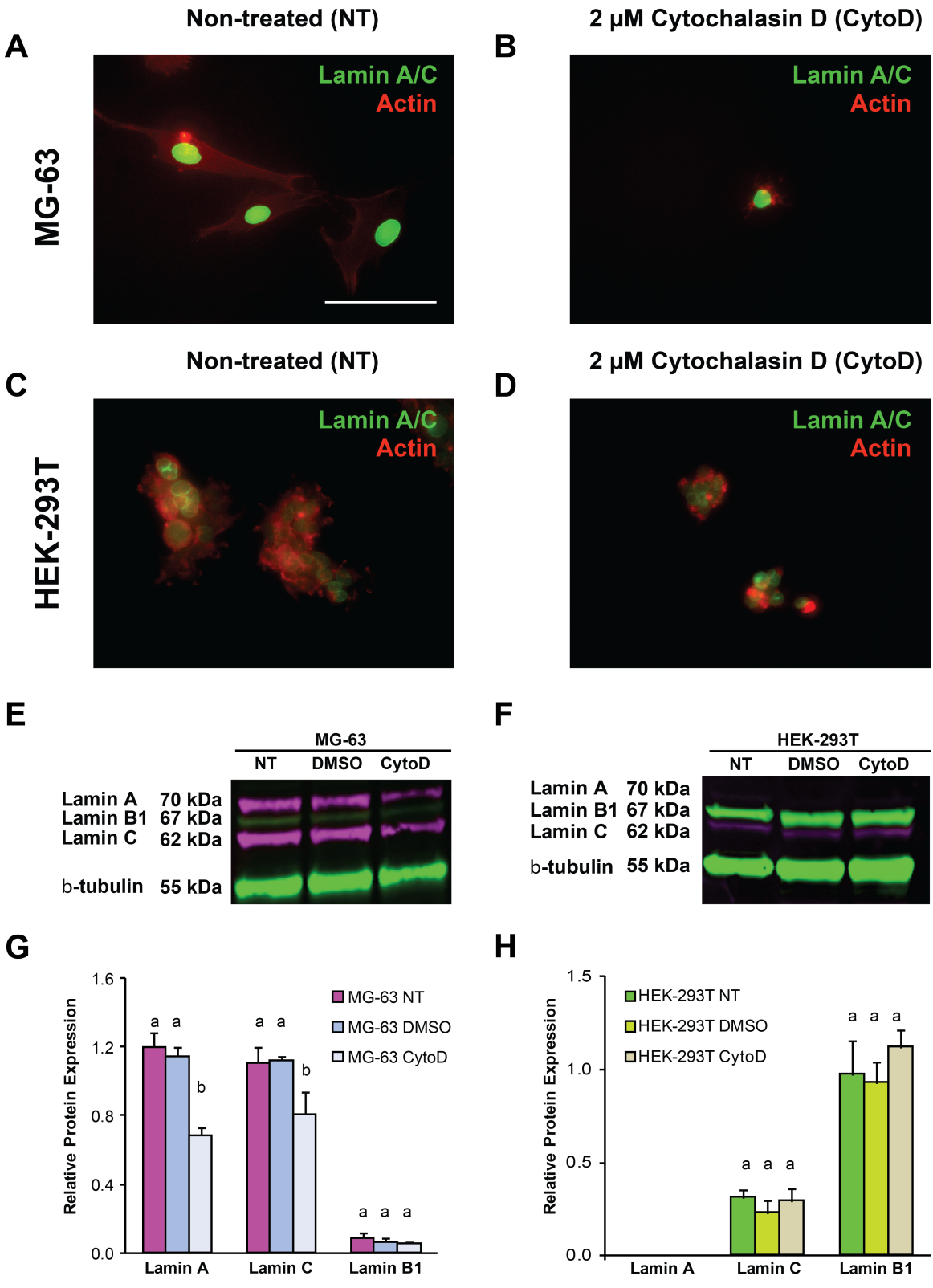

Figure 4: Robust lamin A/C protein expression in stiff MG-63 cells is dependent on actin cytoskeletal organization, whereas weak expression in soft HEK-293T cells is not. (A) Non-treated and (B) CytoD-treated MG-63 cells exhibited a qualitative decrease in lamin A/C levels and dramatic changes in actin

organization. (C) Non-treated and (D) CytoD-treated HEK-293T cells both exhibited similar lamin A/C levels, regardless of cytoskeletal disruption, that were much lower than MG-63 cells. (E) Lamin protein expressions from MG-63 cells exposed to no treatment (NT), 0.05% DMSO for 1 hour (DMSO), or 0.05% DMSO and 2 μM CytoD for 1 hour (CytoD). (F) Representative relative lamin protein expression quantification for NT-, DMSO- and CytoD-treated MG-63 cells. (G) Lamin protein expressions from HEK-293T cells exposed to the same conditions as described in (E). (H) Representative relative lamin protein expression quantification for NT-, DMSO- and CytoD-treated HEK-293T cells. Lamin A (70 kDa) and C (62 kDa) bands are shown in magenta fluorescence while lamin B1 (67 kDa) and β-tubulin (55 kDa) bands are shown in green fluorescence. Relative protein expression was determined by normalizing all protein expression to β-tubulin (loading control). Statistical significance ($p < 0.05$) was determined using one-way ANOVA with Tukey post hoc tests. Groups with different lowercase letters exhibited statistically significant differences.

Immunostaining of lamin A and C proteins, along with actin cytoskeleton, in untreated and CytoD-treated cells showed lower lamin fluorescence intensity in CytoD-treated MG-63 cells than in untreated groups (Figs. 4A and 4B). In HEK-293T cells, changes in actin cytoskeleton organization were observed between untreated and CytoD-treated cells, but no qualitative difference in lamin A/C intensity was observed between the groups (Figs. 4C and 4D). Representative lamin A and C protein levels by western blot were, respectively, ~70% and ~60% lower in CytoD-treated MG-63 cells compared to untreated cells (Figs. 4E and 4F). Lamin B1 protein expression was negligible in both groups. "Soft" HEK-293T cells treated with CytoD also exhibited a substantial reduction in elastic and viscoelastic properties (Fig. 3B, $p < 0.05$). Lamin A protein expression was negligible in both non-treated and CytoD-treated HEK- 293T cells while lamin B1 and C expression levels remained unchanged in all HEK-293T cell groups (Figs. 4G and 4H). Similar to what was observed in actin disruption experiments, MG-63 cells treated with 50 nM *siLMNA* for three days were significantly softer than cells treated with 50 nM *siScramble* (Fig. 5, $p < 0.05$). Specifically, $E_{elastic}$ and E_R parameters, but not μ_{app} ($p = 0.06$), were significantly decreased between *siLMNA*- and *siScramble*-treated MG-63 cells.

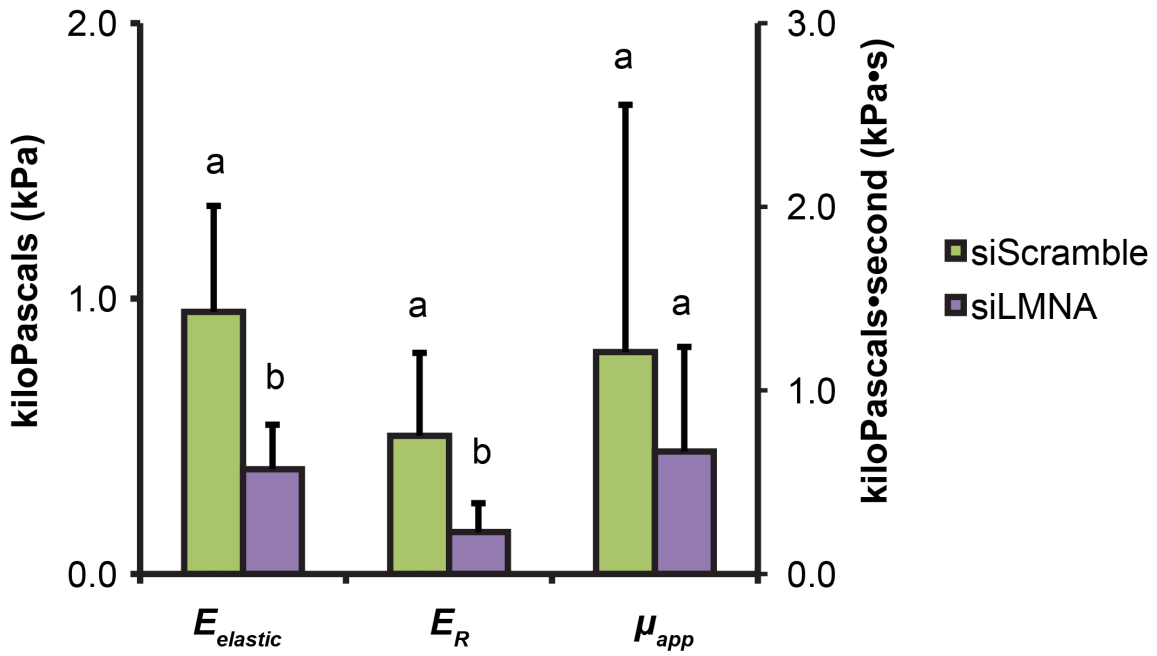

Figure 5: Lamin A/C knockdown via siRNA treatment reduces elastic and viscoelastic properties in stiff cell types. MG-63 cells were treated with either 50 nM *siLMNA* or 50 nM *siScramble* for a three-day period before mechanical testing. Statistical significance was determined using Student's t test ($p > 0.05$). Groups with different letters exhibited statistically significant differences.

4.5 DISCUSSION

Nuclear lamina proteins are known to play critical roles in cellular mechanotransduction machinery and maintenance of nuclear structural integrity.[34] Therefore, we hypothesized that lamin A, B1, and C protein expression would strongly correlate to whole-cell elastic and viscoelastic properties. Because of their involvement in mechanotransduction and nuclearcytoskeletal anchorage, we also hypothesized that nuclear lamin A, B1, and C protein expression were dependent on the integrity of the actin cytoskeleton. Findings showed that cells derived from different lineages exhibited distinct mechanical properties and lamin protein expression profiles. Specifically, stiffer and more viscous cell types exhibited higher lamin A and C protein expression than "soft" cell types, which predominantly expressed lamin B1. Correlations between

individual lamin A, B1, and C protein expression and cellular elastic/viscoelastic properties showed that lamin C protein exhibited the strongest linear correlation to cellular mechanophenotype. Meanwhile, lamin A and B1 protein expression exhibited moderate but statistically insignificant correlations to these mechanical properties. Disruption of the actin cytoskeleton via CytoD decreased elasticity, viscoelasticity, and lamin A and C protein expression in stiff cells. Similarly, lamin A/C knockdown also reduced elasticity and viscoelasticity in stiff cells. Altogether, these results validate the importance of lamin proteins in the mechanotransductive linkage between actin cytoskeleton and nuclear lamina. The current work showed that lamin C protein is a strong indicator of whole-cell mechanophenotype. Therefore, lamin C could represent an important, yet under-investigated, mechanical biomarker. Previous studies have demonstrated that both lamin A and C proteins can influence cellular mechanotransduction,[15] nuclear stiffness,[14] ECM elasticity sensing,[19] and tissue microelasticity,[20] suggesting the isotypes share functions that are connected to cellular mechanical characteristics. Lamins A and C are highly similar in their amino acid (aa) primary structure and composition of their N-terminus, being different only in length (664 and 572 aa).[35] They share two protein domains, 1B and 2B, that are responsible for imparting the characteristic elastic properties of both lamins.[36] The functional redundancy of these lamin isotypes has been reported for nuclear deformation characteristics in cells expressing both lamin A and C compared to lamin C alone.[14, 37] That said, lamins A and C have been shown to contribute differently to microtissue elasticity.[20] Both isotypes correlate highly, but lamin A scales more strongly than lamin C. In the current work, correlation to whole-cell mechanical properties was investigated as opposed to tissue

microelasticity. For this comparison, lamin C was the isotype that correlated more strongly to mechanical properties rather than lamin A. Our study also showed that lamin A and C expression levels were different across cell types of different stiffness, with lamin A being expressed only in the stiffest of cell types while lamin C was expressed in cell types regardless of their stiffness. This result suggests that lamin A and C could have different mechanical roles that are connected to inherent cellular mechanical properties and the tissue microenvironment. It is possible such differences could contribute to the discrepancies between lamins A and C vs. mechanophenotype observed in our study compared to previous work. A secondary finding of our work was that protein extraction techniques could potentially bias resulting data due to variations in protein solubilization. This will be discussed further below but is a possible contributor to the discrepancies between our work and previously published studies. Regardless of extraction technique, we hypothesize that the small differences in amino acid sequence and consequent supramolecular assembly could account for differences in scaling between lamin A and C. These differences are further compounded by cell-specific expression of lamin A/C proteins within given microenvironments, all of which merits further study. The functional redundancy of lamin A and C proteins could be important for a given phenotype because not all cells express the proteins to the same degree. This is especially true if one isotype is not expressed at all, making the other lamin a better biomarker given the biological context. For example, lamin A expression in murine brain has been shown to be limited to endothelial and meningeal cells, whereas neurons and glia only express lamin C.[38] In the current study, we found that NHF and KGN cells had higher lamin C than A protein expression but MG-63 cells showed the reverse. This differential

expression between lamin A and C composition across evaluated cell types could be lineage-specific and has been observed previously in tissues of varying stiffness.[20] Low compliance tissues like bone and cartilage expressed higher levels of lamin A protein than C while softer tissues such kidney, liver, and heart expressed higher levels of lamin C than A.[20] Additionally, these lamin expression differences could be dependent on environmental signals that favor the expression of one lamin protein over another. Previous work showed that altering the expression of spliceosome proteins such as serine/arginine-rich splicing factors (SRSFs) changed lamin A to C protein ratios.[39] Specifically, silencing the expression of SRSF2 resulted in an increase in lamin C and a reduction in lamin A by preventing prelamin A synthesis. The expression of these splicing factors can be altered by inducing changes in physical cues such as substrate stiffness,[40] which is a well-known physical cue that modulates cell phenotype and fate. Altogether, these findings contribute to understanding how different Altogether, these findings contribute to understanding how different lamin A and C compositions affect whole-cell mechanical properties in different cells types and how different environments could lead to shifts in cellular lamina composition.

Results related to lamin B1 protein expression agreed with previous reports indicating that lamin B1, as well as lamin B2, play no significant role in nuclear- and tissue-level mechanical properties.[14, 20] In fact, lamin B1 has been reported to scale very weakly with tissue microelasticity, while lamin B2 does not scale at all.[20] In our study, LMNB1 gene expression was similar in “soft” HEK-293T cells and “stiff” MG-63 cells. However, lamin B1 protein expression was variable across tested cells. This phenomenon

is attributed to lineage-specific, post-transcriptional regulation of lamin B1. Actin is the cytoskeletal element most responsible for determining cellular elastic and viscoelastic properties.[41, 42] From a mechanotransduction standpoint, actin microfilaments bind to LINC complex proteins that ultimately relay mechanical cues, such as cellular tension, to the nuclear lamina.[43] Therefore, it was hypothesized that disrupting the actin microfilament network via CytoD treatment would not only decrease elastic and viscoelastic properties but also affect lamin A, C, and B1 protein expression. CytoD treatment for 1 hour significantly reduced elastic and viscoelastic properties in stiff and soft cell types, confirming the importance of the actin cytoskeleton to whole-cell mechanical properties. Since the CytoD treatment regimen was successful in depolymerizing actin filaments and inducing a sharp reduction in cellular mechanical properties, we hypothesized CytoD would also lower lamin A/C expression. Despite lamin A/C being a very stable protein in undisturbed conditions, previous reports suggest that disruption of the actomyosin cytoskeleton triggers changes in lamin-A dependent nuclear behavior that is concomitant with intracellular tension loss.[44, 45] Specifically, perturbations of the actomyosin cytoskeleton result in loss of intracellular tension sufficient to increase fluidity and dynamics of nuclear heterochromatin in only 30 minutes after CytoD treatment[44] and alter nuclear envelope lamin A/C polarization and size by 1 hour after CytoD treatment,[45] thus showing that the lamin A/C protein meshwork and its structural functionality are rapidly compromised after Cyto D treatment. Another study used a 2-hour treatment with blebbistatin, which inhibits myosin, to disrupt intracellular tension and likewise induce rapid lamin A/C protein changes.[46] Lamin turnover was shown to occur in only 10 minutes after attached cells

were uplifted, which results in a drastic cytoskeletal rearrangement (i.e., from spread to spherical morphology) that is accompanied by loss of intracellular tension. These reports, combined with the present findings, provide evidence that lamin A/C expression and mechanical properties can respond quickly and dramatically to perturbations of the actomyosin cytoskeleton, serving as responsive biomarkers. Additionally, transient silencing of the *LMNA* gene in stiff MG-63 cells resulted in a significant reduction in elastic and viscoelastic properties, which further demonstrates the connection between lamin A/C expression and cellular mechanophenotype. In cells predominantly expressing lamin A and C (stiff cells), a significant decrease in these proteins was observed, which was anticipated since cytoskeletal disruption has previously been reported to affect nuclear compliance and promote lamin A and C protein turnover.[46,47] Interestingly, in cells predominantly expressing lamin B1 (soft cells), negligible changes were observed, suggesting that this protein is neither affected by the disruption of actin cytoskeletal structures nor involved in actin-mediated mechanotransduction processes. It is important to clarify that while CytoD-treated cells are significantly softer than untreated cells, the amount of reduction in elastic properties is very different for MG-63 vs. HEK-293T cell types. Specifically, stiff cells like MG-63 cells lose most of their profuse cytoskeletal connections and the entire actin-dependent mechanotransduction machinery.[41] As such, the connection between actin-mediated mechanotransduction and lamin A/C force transduction is severed and this loss of intracellular tension is accompanied by downregulation of lamin A/C protein,[46] which is consistent with our finding that siLMNA-treated MG-63 cells were significantly softer than their siScramble-treated counterparts. However, HEK-293T cells have a predominantly cortical actin cytoskeleton

that is not robustly linked to the nucleus and employ entirely different mechanotransduction machinery that appears to depend very little on lamin A/C expression, as observed in the CytoD-treatment experiments. Thus, lamin B1 protein was disregarded as a contributor to whole-cell mechanophenotype. One major distinction between the current study and others is the special attention given to how specific protein extraction methods can potentially bias lamin protein expression experiments. Specifically, the work presented here used an SDS/urea-based lysis buffer to maximize the solubilization of lamin proteins rather than a RIPA-based lysis buffer that is routinely used in other studies.[20] RIPA lysis buffers have been found to be suboptimal for solubilizing hydrophobic proteins such as lamins and, therefore, could result in underestimation of actual protein concentration by 20-30%.[33] Therefore, correlative and comparative lamin A/C studies that used RIPA buffers for protein extraction may have reported lamin concentrations that are lower than in actuality and, as result, arrived at inaccurate conclusions. For direct comparison purposes, we also included experiments in the current study that used cell lysates extracted with RIPA buffer. Total protein concentrations for these samples were substantially lower than SDS/urea lysates, indicating that fewer proteins, including lamin and β-tubulin proteins, were extracted (Fig. S2). However, correlative analyses between lamin proteins and whole-cell mechanical properties showed similar findings regardless of lysis extraction buffer, with lamin C being the strongest predictor of whole-cell mechanical properties, although for RIPA samples, this was not to the same level of statistical significance (Fig. S3). Qualitatively, when cells were lysed with RIPA buffer, a supernatant and an insoluble pellet were generated. The supernatant was used for protein expression analyses while the

insoluble pellet, which could include a disproportionally higher concentration of lamin proteins, was discarded. When cells were lysed with SDS/urea buffer, no insoluble pellet remained, as observed by us and others,[48] suggesting that a much greater proportion of the material was successfully solubilized. This conclusion was supported by the presence of more intense lamin and β-tubulin protein bands for SDS/urea vs. RIPA samples in western blot experiments. The extraction efficiency of the two buffers for lamins A/B1/C, β-tubulin, and potentially other proteins of interest could dramatically influence resulting data and should be carefully considered for studies involving nucleocytoskeletal components. One experimental approach that did result in replication of previously reported findings was to use a less sensitive western blot imaging system. RIPA-extracted samples assessed using chemiluminescent detection showed lamin A as the strongest predictor of whole-cell properties (Fig. S4). However, use of a highly sensitive fluorescence-based detection system, along with increased solubilization of proteins should provide a more accurate representation of these lamin-mechanophenotype relationships. While lamin A does correlate with whole-cell properties, using a more appropriate protein extraction method showed that lamin C was actually the strongest predictor. That said, the current study includes a relatively modest number of points to establish these correlations. While increasing this sample set could potentially alter the shape of the trendlines (e.g., linear to exponential) or even change which lamin isotype has the strongest relationship with whole-cell mechanophenotype, the protein extraction method is still expected to be a key factor in any discrepancies between the current work and other reported correlations.

4.6 CONCLUSION

This is the first study to demonstrate strong correlation between lamin C protein and whole-cell, elastic and viscoelastic properties. Due to this link, lamin C can potentially be used as a tool to characterize cellular mechanophenotype. Additionally, future studies exploring involvement of lamin C in mechanotransduction pathways could provide further insight into the specific roles it plays in determining the mechanophenotype of cells in a variety of biological scenarios of clinical relevance, such as stem cell differentiation, cancer progression, and a plethora of laminopathies.

4.7 AUTHOR CONTRIBUTIONS

R.D.G.C. and E.M.D. designed all experiments. R.D.G.C. conducted all AFM experiments. R.D.G.C. and V.C.F. conducted all western blot experiments. J.S.S. conduced all qPCR experiments. R.D.G.C. and E.M.D. analyzed the data and wrote the manuscript. Authors RDGC, JSS, VCF, and EMD have no conflict of interest.

4.8 ACKNOWLEDGEMENTS

We would like to thank Dr. Jeffrey Morgan for his gift of NHF cells. We would also like to acknowledge the Brown Genomics Core Facility and Dr. Christoph Schorl for assistance with fluorescence-based western blot detection. This work by supported by NIH grants R01 AR063642 and P20 GM104937 (EMD) and R25 GM083270 (RDGC) and NSF CAREER Award CBET 1253189 (EMD).

4.9 REFERENCES

1. Gonzalez-Cruz, R.D., V.C. Fonseca, and E.M. Darling, Cellular mechanical properties reflect the differentiation potential of adipose-derived mesenchymal stem cells. Proc Natl Acad Sci U S A. 109(24): p. E1523-9.2012

2. Cross, S.E., Y.S. Jin, J. Rao, and J.K. Gimzewski, Nanomechanical analysis of cells from cancer patients. Nat Nanotechnol. 2(12): p. 780-3.2007

3. Suresh, S., Biomechanics and biophysics of cancer cells. Acta Biomater. 3(4): p. 413-38.2007

4. Mellad, J.A., D.T. Warren, and C.M. Shanahan, Nesprins linc the nucleus and cytoskeleton. Curr Opin Cell Biol. 23(1): p. 47-54.2011

5. Darling, E.M., M. Topel, S. Zauscher, T.P. Vail, and F. Guilak, Viscoelastic properties of human mesenchymally-derived stem cells and primary osteoblasts, chondrocytes, and adipocytes. J Biomech. 41(2): p. 454-64.2008

6. Titushkin, I. and M. Cho, Modulation of cellular mechanics during osteogenic differentiation of human mesenchymal stem cells. Biophys J. 93(10): p. 3693-702.2007

7. Labriola, N.R. and E.M. Darling, Temporal heterogeneity in single-cell gene expression and mechanical properties during adipogenic differentiation. J Biomech. 48(6): p. 1058-66.2015

8. Ho, C.Y. and J. Lammerding, Lamins at a glance. J Cell Sci. 125(Pt 9): p. 2087-93.2012

9. Alam, S.G., Q. Zhang, N. Prasad, Y. Li, S. Chamala, R. Kuchibhotla, B. Kc, V. Aggarwal, S. Shrestha, A.L. Jones, S.E. Levy, K.J. Roux, J.A. Nickerson, and T.P. Lele,

The mammalian linc complex regulates genome transcriptional responses to substrate rigidity. Sci Rep. 6: p. 38063.2016

10. Lin, F. and H.J. Worman, Structural organization of the human gene encoding nuclear lamin a and nuclear lamin c. J Biol Chem. 268(22): p. 16321-6.1993

11. Peter, M., G.T. Kitten, C.F. Lehner, K. Vorburger, S.M. Bailer, G. Maridor, and E.A. Nigg, Cloning and sequencing of cdna clones encoding chicken lamins a and b1 and comparison of the primary structures of vertebrate a- and b-type lamins. J Mol Biol. 208(3): p. 393-404.1989

12. Vorburger, K., G.T. Kitten, and E.A. Nigg, Modification of nuclear lamin proteins by a mevalonic acid derivative occurs in reticulocyte lysates and requires the cysteine residue of the cterminal cxxm motif. EMBO J. 8(13): p. 4007-13.1989

13. Lammerding, J. and R.T. Lee, The nuclear membrane and mechanotransduction: Impaired nuclear mechanics and mechanotransduction in lamin a/c deficient cells. Novartis Found Symp. 264: p. 264-73; discussion 273-8.2005

14. Lammerding, J., L.G. Fong, J.Y. Ji, K. Reue, C.L. Stewart, S.G. Young, and R.T. Lee, Lamins a and c but not lamin b1 regulate nuclear mechanics. J Biol Chem. 281(35): p. 25768- 80.2006

15. Lee, J.S., C.M. Hale, P. Panorchan, S.B. Khatau, J.P. George, Y. Tseng, C.L. Stewart, D. Hodzic, and D. Wirtz, Nuclear lamin a/c deficiency induces defects in cell mechanics, polarization, and migration. Biophys J. 93(7): p. 2542-52.2007

16. Harada, T., J. Swift, J. Irianto, J.W. Shin, K.R. Spinler, A. Athirasala, R. Diegmiller, P.C. Dingal, I.L. Ivanovska, and D.E. Discher, Nuclear lamin stiffness is a barrier to 3d migration, but softness can limit survival. J Cell Biol. 204(5): p. 669-82.2014

17. Kolb, T., J. Kraxner, K. Skodzek, M. Haug, D. Crawford, K.K. Maass, K.E. Aifantis, and G. Whyte, Optomechanical measurement of the role of lamins in whole cell deformability. J Biophotonics. 2017

18. Neelam, S., T.J. Chancellor, Y. Li, J.A. Nickerson, K.J. Roux, R.B. Dickinson, and T.P. Lele, Direct force probe reveals the mechanics of nuclear homeostasis in the mammalian cell. Proc Natl Acad Sci U S A. 112(18): p. 5720-5.2015

19. Swift, J. and D.E. Discher, The nuclear lamina is mechano-responsive to ecm elasticity in mature tissue. J Cell Sci. 127(Pt 14): p. 3005-15.2014

20. Swift, J., I.L. Ivanovska, A. Buxboim, T. Harada, P.C. Dingal, J. Pinter, J.D. Pajerowski, K.R. Spinler, J.W. Shin, M. Tewari, F. Rehfeldt, D.W. Speicher, and D.E. Discher, Nuclear lamina scales with tissue stiffness and enhances matrix-directed differentiation. Science. 341(6149): p. 1240104.2013

21. Constantinescu, D., H.L. Gray, P.J. Sammak, G.P. Schatten, and A.B. Csoka, Lamin a/c expression is a marker of mouse and human embryonic stem cell differentiation. Stem Cells. 24(1): p. 177-85.2006

22. Akter, R., D. Rivas, G. Geneau, H. Drissi, and G. Duque, Effect of lamin a/c knockdown on osteoblast differentiation and function. J Bone Miner Res. 24(2): p. 283-93.2009

23. Bermeo, S., C. Vidal, H. Zhou, and G. Duque, Lamin a/c acts as an essential factor in mesenchymal stem cell differentiation through the regulation of the dynamics of the wnt/betacatenin pathway. J Cell Biochem. 116(10): p. 2344-53.2015

24. Scaffidi, P. and T. Misteli, Lamin a-dependent misregulation of adult stem cells associated with accelerated ageing. Nat Cell Biol. 10(4): p. 452-9.2008

25. Lanzicher, T., V. Martinelli, L. Puzzi, G. Del Favero, B. Codan, C.S. Long, L. Mestroni, M.R. Taylor, and O. Sbaizero, The cardiomyopathy lamin a/c d192g mutation disrupts whole-cell biomechanics in cardiomyocytes as measured by atomic force microscopy loading-unloading curve analysis. Sci Rep. 5: p. 13388.2015

26. Ostlund, C., G. Bonne, K. Schwartz, and H.J. Worman, Properties of lamin a mutants found in emery-dreifuss muscular dystrophy, cardiomyopathy and dunnigan-type partial lipodystrophy. J Cell Sci. 114(Pt 24): p. 4435-45.2001

27. Irianto, J., C.R. Pfeifer, I.L. Ivanovska, J. Swift, and D.E. Discher, Nuclear lamins in cancer. Cell Mol Bioeng. 9(2): p. 258-267.2016

28. Vergnes, L., M. Peterfy, M.O. Bergo, S.G. Young, and K. Reue, Lamin b1 is required for mouse development and nuclear integrity. Proc Natl Acad Sci U S A. 101(28): p. 10428-33.2004

29. Ji, J.Y., R.T. Lee, L. Vergnes, L.G. Fong, C.L. Stewart, K. Reue, S.G. Young, Q. Zhang, C.M. Shanahan, and J. Lammerding, Cell nuclei spin in the absence of lamin b1. J Biol Chem. 282(27): p. 20015-26.2007

30. Dimitriadis, E.K., F. Horkay, J. Maresca, B. Kachar, and R.S. Chadwick, Determination of elastic moduli of thin layers of soft material using the atomic force microscope. Biophys J. 82(5): p. 2798-810.2002

31. Shin, J.W., K.R. Spinler, J. Swift, J.A. Chasis, N. Mohandas, and D.E. Discher, Lamins regulate cell trafficking and lineage maturation of adult human hematopoietic cells. Proc Natl Acad Sci U S A. 110(47): p. 18892-7.2013

32. Darling, E.M., S. Zauscher, and F. Guilak, Viscoelastic properties of zonal articular chondrocytes measured by atomic force microscopy. Osteoarthritis Cartilage. 14(6): p. 571-9.2006

33. Janes, K.A., An analysis of critical factors for quantitative immunoblotting. Sci Signal. 8(371): p. rs2.2015

34. Dahl, K.N., A.J. Ribeiro, and J. Lammerding, Nuclear shape, mechanics, and mechanotransduction. Circ Res. 102(11): p. 1307-18.2008

35. Fisher, D.Z., N. Chaudhary, and G. Blobel, Cdna sequencing of nuclear lamins a and c reveals primary and secondary structural homology to intermediate filament proteins. Proc Natl Acad Sci U S A. 83(17): p. 6450-4.1986

36. Bera, M., S.R. Ainavarapu, and K. Sengupta, Significance of 1b and 2b domains in modulating elastic properties of lamin a. Sci Rep. 6: p. 27879.2016

37. Fong, L.G., J.K. Ng, J. Lammerding, T.A. Vickers, M. Meta, N. Cote, B. Gavino, X. Qiao, S.Y. Chang, S.R. Young, S.H. Yang, C.L. Stewart, R.T. Lee, C.F. Bennett, M.O. Bergo, and S.G. Young, Prelamin a and lamin a appear to be dispensable in the nuclear lamina. J Clin Invest. 116(3): p. 743-52.2006

38. Jung, H.J., C. Coffinier, Y. Choe, A.P. Beigneux, B.S. Davies, S.H. Yang, R.H. Barnes, 2nd, J. Hong, T. Sun, S.J. Pleasure, S.G. Young, and L.G. Fong, Regulation of prelamin a but not lamin c by mir-9, a brain-specific microrna. Proc Natl Acad Sci U S A. 109(7): p. E423-31.2012

39. Lee, J.M., C. Nobumori, Y. Tu, C. Choi, S.H. Yang, H.J. Jung, T.A. Vickers, F. Rigo, C.F. Bennett, S.G. Young, and L.G. Fong, Modulation of lmna splicing as a strategy to treat prelamin a diseases. J Clin Invest. 126(4): p. 1592-602.2016

40. Bordeleau, F., J.P. Califano, Y.L. Negron Abril, B.N. Mason, D.J. LaValley, S.J. Shin, R.S. Weiss, and C.A. Reinhart-King, Tissue stiffness regulates serine/arginine-rich protein-mediated splicing of the extra domain b-fibronectin isoform in tumors. Proc Natl Acad Sci U S A. 112(27): p. 8314-9.2015

41. Rotsch, C. and M. Radmacher, Drug-induced changes of cytoskeletal structure and mechanics in fibroblasts: An atomic force microscopy study. Biophys J. 78(1): p. 520-35.2000

42. Pan, W., E. Petersen, N. Cai, G. Ma, J. Run Lee, Z. Feng, K. Liao, and K. Leong, Viscoelastic properties of human mesenchymal stem cells. Conf Proc IEEE Eng Med Biol Soc. 5: p. 4854-7.2005

43. Stewart-Hutchinson, P.J., C.M. Hale, D. Wirtz, and D. Hodzic, Structural requirements for the assembly of linc complexes and their function in cellular mechanical stiffness. Exp Cell Res. 314(8): p. 1892-905.2008

44. Makhija, E., D.S. Jokhun, and G.V. Shivashankar, Nuclear deformability and telomere dynamics are regulated by cell geometric constraints. Proc Natl Acad Sci U S A. 113(1): p. E32- 40.2016

45. Ihalainen, T.O., L. Aires, F.A. Herzog, R. Schwartlander, J. Moeller, and V. Vogel, Differential basal-to-apical accessibility of lamin a/c epitopes in the nuclear lamina regulated by changes in cytoskeletal tension. Nat Mater. 14(12): p. 1252-1261.2015

46. Buxboim, A., J. Swift, J. Irianto, K.R. Spinler, P.C. Dingal, A. Athirasala, Y.R. Kao, S. Cho, T. Harada, J.W. Shin, and D.E. Discher, Matrix elasticity regulates lamin-a,c phosphorylation and turnover with feedback to actomyosin. Curr Biol. 24(16): p. 1909-17.2014

47. Hale, C.M., A.L. Shrestha, S.B. Khatau, P.J. Stewart-Hutchinson, L. Hernandez, C.L. Stewart, D. Hodzic, and D. Wirtz, Dysfunctional connections between the nucleus and the actin and microtubule networks in laminopathic models. Biophys J. 95(11): p. 5462-75.2008

48. Ngoka, L.C., Sample prep for proteomics of breast cancer: Proteomics and gene ontology reveal dramatic differences in protein solubilization preferences of radioimmunoprecipitation assay and urea lysis buffers. Proteome Sci. 6: p. 30.2008

4.10 SUPPLEMENTARY INFORMATION

Table S1: Elastic and relaxed moduli, apparent viscosity, and height measurements for NHF, MG-63, KGN, HEK-293T and SH-SY5Y cells

Spread morphology	$E_{elastic}$ (kPa)	E_R (kPa)	μ_{app} (kPa•s)	Height (μm)
NHF	2.4 ± 1.3	1.8 ± 1.0	3.4 ± 2.0	3.9 ± 0.7
MG-63	1.1 ± 0.6	0.8 ± 0.5	2.7 ± 0.9	4.9 ± 1.2
KGN	0.8 ± 0.3	0.5 ± 0.2	1.5 ± 0.9	4.4 ± 1.0
HEK-293T	0.3 ± 0.1	0.2 ± 0.1	0.5 ± 0.3	9.8 ± 4.0
SH-SY5Y	0.2 ± 0.1	0.1 ± 0.1	0.4 ± 0.1	7.0 ± 1.6

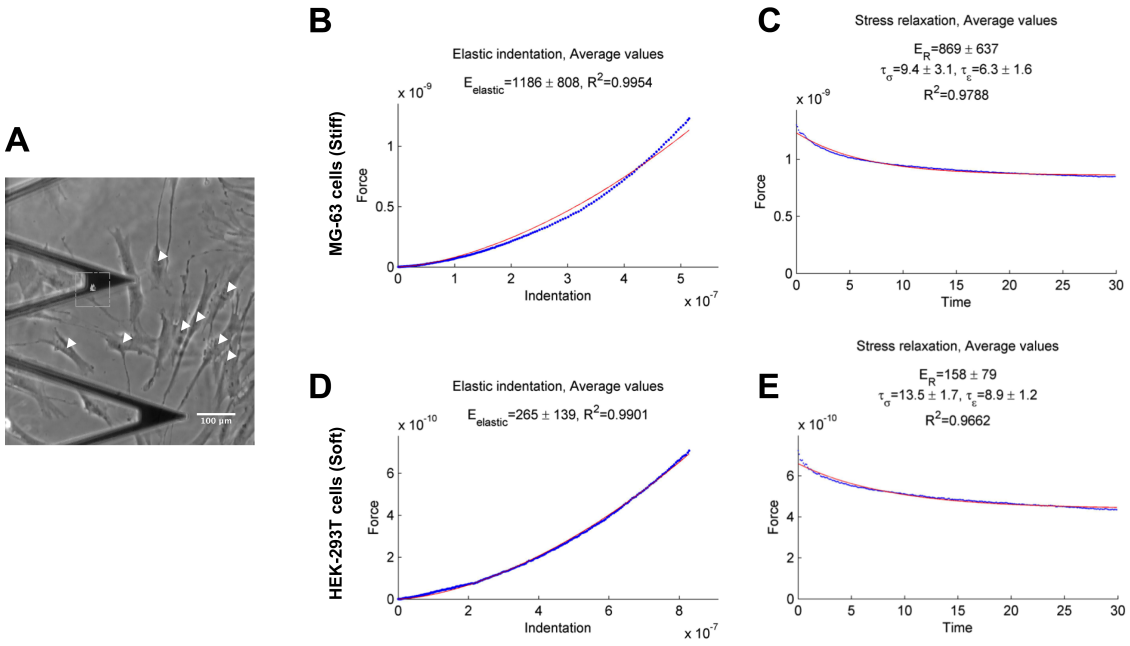

Figure S1: AFM-based force indentation and stress relaxation curves. (A) Representative testing environment on the perinuclear region on a stiff, MG-63 cell to extract elastic and viscoelastic data. Perinuclear region in neighboring cells is indicated by white arrows. Average force vs. indentation curve for (B) MG-63 cells and (D) HEK-293T cells from which elastic moduli were individually extracted using a thin-layer modified Hertz model.[1] Average force vs. time curves for (C) MG-63 cells and (E) HEK-293T cells from which relaxed and instantaneous modulus and apparent viscosity were individually extracted using a modified thin-layer Hertz model.[2] Good quality of fit was evident by high R^2 values associated with each curve.

A

Lysate	TPC (µg/mL) RIPA	SDS+Urea
P7 NHF	525	1278
MG63	583	1040
KGN	718	1203
HEK293T	565	1255
SH-SY5Y	498	1118

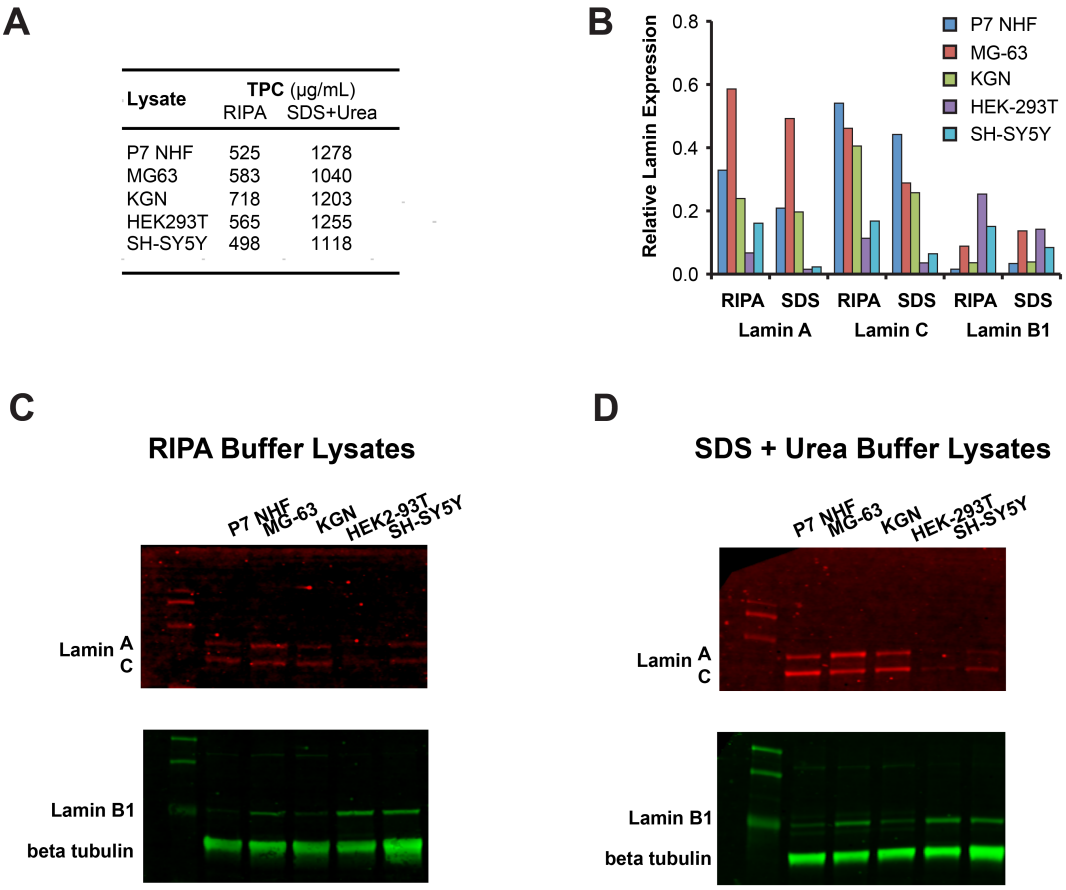

Figure S2: Comparisons between protein lysates extracted with RIPA vs. SDS/urea lysis buffer. (A) BCA assays were conducted to determine total protein concentration (TPC) from near-confluent samples of NHF, MG-63, KGN, HEK293T, and SH-SY5Y protein lysates extracted with either RIPA or SDS/urea (N = 1). Lysates extracted with SDS/urea buffer had, on average, 1.7 times more total protein than lysates extracted with RIPA buffer. (B) Densitometry measurements of protein bands for (C-D) western blots of RIPA and SDS/urea buffer-extracted lysates. Similar protein expression trends were observed regardless of lysis buffer when analyzed using a high-sensitivity, fluorescence-based detection system.

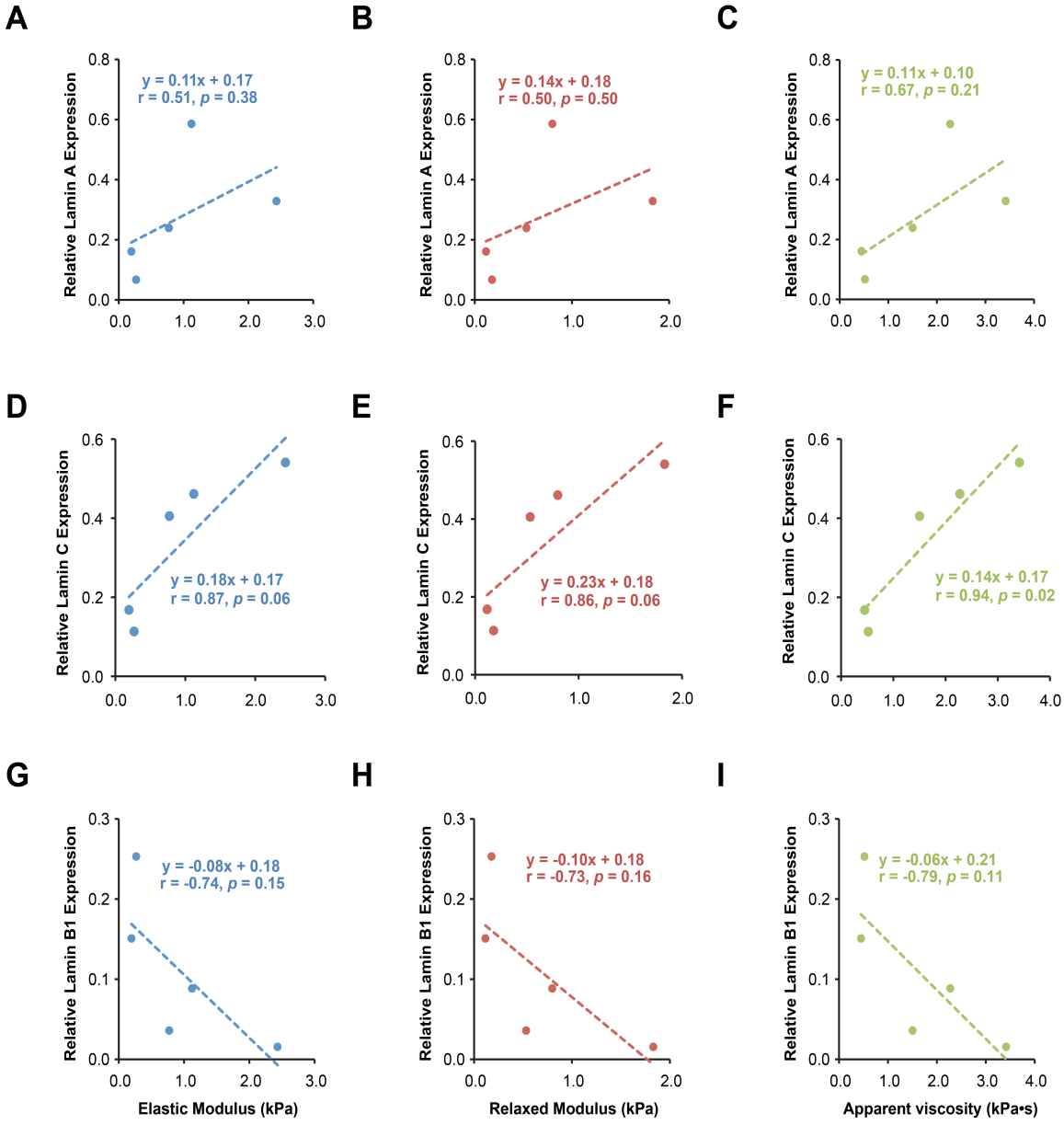

Figure S3: Lamin-mechanical property correlations from lysates extracted using RIPA buffer and detected via fluorescence (N = 1). (A-C) Lamin A protein expression moderately correlated with cellular elastic modulus ($E_{elastic}$), relaxed modulus (E_R), and apparent viscosity (μ_{app}) in a linear fashion, but these correlations were not statistically significant. (D-F) Lamin C protein expression positively correlated to $E_{elastic}$, E_R, and μ_{app}, nearing statistical significance, with Pearson's r coefficients: $r_{Eelastic} = 0.87$ ($p = 0.06$), $r_{ER} = 0.86$ ($p = 0.06$), and $r_{\mu app} = 0.94$ ($p < 0.02$). (G-I) Lamin B1 expression negatively correlated with $E_{elastic}$, E_R, and μ_{app}, and while a clear trend was apparent, these correlations were not statistically significant.

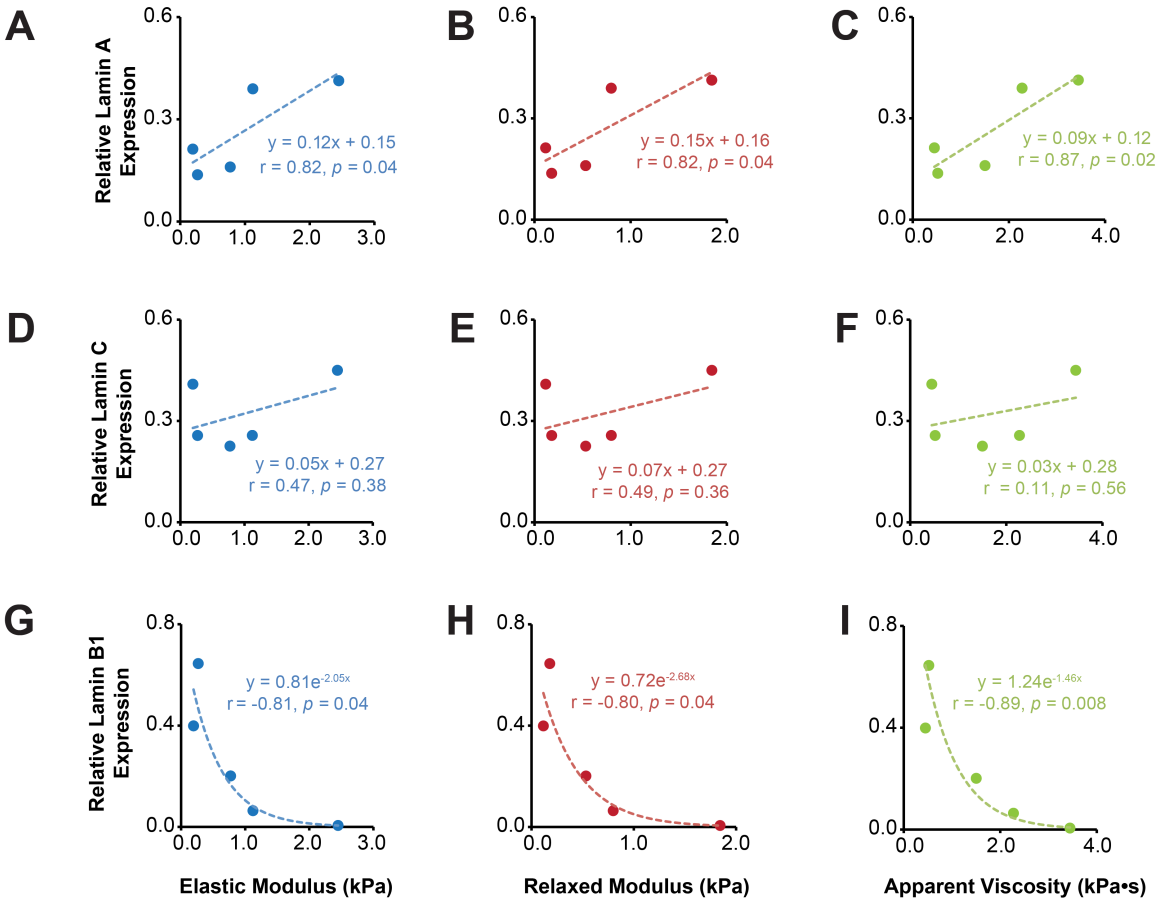

Figure S4: Lamin-mechanical property correlations from lysates extracted using RIPA buffer and detected via chemiluminescence. (A-C) Lamin A protein expression positively correlated with cellular elastic modulus ($E_{elastic}$), relaxed modulus (E_R), and apparent viscosity (μ_{app}) in a statistically significant, linear fashion, with Pearson's r coefficients: $r_{Eelastic} = 0.82$ ($p < 0.05$); $r_{ER} = 0.82$ ($p < 0.05$) and $r_{\mu app} = 0.87$ ($p < 0.05$). (D-F) Lamin C protein expression moderately correlated to $E_{elastic}$, E_R, and μ_{app}, but these correlations were not statistically significant. (G-I) Lamin B1 expression negatively correlated with $E_{elastic}$, E_R, and μ_{app}, exhibiting an inverse exponential relationship, with Pearson's r coefficients: $r_{Eelastic} = -0.81$ ($p < 0.05$); $r_{ER} = -0.80$ ($p < 0.05$) and $r_{\mu app} = -0.89$ ($p < 0.01$). Attention should be given to differences in reported correlations between these data (proteins extracted with RIPA lysis buffer, analyzed by chemiluminescence) and those shown in Figure 2 and S2 (proteins extracted with SDS/urea and RIPA lysis buffer, respectively, analyzed by fluorescence).

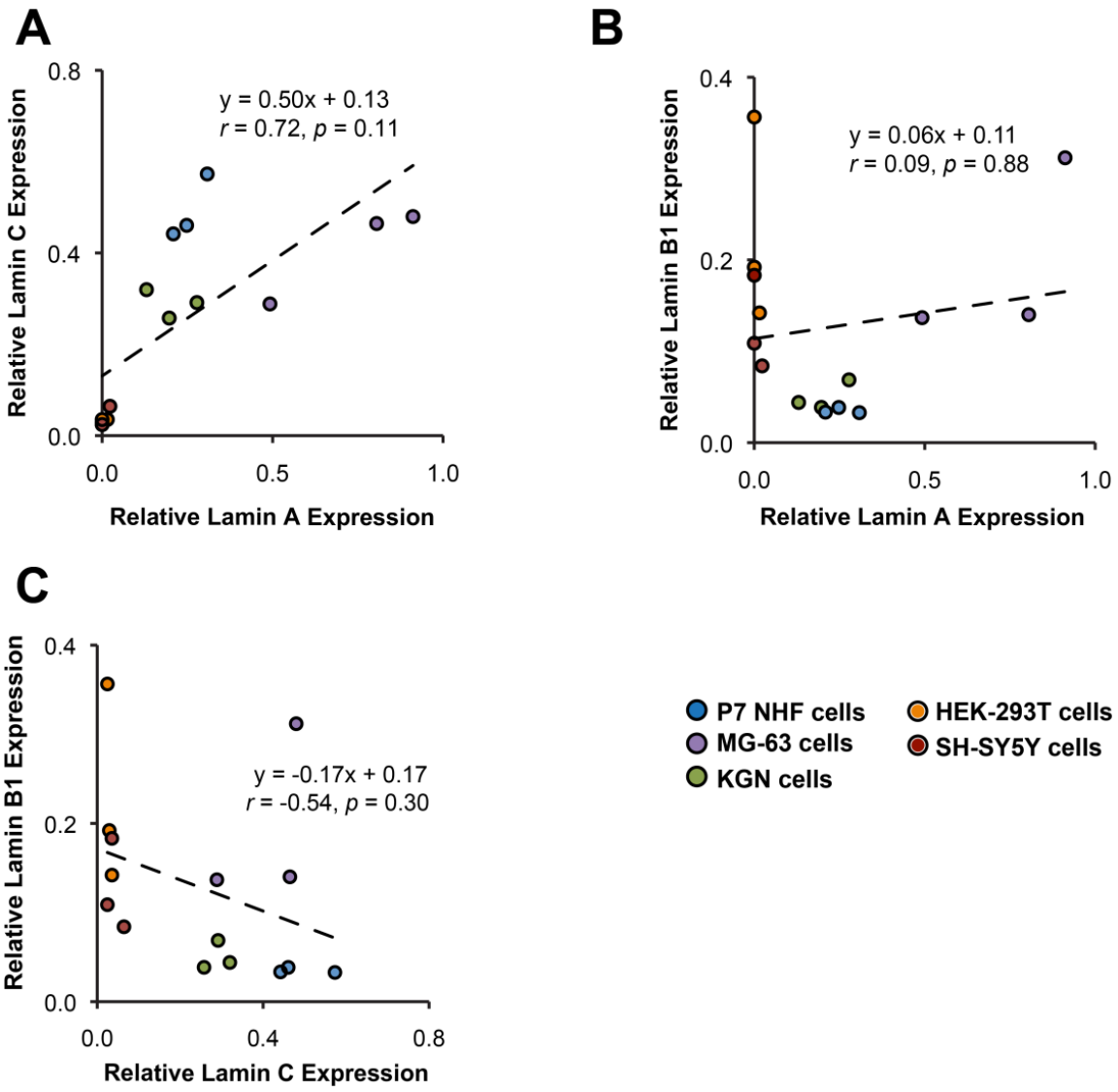

Figure S5: Correlations between the protein expression of (A) lamins C and A, (B) lamins B1 and A, and (C) lamins B1 and C across multiple lineage cell types showed trends indicating a positive relationship between lamins A and C, negative relationship between lamins B1 and C, and no relationship between lamins B1 and A, but no tests were statistically significant. Data points represent lamin protein expression obtained from different SDS-urea treated cell lysates, in triplicate.

REFERENCES

1. Dimitriadis, E.K., F. Horkay, J. Maresca, B. Kachar, and R.S. Chadwick, Determination of elastic moduli of thin layers of soft material using the atomic force microscope. Biophys J. 82(5): p. 2798-810.2002
2. Darling, E.M., S. Zauscher, and F. Guilak, Viscoelastic properties of zonal articular chondrocytes measured by atomic force microscopy. Osteoarthritis Cartilage. 14(6): p. 571-9.2006

CHAPTER 5: CONCLUSION

5.1 CONCLUSION

The body of work presented in this thesis encompasses the use of cellular mechanical properties as phenotypic biomarkers of specific biological scenarios (Chapters 2 & 3) and to validate different macromolecules as biomarkers for mechanophenotype (Chapter 4). It builds on previous studies that demonstrated whole-cell mechanical properties were different between cells of different tissues and that they could be used to predict phenotypic behavior. As a whole, it paves the way for future investigations of high-throughput mechanophenotype using macromolecules that are not only involved in processes mechanotransduction, cell adhesion and cell migration, which are important in process like differentiation and cancer.

Chapter 2 summarizes the study of mechanical characterization of 32 ASC clonal populations with heterogeneous mechanical properties in relation to their lineage-specific differentiation potential. Specifically, it reports moderately strong correlations between stiffer undifferentiated ASCs and their higher preference to undergo osteogenic and chondrogenic differentiation, as evidenced by higher calcium deposition and sulfate glycosaminoglycan production, respectively. It also reports moderately strong correlations between more compliant, undifferentiated ASCs and their higher preference to undergo adipogenesis, as evidenced by higher lipid droplet accumulation. Additionally, its simulated findings suggest that ASCs could differentiate preferentially towards a particular lineage if they have the minimum mechanophenotypic traits associated with that lineage (e.g., E_R > 200 Pa as a threshold for ASCs with osteogenic

lineage or cell height > 12 μm for adipogenic lineages). Prior to this study, elastic and viscoelastic mechanical properties were shown to be different across cells from different tissues and were gaining interest as descriptors in the context of disease and phenotype but their roles as predictors of lineage-specific stem cell differentiation was unknown.[1] At the time of its publication, this study was the first to demonstrate the connection between mechanophenotype of undifferentiated ASCs and their potential to differentiate towards particular lineages.

However, the wide spread use of mechanical properties as biomarkers is limited by the low throughput of the current mechanical testing methods used to measure them, especially when considering some of these methods for clinical applications. While many mechanical testing methods (e.g., AFM, micropipette aspiration, etc.) can provide specific information for the mechanophenotype of single cells, adhesion forces, and test material properties of surface and internal macromolecules and organelles, they work as end-point characterizations (testing environment is unsterile or sample is damaged/destroyed) with limited high-throughput capabilities. To be fair, most of these techniques were not designed for high-throughput characterization or sorting but have nevertheless served to begin lines of investigations where the measured forces or moduli are signatures of the cells or organelles being tested. Having said that, these limitations severely hinder the extrapolation of mechanical properties as mechanophenotypic biomarkers to any studies of clinical importance that require large numbers of living cells that are needed for assays beyond the mechanical characterization phase. Some attempts to increase the throughput of cell mechanical test have been achieved by microfluidic

devices that can perform deformation-based cytometry.[2] Specifically, these devices have been able to test 100 cells/s without labeling cells with antibodies and provide better yields of stiffness-based sorting (and in this sense, mechanical characterization as well) than micropipette aspiration or AFM (1 cell/s for elastic property measurements; 1 cell/30 s for viscoelastic property measurements).[2-4] These devices have been useful to follow cell-cycle changes, rare cell detection, drug response and provide larger numbers for data analysis that may be feasible to answer basic science or proof of concept experiments with enough statistical power.[5, 6] Specifically, these devices seem to be able to differentiate cells with distinct mechanical phenotypes, as shown in studies using devices of this kind to characterize different types of blood cells[7] and could have great potential as medium-throughput sorters or diagnostic tools; perhaps one day, they might rival the throughputs of conventional cell sorters while providing specific mechanical property information. Future advances in this area of research could implement the mechanobiological correlation analysis discussed in Chapter 2 and 4 to include macromolecules or metabolite labeling in combination with deformation-based cytometry to demonstrate the concept that mechanically sorted cells have macromolecules whose presence (or absence) correspond to specific mechanopheotypes.

Chapter 3 expands on the findings reported in Chapter 2 to demonstrate that passage number is an important criteria in the mechanophenotype of cells, which is a finding of great relevance for mechanophenotypic studies using primary cells such as ASCs. Specifically, in the context of ASCs, cells not only change their immunophenotype during passage number but they also change their differentiation

potential preferences. It has been shown by previous researchers that early-passage ASCs have better adipogenic potential than ASCs from later passages. These later-passage ASCs have better osteogenic and chondrogenic potential. Since these findings would suggest that passage number could be targeted as a variable to maximize differentiation potential of ASCs into a particular lineage, the role of mechanical properties could be extremely important in determining whether a batch of cells at a given passage will be successful in differentiation towards a particular lineage. As a result, researchers would know the differentiation potential of a batch of ASCs prior to differentiation based on passage number and mechanical characterization.

Chapter 4 demonstrated that lamin C protein expression is a potential biomarker for whole-cell mechanophenotype. Its expression was significantly different in cells from different lineages (mesenchymal > epithelial > neural) and this difference was concomitant with the distinct mechanical properties exhibited by these cells. The differences in lamin C expression depended on an intact cytoskeleton in stiff but not soft cells and demonstrated that alterations to *LMNA* gene, which is responsible for coding lamin A and C proteins, affect whole-cell mechanophenotype. Lamin C, together with lamin A, have been demonstrated to be important macromolecules for determining mechanical phenotype since the mutations of both proteins make cell nucleui unable to resist deformations that trigger nuclear rupture as well disturb the mechanotransduction cascade. Additionally, lamin A/C proteins are at the center of the mechanotransduction cascade and, therefore, are in part responsible for gene expression modulation triggered by both physical and chemical cues. In the context of stem cell differentiation, lamin A/C

expression increases in osteogenic-inducing environments, whether these environments are modulated by osteogenic/adipogenic media cocktails, stimulation of specific signaling pathways like Wnt or retinoic acid, and/or material compliance effects due to the underlying substrate.[8-13]

The study presented in this chapter is also the first of its own kind to demonstrate that lamin C but not lamin A is the macromolecule with the strongest correlation to whole-cell mechanophenotype. This finding is interesting in the sense that previous studies had placed bigger importance on lamin A[10], despite evidence for lamin C to be an important contributor to mechanical phenotype.[14] In this chapter, it was shown that lamin A was not significantly correlated to whole-cell mechanical properties, as opposed to a previous study. The main differences between that study and the one presented here lies in the protein extraction methods used to obtain nuclear protein content such as lamins, which are known to be hydrophobic proteins and not readily soluble in conventional cell lysis buffers like RIPA.[15] As a result, the reported nuclear lamin concentrations in previous studies were likely underestimated and the conclusions made about them potentially have some degree of inaccuracy. The extraction method use in our study allowed for the extraction of higher protein content, and it is possible the improved approach revealed this trend for lamin C. The study presented in this chapter does have a limitation regarding a low sample number of cell types and it is possible that the relationship between lamin A/C and mechanical properties could change somewhat from what was reported if more cell types were tested. Additionally, the use of lamin C as a biomarker for whole-cell mechanophenotyping is more likely to be successful when

comparing cells exhibiting substantial differences in mechanical properties or lamin profiles, which suggests that cells with similar mechanical properties and lamin profiles will be nearly impossible to discriminate using this marker.

The studies presented in this thesis serve to show that mechanical properties are biomarkers of biological traits or cell fate as well as to cement the role of lamin C as a biomarker that correlates to mechanopehnotype at a whole-cell perspective. However, it strongly suggests that, in order to achieve high-throughput mechanophenotypic characterization of cells, the sorting of cells with distinct mechanical properties still needs to be tied up to biomarkers that not only relate to the mechanophenotype but also to the mechanical phenomena under study. To address these limitations, I propose an alternative approach to discover and validate cell surface markers as novel mechanophenotypic biomarkers based on a combination of proteomics, cell sorting, and AFM-based mechanical characterization. As preliminary supporting evidence for this approach, it is possible to sort cells from a mechanical heterogeneous population (such as ASCs) based on their lamin A/C expression. Since lamin A/C protein, particularly lamin C, has been demonstrated to be a biomarker for mechanophenotype (Chapter 3), one could label mechanically heterogeneous cell populations with lamin A/C antibodies and sort the bottom and top 20% of labeled cells while hypothesizing these two populations exhibit distinct mechanical phenotypes. Specifically, this preliminary hypothesis was tested by expanding ASCs in culture for five passages, fixing them using 4% PFA, labeling them with fluorescently-tagged lamin A/C antibodies and sorting them using FACS. For these cell-sorting experiments, the sorter was programmed to collect only the

top and bottom 20% of cells expressing lamin A/C, as evidenced by the fluorescence associated with high and low gatings. The collected cells were then lysed to extract their whole protein content using the **f**ormaldehyde-fixed, **i**ntracellular **t**arget **s**orting, **a**ntigen **r**etrieval (FITSAR) method (see Apendix B).[16] Once the lysates were collected, a subset of them was analyzed via Western blot to compare the lamin A/C expression between the lysates from the sorted cells. While this pilot assay was just one experimental run, it was found that, as should be expected, ASCs enriched for high-lamin A/C content have more lamin C by western blot than ASCs enriched for low-lamin A/C content. Interestingly, expression differences between lamin A between the two sorted populations are less dramatic. Detailed information on this preliminary run can be found in Appendix A. Another subset of the lysates was sent to a commercial facility for proteomic analysis to analyze the overall protein content of the sorted cells, with particular emphasis on cell surfaces markers that are predominant in cells exhibiting high lamin A/C expression only as well as those expressed in cells exhibiting low lamin A/C expression. With the proteomics results, a series of surface biomarkers can potentially be identified and used to define a surface marker panel for sorting live cells based on their mechanophenotype. Then the sorted cells can be mechanically characterized via AFM to validate that the differences in elastic and viscoelastic properties between the sorted populations based on the presence of these biomarkers (Fig. 1).

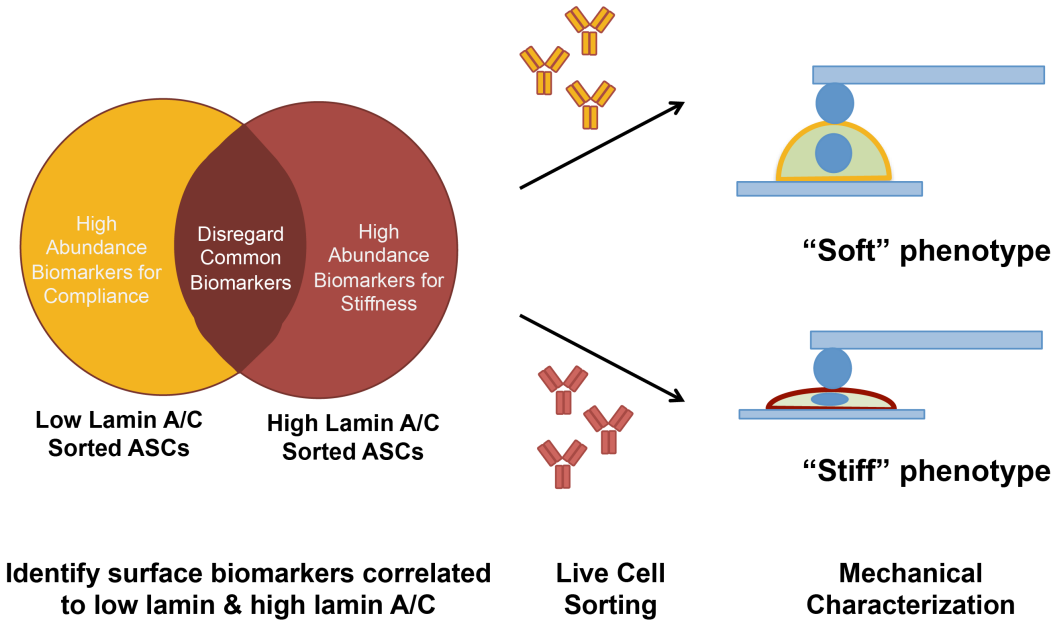

Figure 1. Proposed mechanical validation of cell surface biomarkers identified via proteomics-based analysis. Fixed, lamin A/C-antibody labeled ASCs can sorted via FACS using top and bottom 20% lamin A/C expression thresholds (as determined by fluorescence corresponding to cell counts at those thresholds, see Apendix A) to get ASC populations that are, hypothetically, mechanically distinct from each other (i.e., stiff and soft ASCs). Each sorted population would be lysed to extract proteins using the FITSAR method for protein extraction. The resulting lysates would be subjected to proteomic analysis to determine the identity and abundance of surface proteins that are uniquely expressed in high or low lamin A/C labeled cells. Based on these results, surface marker panels can be defined and used to sort live cells into populations whose mechanophenotype can be validated using mechanical testing methods such as AFM-based single cell indentations.

Once these biomarkers are validated as reliable mechanophenotypic descriptors, the makers could be used to sort cells from heterogeneous populations in large numbers, knowing that the sorted populations have differences in mechanophenotype. Furthermore, other markers that are of biological significance to the cells under study can be incorporated with the validated mechanical biomarkers for more specific sorting schemes in studies involving living cells.

5.2 REFERENCES

1. Darling, E.M., M. Topel, S. Zauscher, T.P. Vail, and F. Guilak, Viscoelastic properties of human mesenchymally-derived stem cells and primary osteoblasts, chondrocytes, and adipocytes. J Biomech. 41(2): p. 454-64.2008

2. Otto, O., P. Rosendahl, A. Mietke, S. Golfier, C. Herold, D. Klaue, S. Girardo, S. Pagliara, A. Ekpenyong, A. Jacobi, M. Wobus, N. Topfner, U.F. Keyser, J. Mansfeld, E. Fischer-Friedrich, and J. Guck, Real-time deformability cytometry: On-the-fly cell mechanical phenotyping. Nat Methods. 12(3): p. 199-202, 4 p following 202.2015

3. Gonzalez-Cruz, R.D., V.C. Fonseca, and E.M. Darling, Cellular mechanical properties reflect the differentiation potential of adipose-derived mesenchymal stem cells. Proc Natl Acad Sci U S A. 109(24): p. E1523-9.2012

4. Hogan, B., A. Babataheri, Y. Hwang, A.I. Barakat, and J. Husson, Characterizing cell adhesion by using micropipette aspiration. Biophys J. 109(2): p. 209-19.2015

5. Gossett, D.R., W.M. Weaver, A.J. Mach, S.C. Hur, H.T. Tse, W. Lee, H. Amini, and D. Di Carlo, Label-free cell separation and sorting in microfluidic systems. Anal Bioanal Chem. 397(8): p. 3249-67.2010

6. Gossett, D.R., H.T. Tse, S.A. Lee, Y. Ying, A.G. Lindgren, O.O. Yang, J. Rao, A.T. Clark, and D. Di Carlo, Hydrodynamic stretching of single cells for large population mechanical phenotyping. Proc Natl Acad Sci U S A. 109(20): p. 7630-5.2012

7. Toepfner, N., C. Herold, O. Otto, P. Rosendahl, A. Jacobi, M. Krater, J. Stachele, L. Menschner, M. Herbig, L. Ciuffreda, L. Ranford-Cartwright, M. Grzybek, U. Coskun, E. Reithuber, G. Garriss, P. Mellroth, B. Henriques-Normark, N. Tregay, M. Suttorp, M.

Bornhauser, E.R. Chilvers, R. Berner, and J. Guck, Detection of human disease conditions by single-cell morpho-rheological phenotyping of blood. Elife. 7.2018

8. Bermeo, S., C. Vidal, H. Zhou, and G. Duque, Lamin a/c acts as an essential factor in mesenchymal stem cell differentiation through the regulation of the dynamics of the wnt/beta-catenin pathway. J Cell Biochem. 116(10): p. 2344-53.2015

9. Du, J., Y. Zu, J. Li, S. Du, Y. Xu, L. Zhang, L. Jiang, Z. Wang, S. Chien, and C. Yang, Extracellular matrix stiffness dictates wnt expression through integrin pathway. Sci Rep. 6: p. 20395.2016

10. Swift, J., I.L. Ivanovska, A. Buxboim, T. Harada, P.C. Dingal, J. Pinter, J.D. Pajerowski, K.R. Spinler, J.W. Shin, M. Tewari, F. Rehfeldt, D.W. Speicher, and D.E. Discher, Nuclear lamin-a scales with tissue stiffness and enhances matrix-directed differentiation. Science. 341(6149): p. 1240104.2013

11. Buxboim, A., J. Swift, J. Irianto, K.R. Spinler, P.C. Dingal, A. Athirasala, Y.R. Kao, S. Cho, T. Harada, J.W. Shin, and D.E. Discher, Matrix elasticity regulates lamin-a,c phosphorylation and turnover with feedback to actomyosin. Curr Biol. 24(16): p. 1909-17.2014

12. Swift, J. and D.E. Discher, The nuclear lamina is mechano-responsive to ecm elasticity in mature tissue. J Cell Sci. 127(Pt 14): p. 3005-15.2014

13. Ivanovska, I.L., J. Swift, K. Spinler, D. Dingal, S. Cho, and D.E. Discher, Cross-linked matrix rigidity and soluble retinoids synergize in nuclear lamina regulation of stem cell differentiation. Mol Biol Cell. 28(14): p. 2010-2022.2017

14. Lammerding, J., L.G. Fong, J.Y. Ji, K. Reue, C.L. Stewart, S.G. Young, and R.T. Lee, Lamins a and c but not lamin b1 regulate nuclear mechanics. J Biol Chem. 281(35): p. 25768-80.2006

15. Janes, K.A., An analysis of critical factors for quantitative immunoblotting. Sci Signal. 8(371): p. rs2.2015

16. Sadick, J.S., M.E. Boutin, D. Hoffman-Kim, and E.M. Darling, Protein characterization of intracellular target-sorted, formalin-fixed cell subpopulations. Sci Rep. 6: p. 33999.2016

Appendix A

Effects of *LMNA* gene silencing on whole-cell mechanophenotype of ASCs

A.1 INTRODUCTION

Nuclear lamin proteins A and C have been shown to be involved in the mechanical properties of microtissues and cellular mechanotransduction. These two proteins arise from two *LMNA* mRNA splice variants that are encoded by the *LMNA* gene. Cells with mutations in the *LMNA* gene exhibit aberrant mechanotransduction, and have nuclei with enhanced deformability due to either the absence or faulty production of lamins A and C, which is a mechanophenotypic feature of a series of diseases called laminopathies. The *LMNA* gene expression is also responsive to changes in the cells' mechanical environment, such as alterations in the substrate's stiffness, and can be different between cells with drastic differences in their elastic and viscoelastic properties. Furthermore, stem cells differentiating towards stiffer cell types, such as osteoblasts, exhibit an increase in *LMNA* gene expression that is concomitant to upregulation of osteogenic gene expression. Additionally, metastatic cells exhibit changes in their *LMNA* gene expression that are consistent with the cells' potential to migrate into other tissues. Altogether, this body of research demonstrates that *LMNA* gene expression can affect mechanophenotypic traits in a number of different cell scenarios.

In this thesis, it was shown in Chapter 4 that cells with distinct mechanical properties exhibit differences in lamin A/C expression, with lamin C exhibiting the highest correlation to whole-cell elastic and viscoelastic properties. It was also shown that lamin A/C proteins are expressed in greater amounts in stiffer cells than in softer cells and that downregulation of *LMNA* gene reduce both elastic and viscoelastic properties in stiff cells. Given the evidence that lamin C can serve as a potential

mechanical biomarker for whole-cell mechanophenotype, we wanted to know if cells with differences in mechanical properties could exhibit differences in lamin A/C and therefore propose lamin A/C-based ASC sorting experiments. We tested the feasibility of lamin A/C-based sorting of ASCs was tested by subjecting subsets of ASCs to *LMNA* gene downregulation via *LMNA* siRNA treatments and then observing their lamin A/C profile using flow cytometry. Differences in lamin A/C expression were detected between treated and non-treated ASCs based on flow cytometry profiles. Additionally, we confirmed their differences in whole-cell mechanophenotype using AFM-single cell indentation experiments. Therefore, lamin A/C can be used to distinguish between mechanically distinct populations and is a good biomarker for flow cytometry experiments.

A.2 METHODS

A.2.1 ASC isolation and culture

ASCs were isolated from human lipoaspirate tissue obtained from collaborators at Rhode Island following an approved protocol (IRB Registration #0000396, 00004624, CMTT/PROJ: 210312). 100 mL of lipoaspirate tissue were extracted and processed from the axillary region of a consenting female donor experiencing symptomatic macromastia (age 34). To isolate the stromal vascular fraction (SVF) containing the ASCs, lipoaspirate adipose tissue samples were washed 3-5x times in equal volumes of phosphate buffered saline (PBS 1X) warmed to 37˚C to remove blood and tumescent fluid. Following these washes, the tissue samples were digested with equal volumes of a collagenase solution

(0.1% w/v collagenase, 1% v/v bovine serum albumin fraction V (BSA, Invitrogen), and 2mM calcium chloride) diluted in PBS 1X while shaking for 1 hour at 37˚C. The digested tissue samples were then centrifuged at 300g for 5 minutes at room temperature. The resulting supernatant was aspirated and discarded while the remaining cell pellet was resuspended in stromal media (DMEM/F-12, 10% fetal bovine serum (FBS, Zen-Bio), and 1% antibiotic/antimycotic (A/A)). The resuspended cells were filtered sequentially through 100 μM and 70 μM filters, centrifuged again as mentioned above and resuspended in red blood cell lysis buffer (155 mM ammonium chloride, 10 mM potassium carbonate, 0.1 mM EDTA) for 10 minutes at room temperature and centrifuged at 400g. Then the cells were resuspended in stromal media to a concentration of 5.7 x 10^6 cells/mL and either frozen using ASC freezing media (80% FBS, 10% stromal media and 10% dimethyl sulfoxide) and stored at -80˚C or plated at that concentration in T-182 flasks containing ASC expansion media (80% DMEM/F-12, 10% FBS, 5 ng/ml human epidermal growth factor, 1 ng/mL recombinant human fibroblastic growth factor, 0.25 ng/mL transforming growth factor beta-1 and 1% A.A). ASCs were passaged 5 times in expansion media and grown to 90% confluence to prior to experiments.

A.2.2 *LMNA* gene knockdown experiments and flow cytometry experiments

P5 ASCs were treated with either 50 nM *LMNA* siRNA (*siLMNA*, s8221, 4390824, sense: 5′-CCAAAAAGCGCAAACUGGATT-3′, antisense: 5′-UCCAGUUUGCGCUUUUUGGTG-3′, *LMNA* Silencer Select Validated siRNA, Ambion, Thermo Fisher Scientific) or 50 nM Scramble siRNA (siScramble, 4390843,

Silencer Select Negative Control #1 siRNA, Ambion, Thermo Fisher Scientific) for 72 hours before mechanical testing. Sample sizes for mechanical characterization of all cell types are as follows: untreated ASCs (n = 47), *siScramble*-treated ASCs (n = 49), and *siLMNA*-treated ASCs (n = 56). Once the siRNA treatments were completed, ASCs were uplifted, fixed with 4% paraformaldehyde. Fixed ASCs were permeabilized using 1% v/v Triton X-100 (Fisher Scientific)/PBS 1X for 15 minutes at room temperature, blocked with 3% v/v BSA/PBS 1X for 1 hour, and then incubated with Alexa Fluor 488-conjugated mouse anti-human lamin A/C primary antibody (4C11, 8617S, Cell Signaling Technology) at a 1:50 dilution in 1% v/v BSA/PBS 1X. Lamin A/C expression profiles for untreated, si*Scramble*- and si*LMNA*-treated ASCs, either unlabeled or labeled with with fluorescently-tagged lamin A/C antibody, were obtained using a Guava easyCyte flow cytometer that has a 488nm blue laser and 642nm red laser (Millipore Sigma, MA). A total of 10,000 cell events were counted for each sample subjected to flow cytometry.

A.2.3 AFM-based mechanical characterization

AFM-based, single cell indentation tests were used to measure whole-cell mechanical properties (MFP-3D-Bio, Asylum Research, CA). Spherically tipped cantilevers (diameter = 5 μm, Novascan Technologies, IA) had a nominal stiffness of k = 0.03 N/m. Cells were indented over the perinuclear region at a constant indentation velocity of 10 μm/s using a force trigger of 1 nN, yielding cell strains < 10%. Stress relaxation experiments maintained an approximately constant indentation for 30 seconds prior to retracting. Indentation and force data were used to determine cellular elasticity ($E_{elastic}$) and viscoelasticity (relaxed modulus, E_R; and apparent viscosity, μ_{app}) using a modified

Hertz contact model and thin-layer stress relaxation model, as mentioned in Chapters 2 and 4.

A.3 RESULTS

ASCs treated with 50 nM *LMNA* siRNA exhibited a softer phenotype than untreated and siScramble-treated ASCs. Similarly, si*LMNA*-treated ASCs also displayed a shift in their lamin A/C expression profiles towards lower fluorescence when compared to siScramble-treated ASCs. This shift in lamin A/C profile was observed for 39± 2 % of si*LMNA*-treated cells. However, the *LMNA* gene silencing procedure was observed in all treated ASCs since not widely successful since a population of the lamin A/C-labeled, si*LMNA*-treated cells displayed fluorescence levels with 61% si*LMNA*-treated ASCs display a noticeable difference in their lamin A/C profiles when compared to si*Scramble*-treated ASCs while 39% of si*LMNA*-treated ASCs displayed lamin A/C expression profiles that were similar to si*Scramble*-treated ASCs.

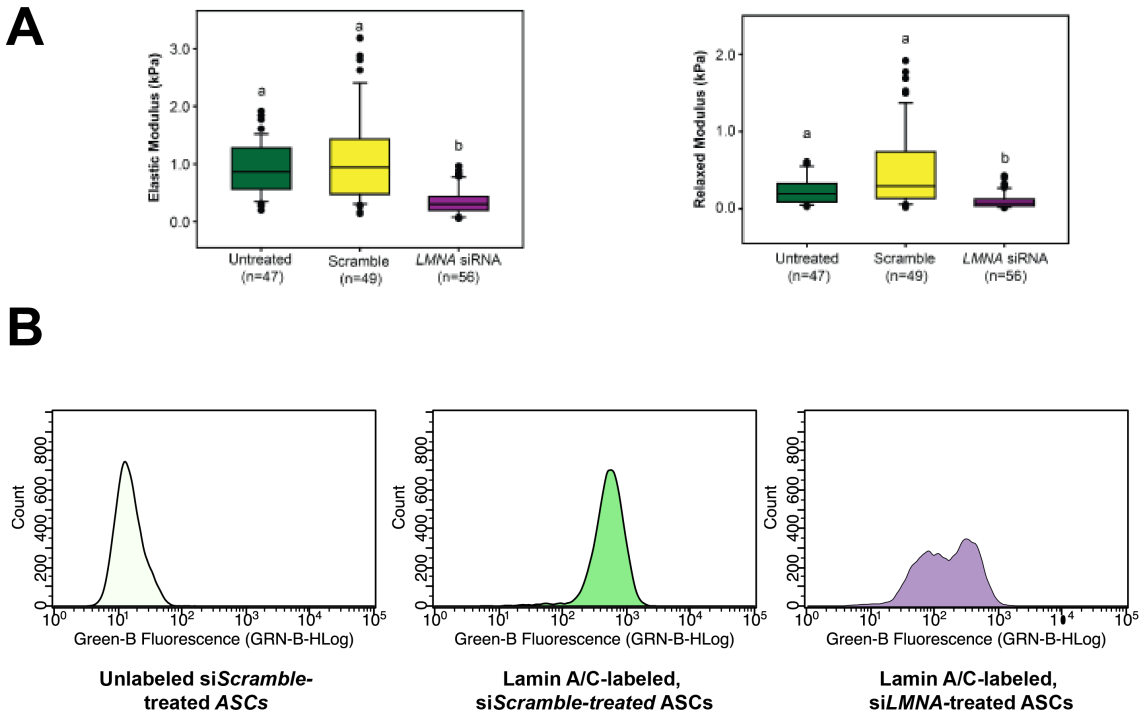

Figure A.1: *LMNA* siRNA treatment alters mechanical properties and lamin A/C expression profiles in adipose-derived stem cells (A-B). AFM-based single cell indentation experiments were used to determine the elastic and viscoelastic properties of untreated, 50 nM siScramble-treated and 50 nM siLMNA-treated ASCs. Data shown as median±interquartile range (A).

A.4 DISCUSSION

Lamin A/C protein expression has been demonstrated to be important for cellular mechanotransduction in previous studies and in this thesis, lamin C was found to exhibit the strongest correlation to whole-cell mechanophenotype. Those findings strongly suggest lamin C could be a novel biomarker for whole-cell mechanophenotyping. In this appendix, it was hypothesized that altering the lamin A/C expression via *LMNA* siRNA knockdown could not only affect whole-cell mechanophenotype but also demonstrate that mechanically distinct cells would be detected differently in a flow cytometry experiment. It was shown that si*LMNA*-treated ASCs had a more compliant phenotype as well as

lower lamin A/C expression profile that are different from untreated, stiffer ASCs. Therefore, it is possible to resolve drastic differences in lamin A/C expression between mechanically heterogeneous populations using flow cytometry. Consequently, these findings pave the way to use lamin A/C as biomarker for high-throughput cell sorting of cells based on their mechanophenotype.

Appendix B

Lamin A/C-based cell sorting and protein extraction from fixed ASCs

B.1 INTRODUCTION

Nuclear lamin proteins A and C have been shown to be important in mechanotransduction, mechanophenotype and cell differentiation processes. They are important to impart nuclear resistance to deformation, transduce mechanical cues from the local microenvironment and alter gene expression to initiate genetic programming in stem cells. Because of their involvement in all these process, lamin A/C proteins could be used as biomarkers of mechanophenotype and as indicators of stem cell fate. In fact, lamin A/C has been demonstrated to serve as a potential biomarker for whole-cell mechanophenotype in Chapter 4 of this thesis and as a protein whose expression scale with tissue microelasticity by others.[1] However, use of these proteins as biomarkers for mechanophenotype is limited to fixed cells since lamin A/C protein labeling with fluorescent antibodies requires cell fixation and plasma/nuclear membrane permeabilization. As a result, most studies using antibodies to label lamin A/C can only serve as end-point, diagnostic markers.

To circumvent this limitation, alternative biomarkers need to be identified. These biomarkers need to be cell surface markers because that would allow labeling and sorting of live cells. Given that there are many cell surface proteins in the plasma membrane, finding a minimum number of potential surface markers to create a mechanophenotype-based surface marker panel can be daunting. It is possible to identify molecules known to affect mechanotransduction processes such as integrins and cadherins but there could be other undiscovered molecules that are important to impart mechanophenotype as well.

This is particularly important in the context of stem cell differentiation or disease because both proteins involved in mechanotransduction/mechanophenotype and differentiation/malignancy may undergo expression changes in a similar fashion or at a similar time. Therefore, an evaluation of the entire proteome is required to identify the most abundant markers that play a role in context-oriented mechanophenotype, with the context in this thesis being limited to stem cell differentiation potential.

It is possible to look at the entire protein expression profile of ASCs in their undifferentiated state as well as undergoing adipogenic[2, 3] and osteogenic differentiation[4, 5] using proteomic analysis. For any proteomics analysis, a critical requirement is to extract enough protein of interest from the cells or tissues under study (Fig. A1). To accomplish this extraction, living or fixed cells and tissues are lysed using different techniques to extract proteins that can either yield whole-protein lysates or proteins from specific cellular compartments. The obtained protein lysates are still very complex to be analyzed in that fashion so they are further processed by either separation of proteins from lysates using isometric point-based, two dimensional electrophoretic (2DE) gel separations followed by in-gel, trypsin-mediated digestion or direct trypsin-mediated digestion of lysates following by liquid chromatographic-based (LC) separations.[6] The choice of protein separation and fragmentation is dependent of depth of analysis required, sensitivity of samples, types of proteins that are the focus of studies, etc. Regardless of the selected fractionation method, each method yields tryptic peptide fragments that can be identified and quantified in relation to the original proteins from which they are obtained because of the unique lysine and arginine residues each peptide fragment

exhibits after digestion. To be able to identify quantify these peptides, the digested peptides are ionized using techniques like matrix-assisted, laser desorption ionization-time of flight (MALDI-TOF) or mass spectrometry (MS). In this step, a laser ionizes the peptides and the generated ions have a specific mass to charge (*m/z*) ratio that is unique to each peptide and can be used as "protein fingerprinting" to qualitatively determine if a protein is expressed in the lysates under study. Additionally, the measurement of the detected ion intensities in relation to their m/z ratios can provide quantitative information about the relative abundance of each peptide, which is useful to determine which proteins are highly expressed in the peptides obtained from the cell or tissue lysates. Depending on the depth of the analysis, different parts of these stages can be combined.

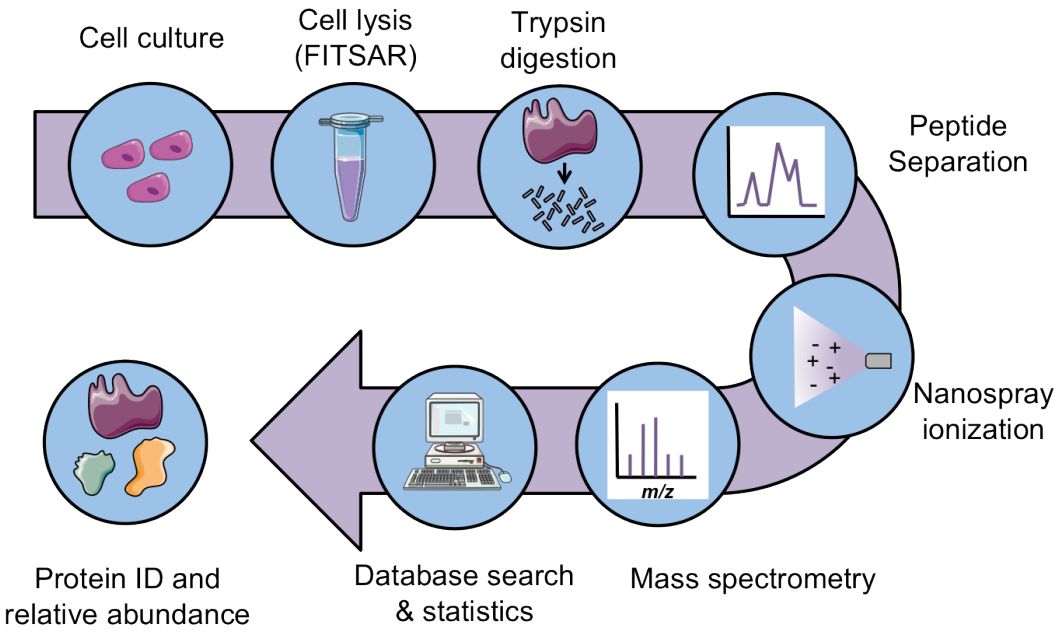

Based on Sadick, JS et al. Sci. Rep. 2016

Figure A.1 Schematic of sample preparation and workflow for proteomics analysis.

While these analyses are typically done using lysates from living cells, it is also possible to extract protein lysates from fixed cells and tissues. However, protein lysates from fixed lysates have additional challenges than lysates obtained from live cells or

tissues. As part of the fixation process, fixative agents such as formaldehyde and formalin bind to the free amines of protein residues and can create chemical crosslinks between different peptide residues. Because of this mode of interaction, these fixative agents prevent analysis of protein fragments because these fixative molecules block any potential amine reaction sites. Therefore, the antigen sites from these proteins must be retrieved if any further fractionation analyses are to be expected.

To circumvent this limitation, researchers have investigated ways to remove the formaldehyde and formalin molecules post fixation and have been successful in retrieving the reaction sites. One such method, formaldehyde-fixed intracellular target antigen retrieval (FITSAR), consists of suspending fixed cell/tissue pellets in a detergent-containing buffer followed by subjecting them to heat-induced denaturation.[7] The use of detergents and denaturation help to decouple the formaldehyde molecules from the peptide residues they are bound to and assist in protein unfolding so that all proteins in the lysate are in their primary structure. This process is important for maximizing sites of interaction for the trypsin digestion. As a later step, the detergent, which in this case imparts a net negative charge to the protein molecules, is removed via column purification to allow proteins to regain their native charges. This step is important for allowing success in the ionizaton portion of the proteomic analysis.

B.2 METHODS

B.2.1 ASC isolation and culture

ASCs were isolated from human lipoaspirate tissue obtained from collaborators at Rhode Island following an approved protocol (IRB Registration #0000396, 00004624, CMTT/PROJ: 210312). 100 mL of lipoaspirate tissue were extracted and processed from the axillary region of a consenting female donor experiencing symptomatic macromastia (age 34). To isolate the stromal vascular fraction (SVF) containing the ASCs, lipoaspirate adipose tissue samples were washed 3-5x times in equal volumes of phosphate buffered saline (PBS 1X) warmed to 37˚C to remove blood and tumescent fluid. Following these washes, the tissue samples were digested with equal volumes of a collagenase solution (0.1% w/v collagenase, 1% v/v bovine serum albumin fraction V (BSA, Invitrogen), and 2mM calcium chloride) diluted in PBS 1X while shaking for 1 hour at 37˚C. The digested tissue samples were then centrifuged at 300g for 5 minutes at room temperature. The resulting supernatant was aspirated and discarded while the remaining cell pellet was resuspended in stromal media (DMEM/F-12, 10% fetal bovine serum (FBS, Zen-Bio), and 1% antibiotic/antimycotic (A/A)). The resuspended cells were filtered sequentially through 100 μM and 70 μM filters, centrifuged again as mentioned above and resuspended in red blood cell lysis buffer (155 mM ammonium chloride, 10 mM potassium carbonate, 0.1 mM EDTA) for 10 minutes at room temperature and centrifuged at 400g. Then the cells were resuspended in stromal media to a concentration of 5.7 x 10^6 cells/mL and either frozen using ASC freezing media (80% FBS, 10% stromal media and 10% dimethyl sulfoxide) and stored at -80˚C or plated at that

concentration in T-182 flasks containing ASC expansion media (80% DMEM/F-12, 10% FBS, 5 ng/ml human epidermal growth factor, 1 ng/mL recombinant human fibroblastic growth factor, 0.25 ng/mL transforming growth factor beta-1 and 1% A.A). ASCs were passaged 5 times in expansion media prior to experiments. A subset of the cultured cells had their culture media replace with serum-free expansion media for 16 hours before uplifting the cells.[8, 9] This serum-free expansion media incubation step was important for preventing signaling swamping of cell-associated proteins by widely abundant serum proteins in the proteomics experiments mentioned below.

B.2.2 Lamin A/C-based cell sorting

Upon reaching 90% confluency, cells were uplifted by incubating them in Accutase™ (Fisher Scientific) for 30 min at 37ºC. The cells were resuspended in serum-free media, counted, and fixed in 4% paraformaldehyde (in PBS 1X) for 10 min at room temperature. A total of four, triplicate ASC samples were uplifted, which provided an average of 38 million cells/sample. Fixed ASCs were permeabilized using 1% v/v Triton X-100 (Fisher Scientific)/PBS 1X for 15 minutes at room temperature, blocked with 3% v/v BSA/PBS 1X for 1 hour, and then incubated with Alexa Fluor 488-conjugated mouse anti-human lamin A/C primary antibody (4C11, 8617S, Cell Signaling Technology) at a 1:50 dilution in 1% v/v BSA/PBS 1X. Lamin A/C antibody-tagged ASCs were sorted using a BD FACSAria Ilu instrument (BD Biosciences). Cells were sorted at a concentration of 10 million cells/mL and at a rate of 2500 cells/s. Specific gates were set to collect the top and bottom 20% of fluorescent ASCs, classified as high and low lamin A/C expressing groups, respectively. Unlabeled ASCs were also subjected to FACS-

based cell sorting to obtain an estimate of background fluorescence. To determine the purity of the top and bottom 20% sorting threshold, aliquots of 10,000 cells were taken from each sample and resorted using the same thresholds. Cell sorting data were analyzed using FlowJo FACS analysis software (TreeStar, Inc., Portland, OR, USA).

B.2.3 Protein extraction from fixed, lamin A/C sorted ASCs

Protein extraction from fixed, lamin A/C-sorted ASCs was achieved via the formaldehyde-fixed, intracellular target-sorted antigen retrieval (FITSAR) method. Briefly, fixed, high-and low-lamin A/C sorted ASCs were lysed by incubating the lysates in 300 mM Tris HCl, pH = 8.0 with 2% v/v SDS at 100ºC for 30 minutes, followed by 60ºC for 2 hours. The samples were centrifuged at 16000g for 10 minutes at 4ºC. The resulting lysate supernatants for each sample were subjected to BCA assay to determine their total protein concentration. Aliquots from these lysates corresponding to 5 µg of total protein were used in Western blot assays with densitrometric analysis to determine relative protein expression (n=1) while aliquots corresponding to 30 µg were stored at -80ºC until they were ready to be sent to a proteomics facility for whole-cell proteomic analysis.

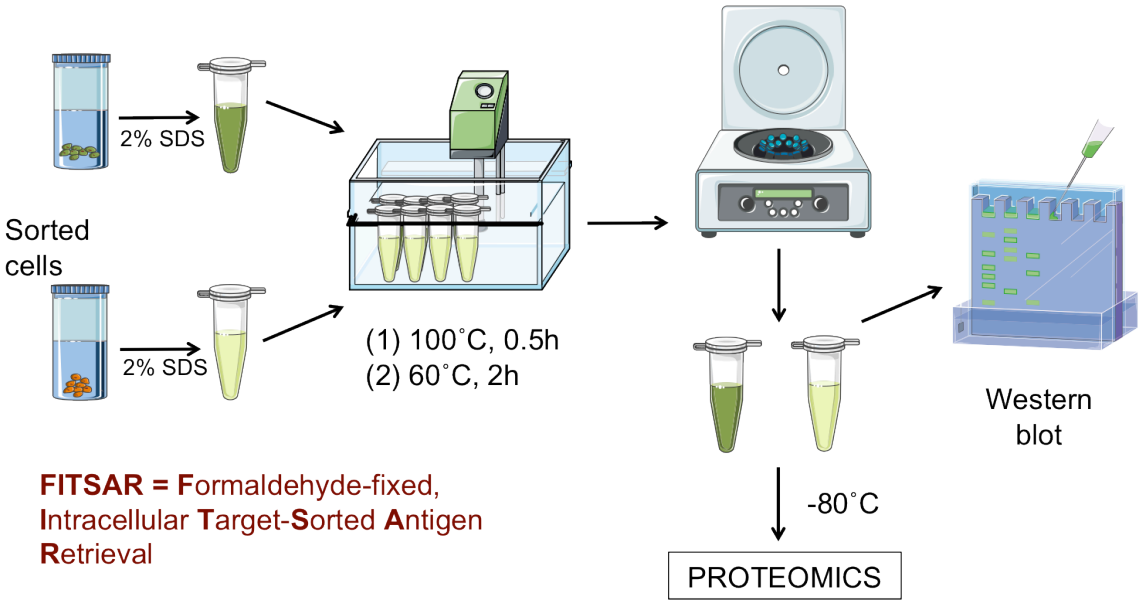

B.3 RESULTS

B.3.1 Lamin A/C-based sorting of ASCs

ASCs enriched based on their lamin A/C expression for the top and bottom 20% cutoffs yielded two cell populations with different lamin A/C expressions (Fig. B2, A–B). An average of 38 million cells were sorted into high and low lamin A/C and the cell loss associated with the sorting scheme was reflected in the sorted populations (Table B1). Specifically, an average of 3.87 millions of ASCs were collected by sorting cells above the top 20% threshold, which represents a cell loss of 50%. Similarly, an average of 3.94 million ASCs were collected by sorting cells below the bottom 20% threshold, which represents a cell loss of 49.2%.

Table B1: Lamin A/C-based ASC sorting cell counts

Samples	Unsorted Cells	High LA/C	Low LA/C	% Loss Top 20	% Loss Bot 20
S1	41×10^6	6×10^6	6×10^6	24	24
S2	38×10^6	3×10^6	3×10^6	64	60
S3	36×10^6	3×10^6	3×10^6	52	52
S4	38×10^6	3×10^6	3×10^6	61	61
Average	38×10^6	4×10^6	4×10^6	50	49

Table B1. Four samples averaging 38 millions cells were subjected to a cell sorting scheme where cells were sorted based on their high and low lamin A/C protein expression. To capture the groups with the biggest differences in lamin A/C expression, the top and bottom 20% of fluorescent cells (or lamin A/C expressing cells) were collected for proteomic analysis.

The purity of this sorting scheme was verified by performing purity checks for the lamin A/C of top and bottom 20% sorted cells. These purity checks consisted on taking 10,000 cells from the high and low lamin A/C-sorted populations and running them through the cell sorter a second time to analyze their distribution with respect to the top and bottom 20% pre-established thresholds (Fig. B2, C–D). By analyzing the purity check data, one can see that most cells sorted on the bottom 20% threshold exhibited lamin A/C expression consistent with that threshold; in other words, cells sorted in the bottom 20% of lamin A/C have low-lamin A/C expression. However, cells that were sorted on the top 20% threshold exhibited a broader distribution of fluorescence values. While this top 20% cell distribution does not substantially overlap with the cell population for the bottom 20% threshold, it suggests that the top 20 of sorted cells still exhibit greater variability in the measured lamin A/C expression within that grouping. This latter result could suggest that the top 20% lamin A/C-sorted cells have subpopulations of cells exhibiting both intermediate and high lamin A/C expression levels or that fluorescence detection at the higher end is less consistent from run-to-run.

B.3.2 Protein expression of high and low lamin A/C-expressing ASCs

Western blot assays of the high and low-lamin A/C sorted cell lysates indicated differences in lamin A and C expression between high and low lamin A/C sorted ASCs (Fig. B3, A–B) While this Western blot pilot run did not provide enough samples to make statistical comparisons, the expression of lamin C seemed to be quite different between high and low lamin A/C-sorted ASCs. Lamin A protein expression, however, was not drastically different between high and low lamin A/C-sorted ASCs.

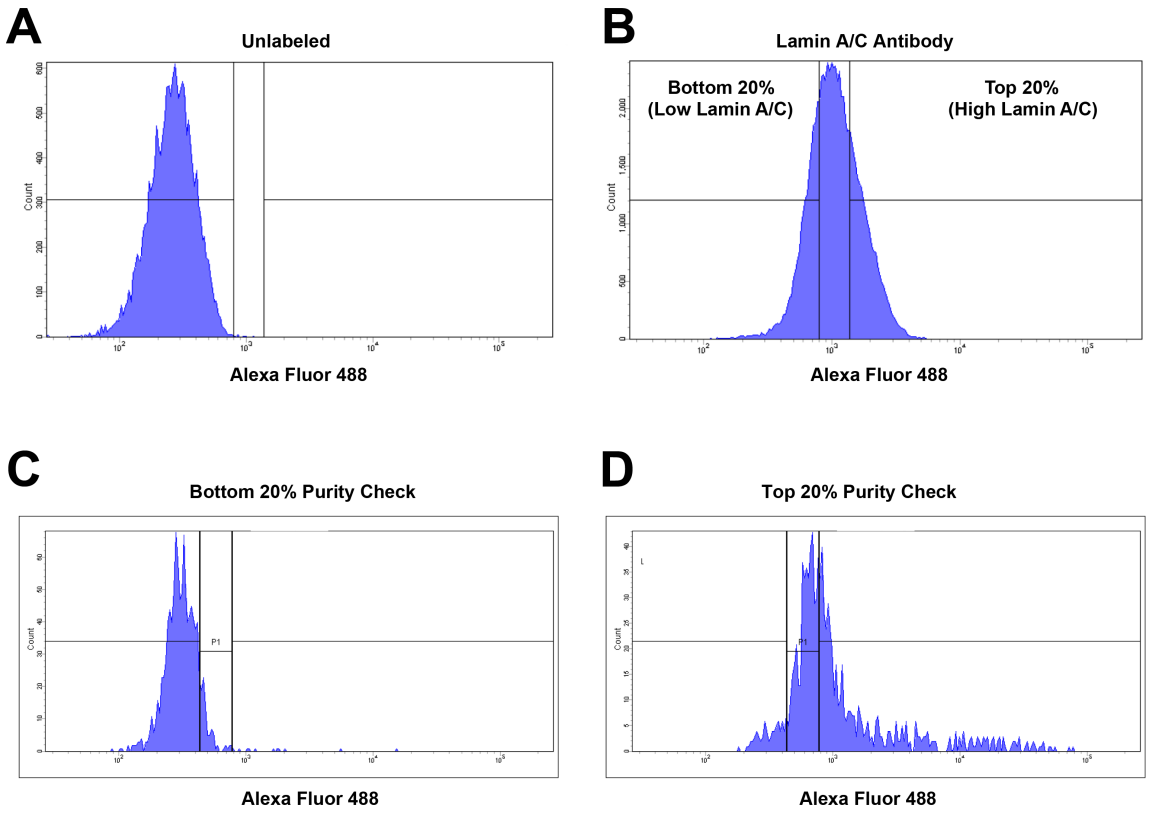

Figure B2. Lamin A/C-based sorting of high and low lamin A/C expressing ASCs. (A) Unlabeled P5 ASCs; (B) Lamin A/C antibody labeled P5 ASCs were sorted in two groups: the top 20% of fluorescent cells (high lamin A/C expressing cells) and the bottom 20% of fluorescent cells (low lamin A/C); (C-D) Sorting of the bottom 20% (C) and top 20% (D) of cells was verified by taking a 10,000 cell aliquot from

the sorted samples for each group and re-sorting them based on the bottom 20% and top 20% thresholds. Data shown are representative of the 4 samples sorted using the previously described criteria.

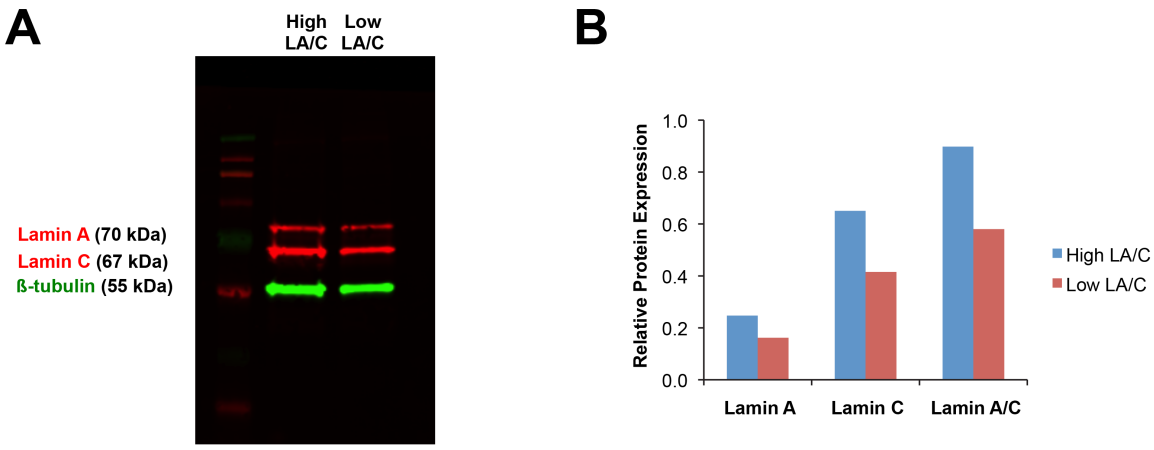

Figure B3. Protein expression analysis of high and low lamin A/C expressing cells. (A) Western blot assay of ASCs sorted by their high lamin A/C (High LA/C) and low lamin A/C (Low LA/C) protein expression (n=1, pilot run). (B) Quantification of relative lamin A/C expression from High LA/C and Low LA/C ASCs. Relative lamin expression was obtained by normalizing lamin expression to that of beta-tubulin (used as a loading control).

A.4 DISCUSSION

The data contained in this appendix represent preliminary evidence that lamin A/C could be used as a biomarker to sort cells with differential lamin A/C in a fashion similar to conventional cell sorters. Specifically, ASCs sorted using the top and bottom 20% of fluorescence thresholds showed differences in lamin A/C expression. These findings indicate the feasibility of using lamin A/C as a marker for acquiring distinct groups of cells, which are hypothesized to have different whole-cell mechanophenotypes based on our previous work. However, the collected cytometric data cannot reveal the extent to which each protein contributes to the observed lamin A/C expression profiles. Because of this limitation, it was important to determine whether the expression of lamin

A and C was different enough between these sorted groups before subjecting the samples to expensive proteomic analyses.

Western blot assays were performed to determine whether the established thresholds provided enough resolution in the differences for lamin A/C expression between high and low lamin A/C-sorted cells. It was observed that lamin C, rather than lamin A, exhibited the largest difference in protein expression between high and low lamin A/C-sorted ASCs. While these data were obtained from a pilot study with insufficient power for determining statistical significance, the finding was consistent with the results reported in Chapter 3, in which lamin C was reported to be the lamin protein with the strongest correlation to mechanophenotype.

The rationale behind running just one Western blot assay was to examine the differential expression of lamin A and C in high and low lamin A/C-sorted cells without sacrificing too much protein content from lysates (5 μg) in the Western blot assay. Instead, a considerable amount of protein (30 μg) was assigned towards proteomics analyses to provide enough starting material for the statistical analysis of protein/peptide fragment abundance. This step will prove to be critical to identify surface proteins that are highly abundant in high lamin A/C-sorted cells and low lamin A/C-sorted cells with statistical validity.

As mentioned above, the entire methods of this section revolve around sorting enough cells with differential lamin A/C expression. However, lamin A and C alone may

not be enough to distinguish cells with intermediate mechanophenotypic traits in heterogeneous populations, as suggested by data from the top 20% threshold's purity checks. Therefore, it could be necessary to identify additional markers that can help distinguish mechanophenotypic differences or sort intermediate to high stiffness ASCs, which could prove to be a non-trivial task. To accomplish this goal, the approach proposed for future investigations of this topic revolves in performing a proteomics analysis on the high and low lamin A/C sorted ASCs to identify markers that have protein abundances that correspond to the cells' mechanophenotype.

Following proteomic analysis, a hypothesized surface marker protein profile corresponding to either high and low lamin A/C ASCs can be used to sort live cells. The sorted cells would then be mechanically tested to characterize the mechanophenotype of the sorted cells. If the mechanically tested, sorted cells exhibit mechanical properties that correspond to other high-abundance surface proteins identified in the proteomics analysis, these biomarkers could also be potentially useful to sort mechanically distinct cells using conventional cell sorters by their mechanophenotype. As a result, this approach would allow for a method to sort and characterize cells based on their mechano- and lineage-specific phenotypic traits whose higher throughput and tunable degree of specificity (based on number of surface markers selected) cannot be currently matched by deformability-based cytometry devices.

A.5 CONCLUSION

This pilot study demonstrates the potential of using lamin A/C as a biomarker to sort cells from mechanically heterogeneous cell populations such as ASCs. As a whole, the presented approach could provide a platform for the discovery of mechanophenotypic biomarkers. These mechanophenotypic biomarkers could be combined with other biologically-relevant biomarkers for studying mechanophenotype in the context of biological processes like cell-matrix & cell-cell adhesion, migration, and mechanotransduction. Additionally, the same biomarkers could also be used to study the phenotype of cells of interests in scenarios that are relevant to tissue engineering, and regenerative medicine.

A.6 REFERENCES

1. Swift, J., I.L. Ivanovska, A. Buxboim, T. Harada, P.C. Dingal, J. Pinter, J.D. Pajerowski, K.R. Spinler, J.W. Shin, M. Tewari, F. Rehfeldt, D.W. Speicher, and D.E. Discher, Nuclear lamin-a scales with tissue stiffness and enhances matrix-directed differentiation. Science. 341(6149): p. 1240104.2013

2. DeLany, J.P., Z.E. Floyd, S. Zvonic, A. Smith, A. Gravois, E. Reiners, X. Wu, G. Kilroy, M. Lefevre, and J.M. Gimble, Proteomic analysis of primary cultures of human adipose-derived stem cells: Modulation by adipogenesis. Mol Cell Proteomics. 4(6): p. 731-40.2005

3. Satish, L., J.M. Krill-Burger, P.H. Gallo, S.D. Etages, F. Liu, B.J. Philips, S. Ravuri, K.G. Marra, W.A. LaFramboise, S. Kathju, and J.P. Rubin, Expression analysis

of human adipose-derived stem cells during in vitro differentiation to an adipocyte lineage. BMC Med Genomics. 8: p. 41.2015

4. Giusta, M.S., H. Andrade, A.V. Santos, P. Castanheira, L. Lamana, A.M. Pimenta, and A.M. Goes, Proteomic analysis of human mesenchymal stromal cells derived from adipose tissue undergoing osteoblast differentiation. Cytotherapy. 12(4): p. 478-90.2010

5. Sun, H.J., Y.Y. Bahk, Y.R. Choi, J.H. Shim, S.H. Han, and J.W. Lee, A proteomic analysis during serial subculture and osteogenic differentiation of human mesenchymal stem cell. J Orthop Res. 24(11): p. 2059-71.2006

6. Mateos, J., P.F. Pernas, J.F. Labora, F. Blanco, and M.D. Arufe, Proteomic applications in the study of human mesenchymal stem cells. Proteomes. 2(1): p. 53-71.2014

7. Sadick, J.S., M.E. Boutin, D. Hoffman-Kim, and E.M. Darling, Protein characterization of intracellular target-sorted, formalin-fixed cell subpopulations. Sci Rep. 6: p. 33999.2016

8. Zvonic, S., M. Lefevre, G. Kilroy, Z.E. Floyd, J.P. DeLany, I. Kheterpal, A. Gravois, R. Dow, A. White, X. Wu, and J.M. Gimble, Secretome of primary cultures of human adipose-derived stem cells: Modulation of serpins by adipogenesis. Mol Cell Proteomics. 6(1): p. 18-28.2007

9. Frazier, T.P., J.M. Gimble, I. Kheterpal, and B.G. Rowan, Impact of low oxygen on the secretome of human adipose-derived stromal/stem cell primary cultures. Biochimie. 95(12): p. 2286-96.2013